

Appendix

7.1 Chapter 3 – supporting information

7.1.1 Peptides and peptide-peptoid hybrids characterisation

7.1.1.1 P006 – VPTDVGPFaf-NH₂

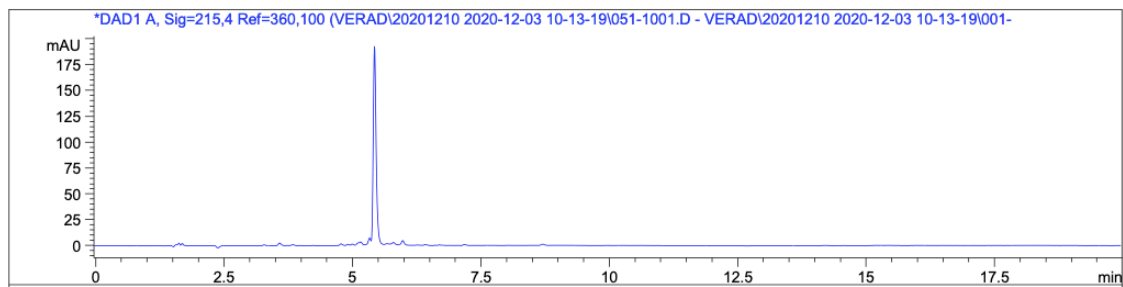


Figure S 1. HPLC chromatogram (215 nm) of P006. Compound purity based on HPLC peak area analysis: 96.6%.

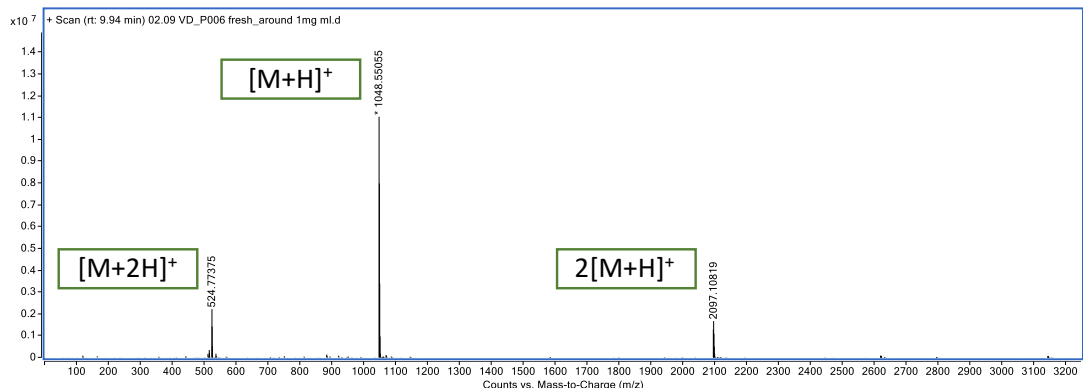


Figure S 2. Accurate mass spectrum of P006.

7.1.1.2 LJMU011 – VPTDVGPFa-4-F-Phe-NH₂

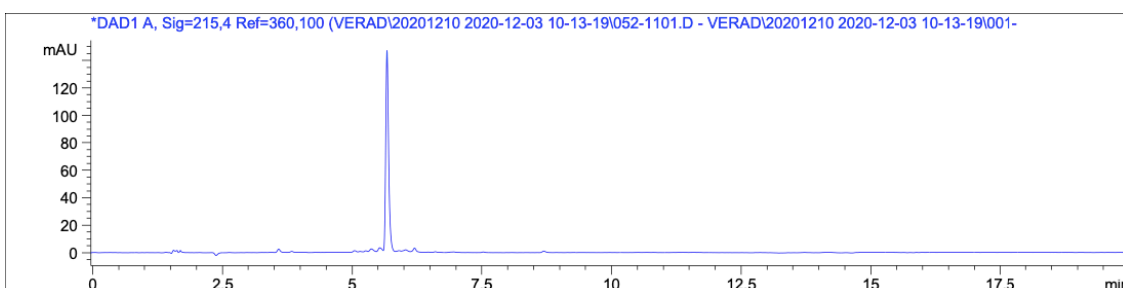


Figure S 3. HPLC chromatogram (215 nm) of LJMU011.

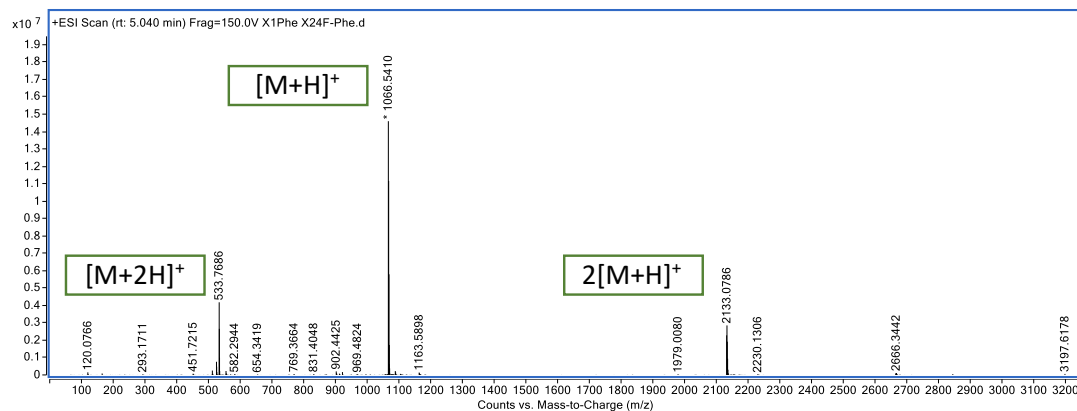


Figure S 4. Accurate mass spectrum of LJM011. Compound purity based on HPLC peak area analysis: 95%.

7.1.1.3 LJM012 – VPTDVG-4-F-Phe-AF-NH₂

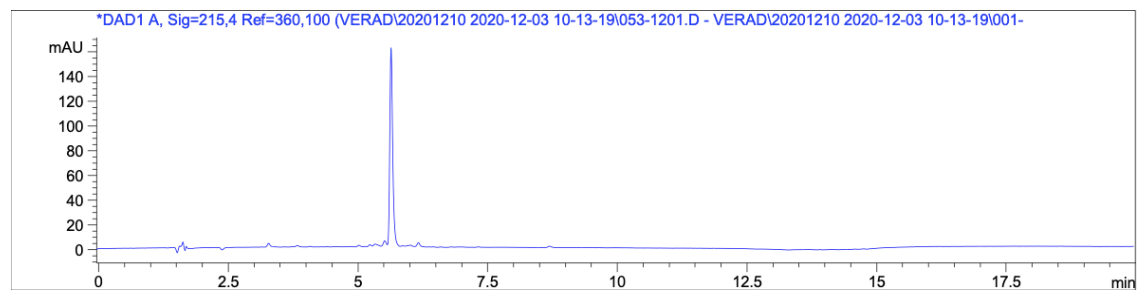


Figure S 5. HPLC chromatogram (215 nm) of LJM012. Compound purity based on HPLC peak area analysis: 94.3%.

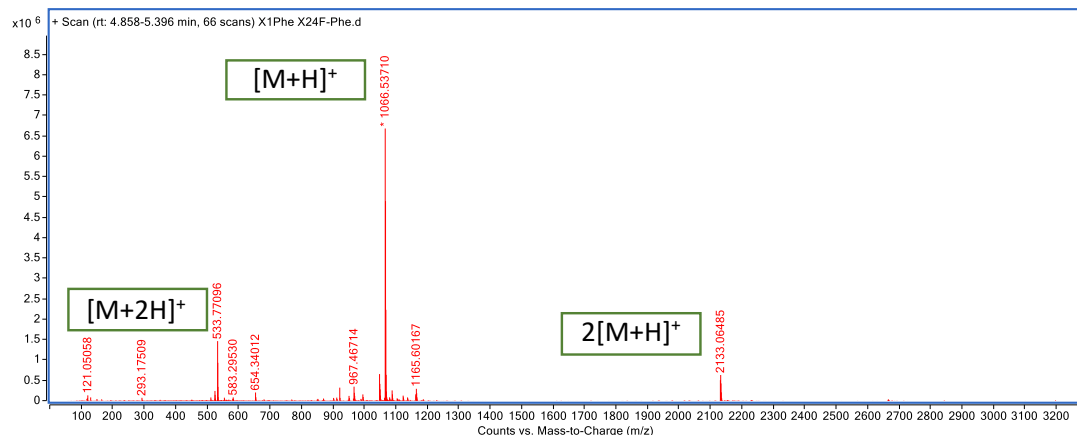


Figure S 6. Accurate mass spectrum of LJM012.

7.1.1.4 LJM013 – VPTDVGPF-4-F-Phe-A-4-F-Phe-NH₂

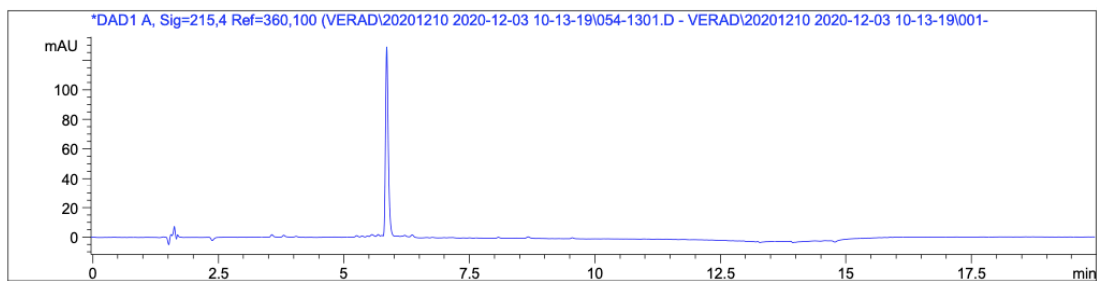


Figure S 7. HPLC chromatogram (215 nm) of LJM013. Compound purity based on HPLC peak area analysis: 98%

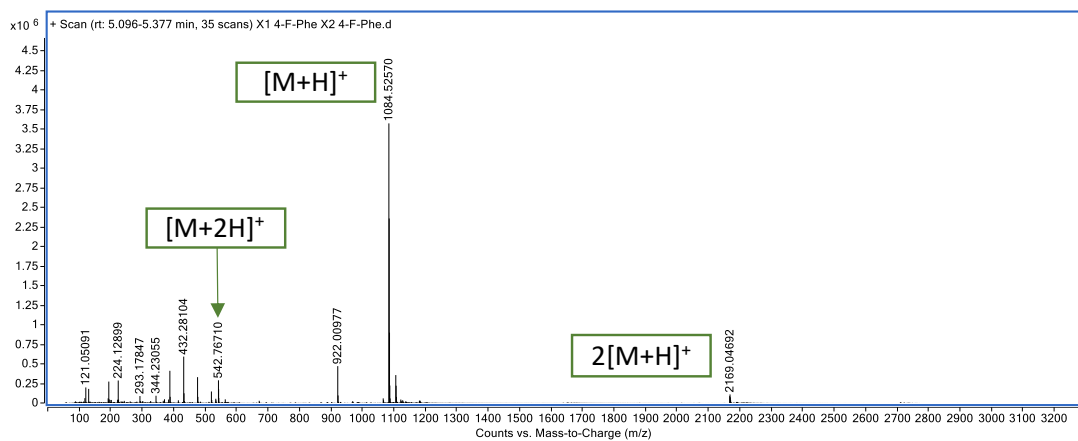


Figure S 8. Accurate mass spectrum of LJM013.

7.1.1.5 LJM014 – VPTDVGPF-F₅-Phe-NH₂

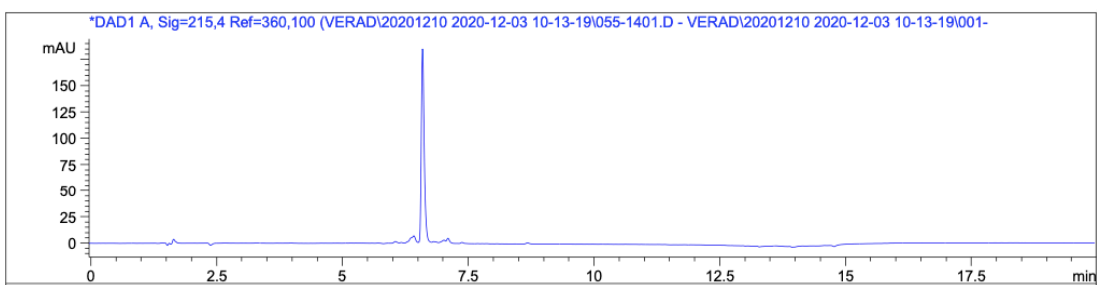


Figure S 9. HPLC chromatogram (215 nm) of LJM014. Compound purity based on HPLC peak area analysis: 90.3%

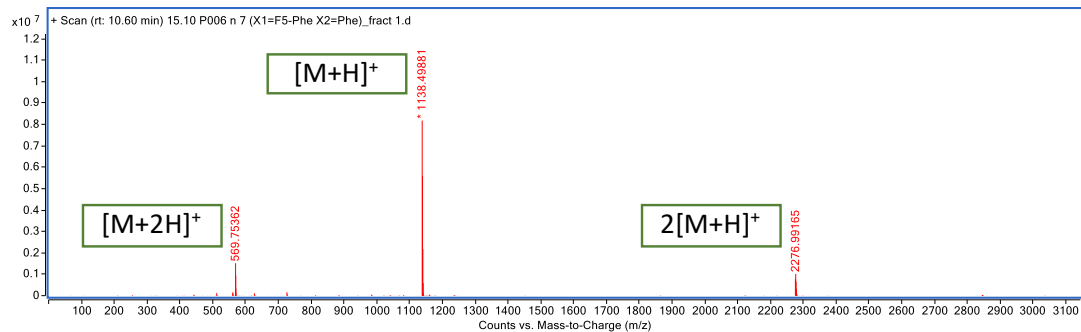


Figure S 10. Accurate mass spectrum of LJM014.

7.1.1.6 LJM015 – VPTDVGPF₅-Phe-AF-NH₂

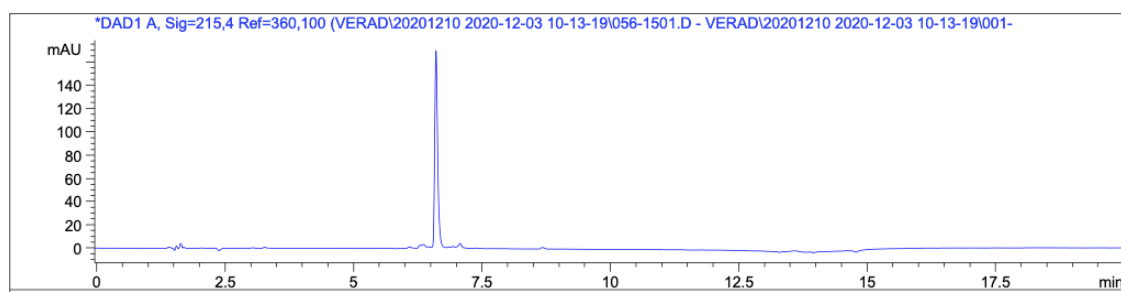


Figure S 11. HPLC chromatogram (215 nm) of LJM015. Compound purity based on HPLC peak area analysis: 92.3%

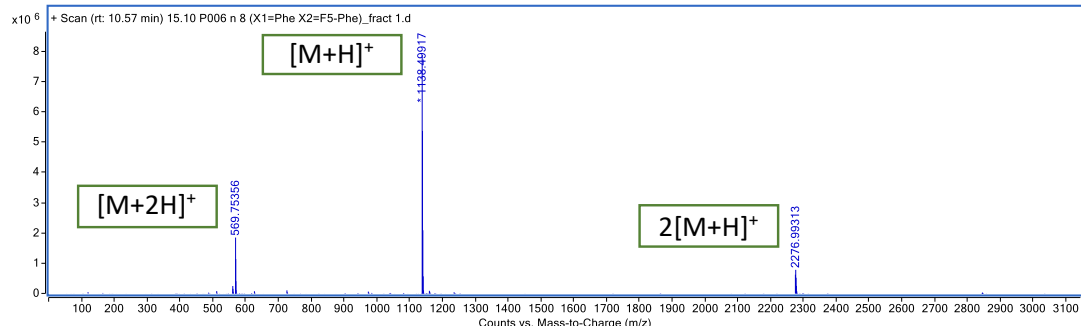


Figure S 12. Accurate mass spectrum of LJM015.

7.1.1.7 LJMU016 – VPTDVGPF₅-Phe-A-F₅-Phe-NH₂

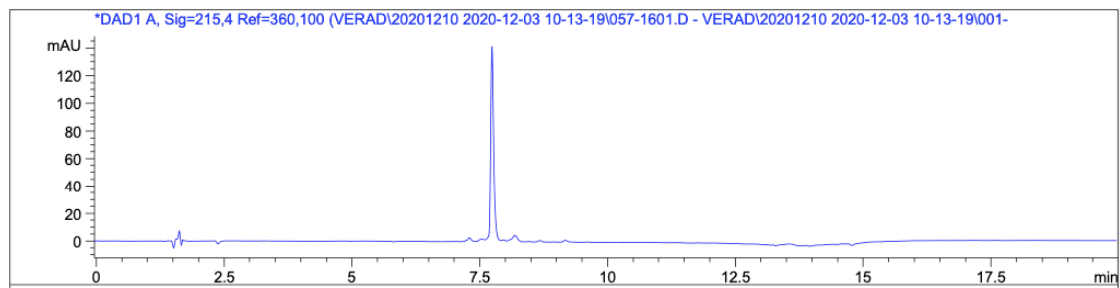


Figure S 13. HPLC chromatogram (215 nm) of LJMU016. Compound purity based on HPLC peak area analysis: 90%

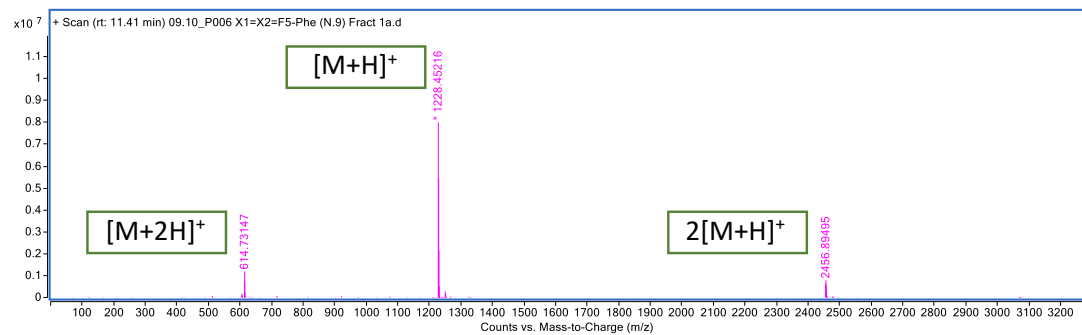


Figure S 14. Accurate mass spectrum of LJMU016.

7.1.1.8 LJMU017 – 4-F-benzoyl-VPTDVGPF₅-NH₂

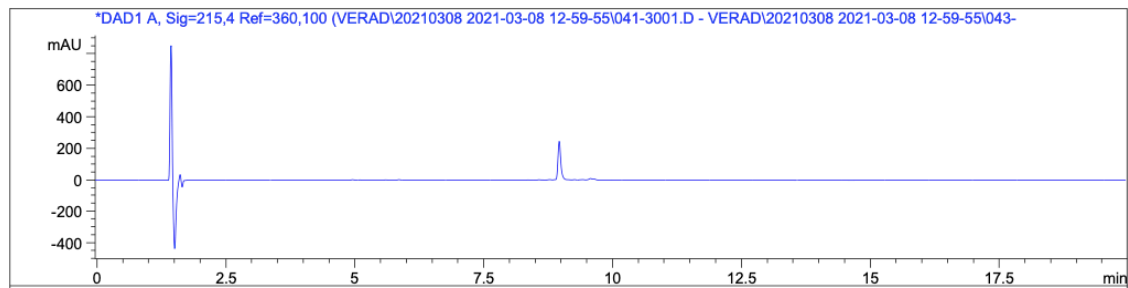


Figure S 15. HPLC chromatogram (215 nm) of LJMU017. Compound purity based on HPLC peak area analysis: 92.6%

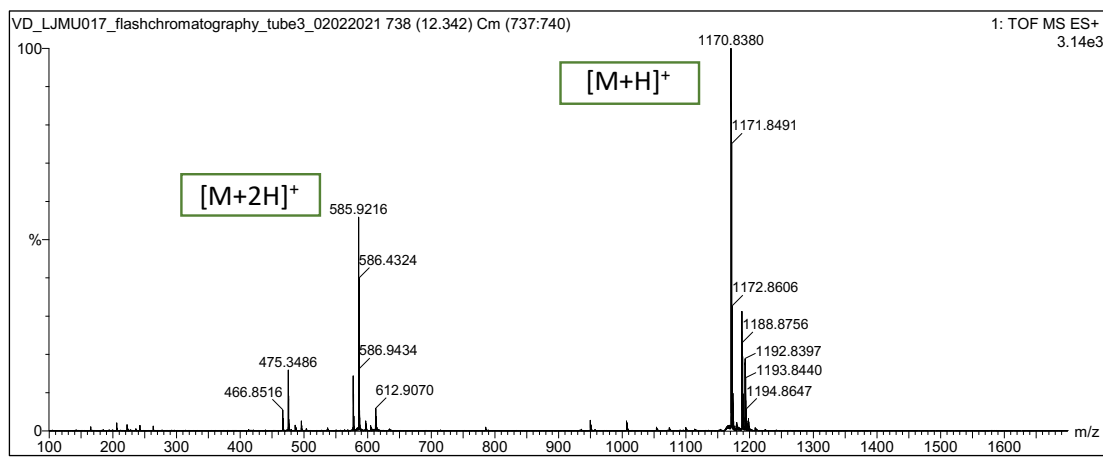


Figure S 16. MS spectrum of LJM017.

7.1.1.9 LJM018 – F₅-benzoyl-VPTDVGPFaf-NH₂

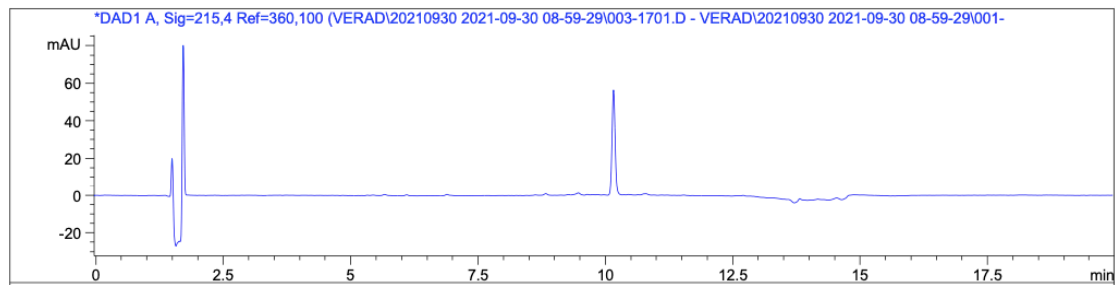


Figure S 17. HPLC chromatogram (215 nm) of LJM018. Compound purity based on HPLC peak area analysis: 99.5%.

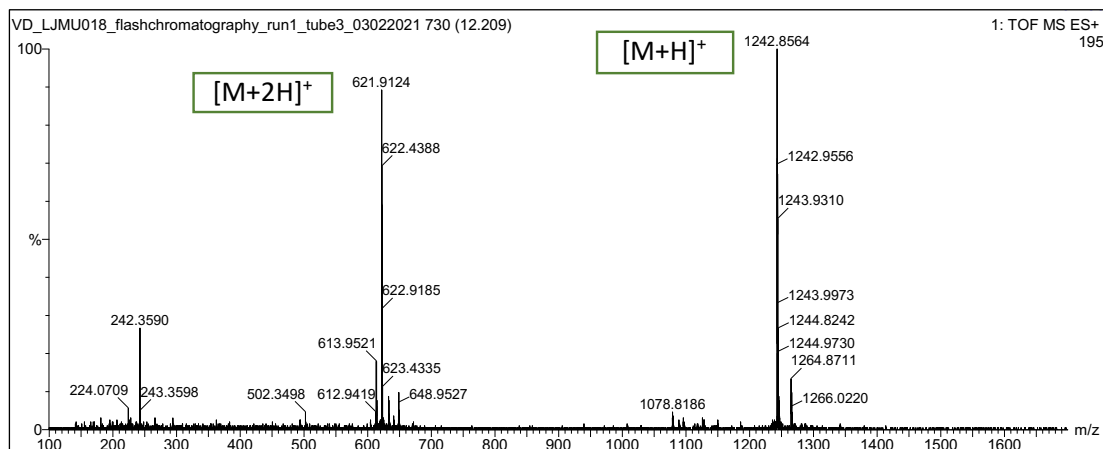


Figure S 18. MS spectrum LJM018.

7.1.1.10 LJM019 – VPTDVGPF-NPhe-NH₂

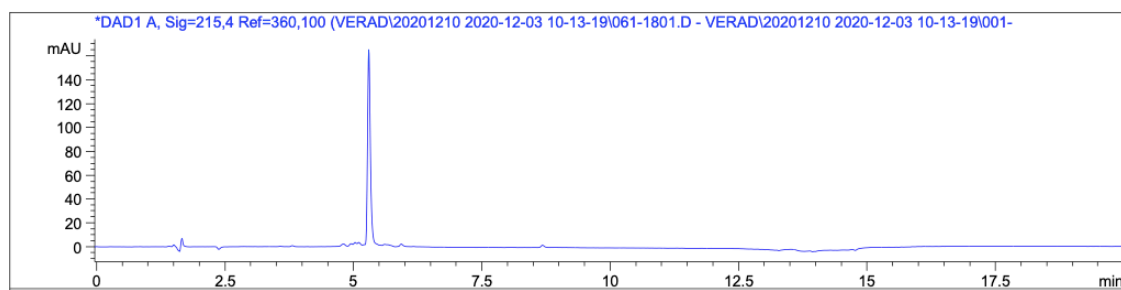


Figure S 19. HPLC chromatogram (215 nm) of LJM019. Compound purity based on HPLC peak area analysis: 91.5%.

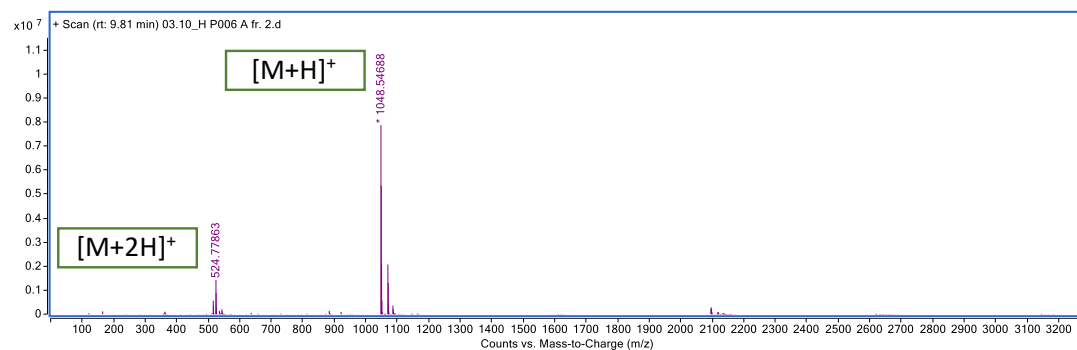


Figure S 20. Accurate mass spectrum of LJM019.

7.1.1.11 LJM020 – VPTDVGPF-NAla-F-NH₂

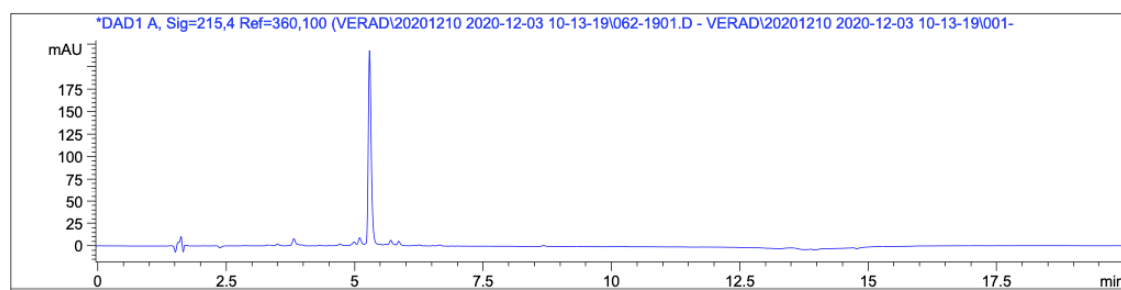


Figure S 21. HPLC chromatogram (215 nm) of LJM020. Compound purity based on HPLC peak area analysis: 87.5%.

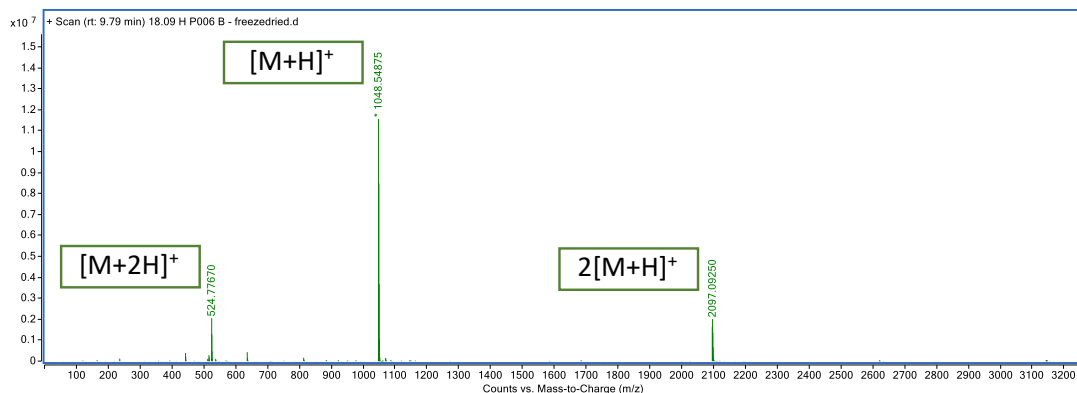


Figure S 22. Accurate mass spectrum of LJM020.

7.1.1.12 LJM021 – VPTDVGP-NPhe-AF-NH₂

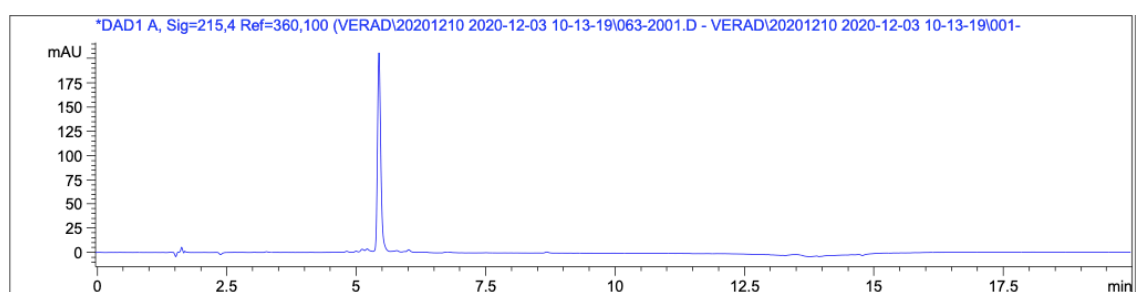


Figure S 23. HPLC chromatogram (215 nm) of LJM021. Compound purity based on HPLC peak area analysis: 97.5%.

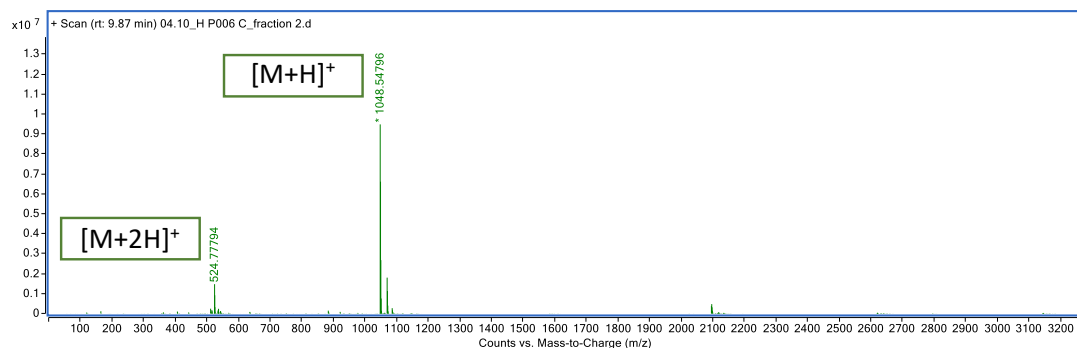


Figure S 24. Accurate mass spectrum of LJM021.

7.1.1.13 LJMU022 – VPTD-NVal-GPFAF-NH₂

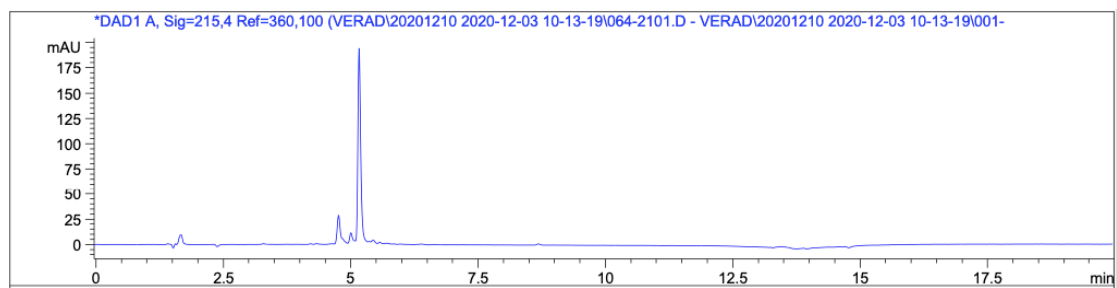


Figure S 25. HPLC chromatogram (215 nm) of LJMU022. Compound purity based on HPLC peak area analysis: 99.7%. Minor peak attributed to VPTDGPFAF-NH₂ due to deletion of NVal.

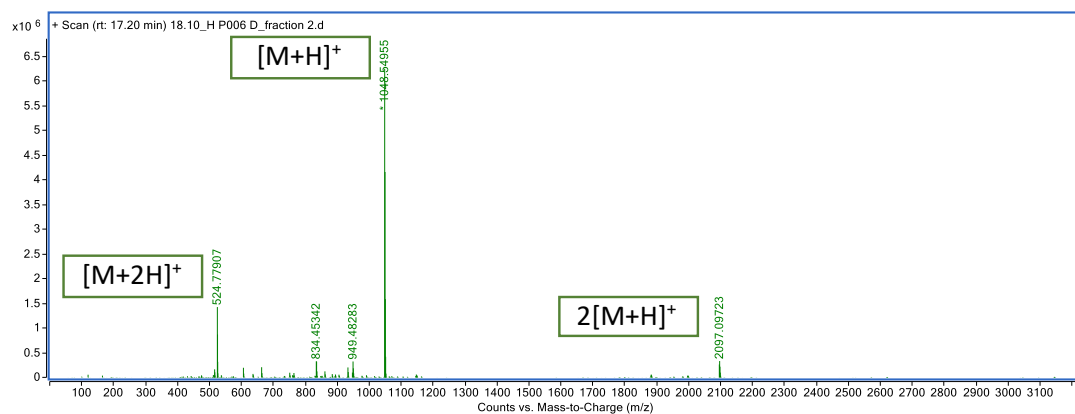


Figure S 26. Accurate mass spectrum of LJMU022.

7.1.1.14 LJMU023 – VPT-NAsp-VGPFAF-NH₂

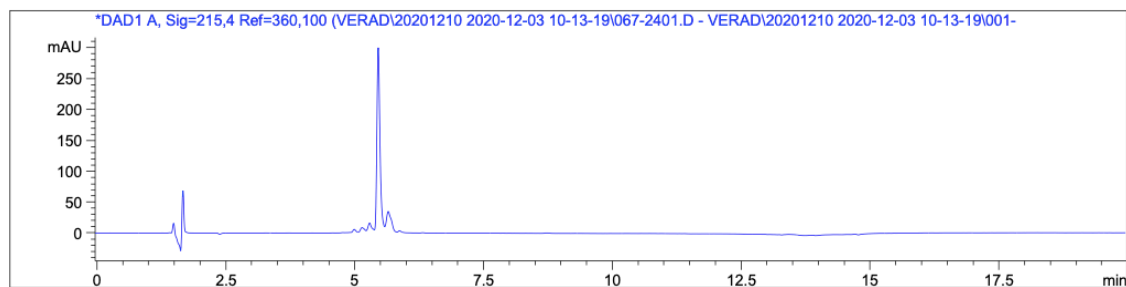


Figure S 27. HPLC chromatogram (215 nm) of LJMU023. Compound purity based on HPLC peak area analysis: 77%

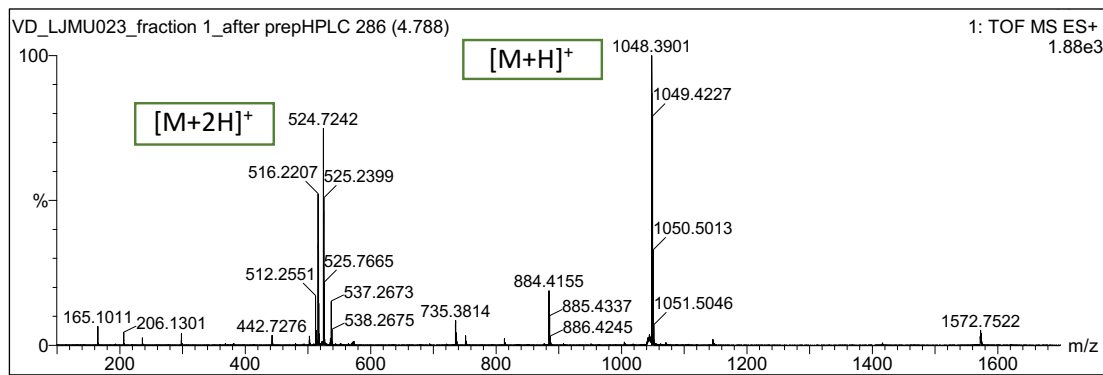


Figure S 28. MS spectrum of LJM023.

7.1.1.15 LJM024 – NVal-PTDVGPFaf-NH₂

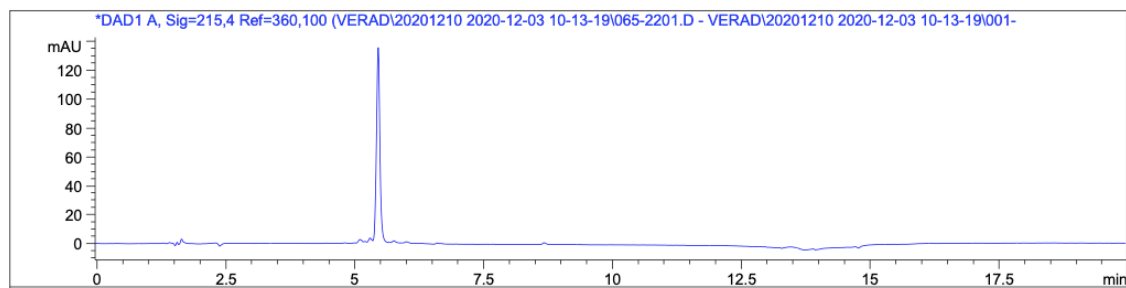


Figure S 29. HPLC chromatogram (215 nm) of LJM024. Compound purity based on HPLC peak area analysis: 95.4%.

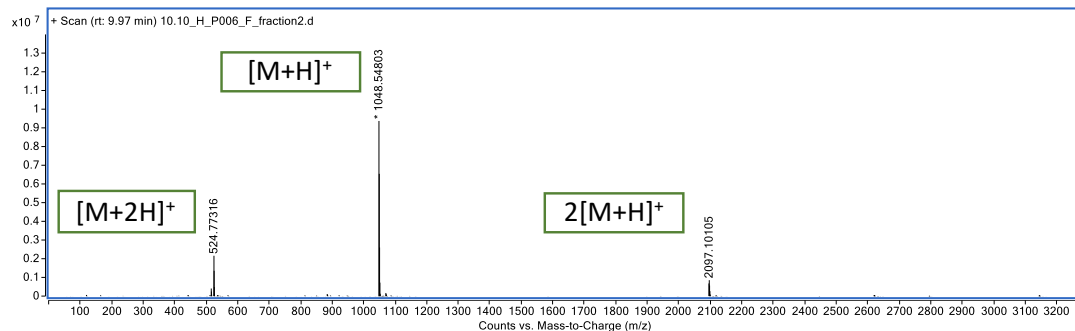


Figure S 30. Accurate mass spectrum of LJM024.

7.1.1.16 LJM025 – TDVGPFAF-NH₂

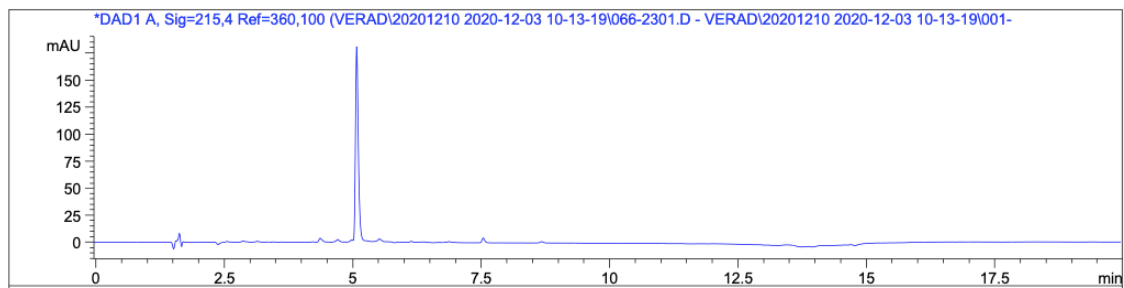


Figure S 31. HPLC chromatogram (215 nm) of LJM025. Compound purity based on HPLC peak area analysis: 96%.

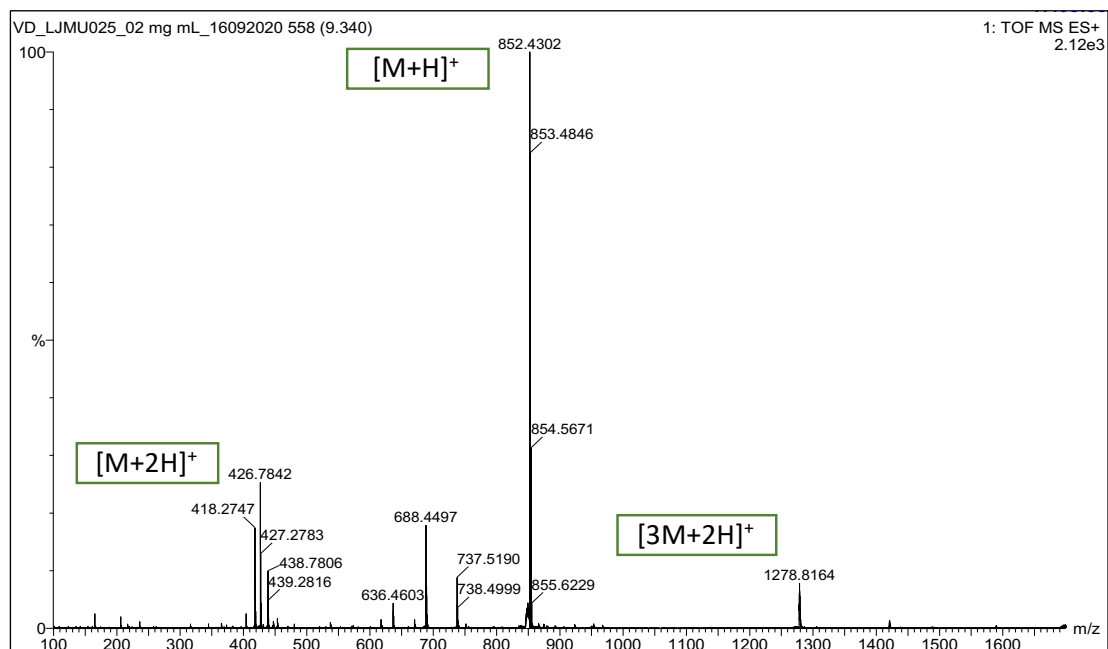


Figure S 32. MS spectrum of LJM025.

7.1.1.17 LJM026 – VPSDVGPFAF-NH₂

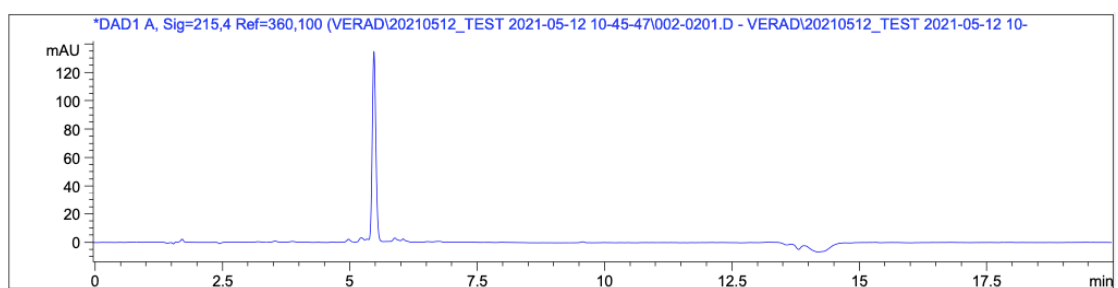


Figure S 33. HPLC chromatogram (215 nm) of LJM026. Compound purity based on HPLC peak area analysis: 91.7%.

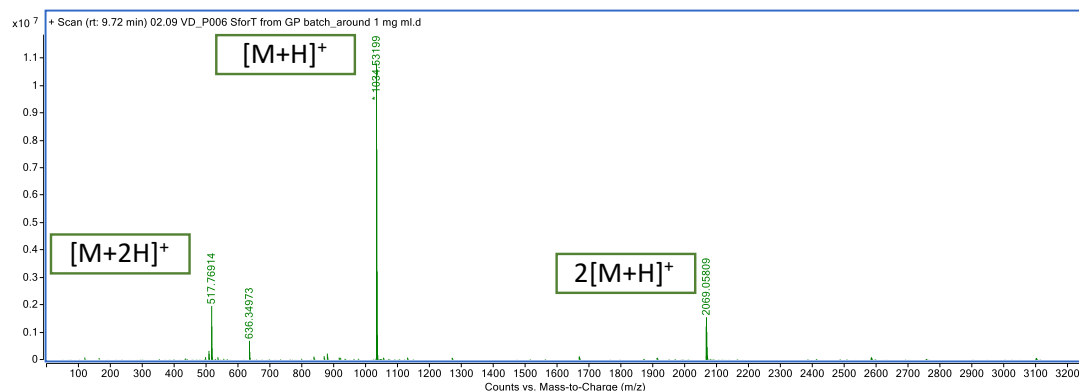


Figure S 34. Accurate mass spectrum of LJMU026.

7.1.1.18 LJMU027 – Benzoyl-VPTDVGPFaf-NH₂

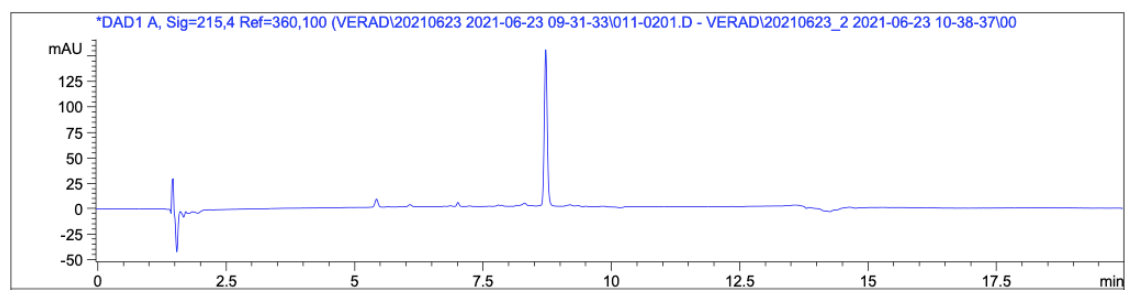


Figure S 35. HPLC chromatogram (215 nm) of LJMU027. Compound purity based on HPLC peak area analysis: 88.9%.

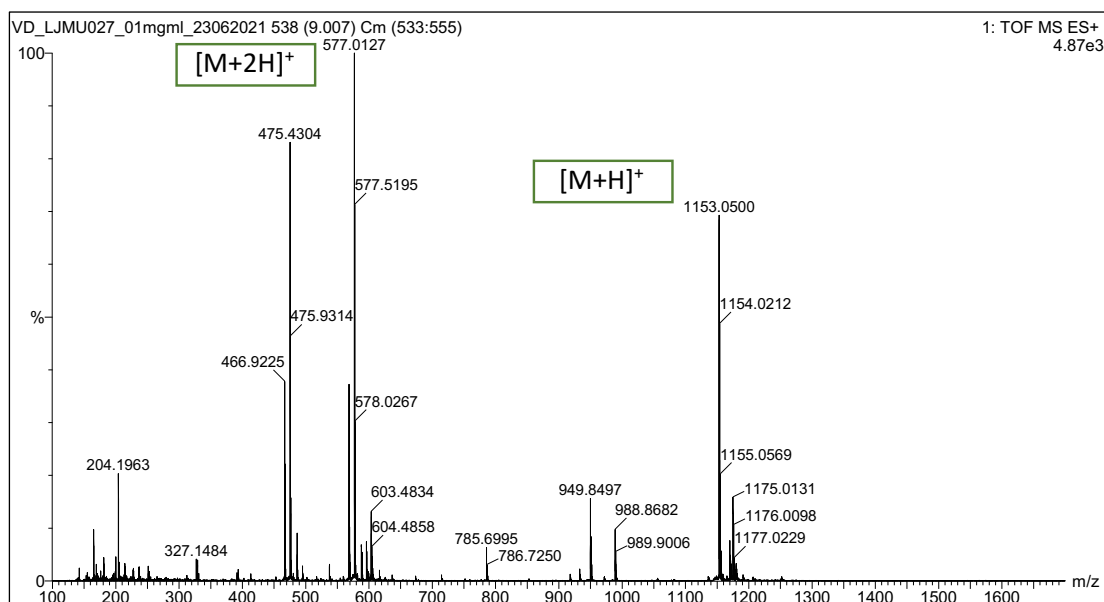


Figure S 36. MS spectrum of LJMU027.

7.1.1.19 CGRP 8-37 – VTHRLAGLLSRSGGVVKNNFVPTNVGSKAF-NH₂

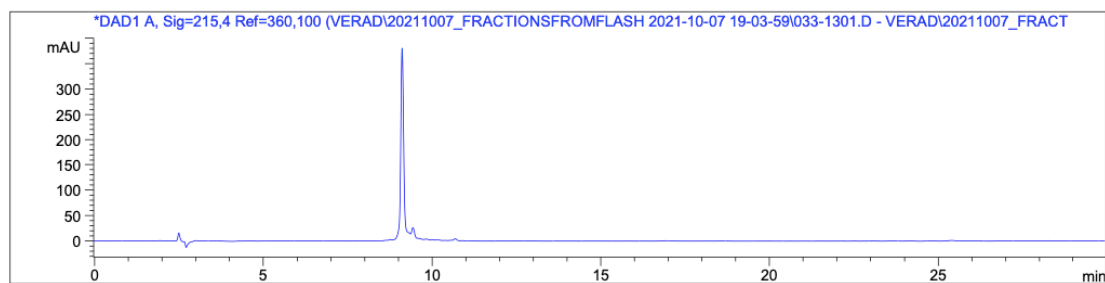


Figure S 37. HPLC chromatogram (215 nm) of CGRP 8-37. Compound purity based on HPLC peak area analysis: 88.5%.

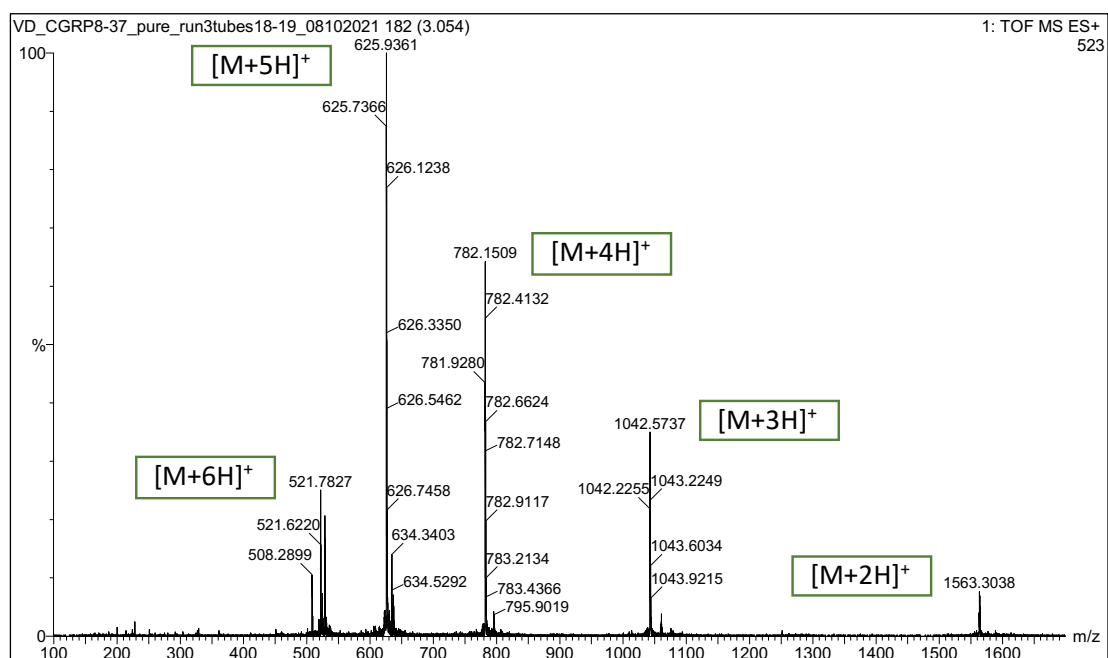


Figure S 38. MS spectrum of CGRP 8-37.

7.1.2 Experimental LogD (shake-flask method)

7.1.2.1 Calibration curves in PBS aq. solution saturated with 1-octanol

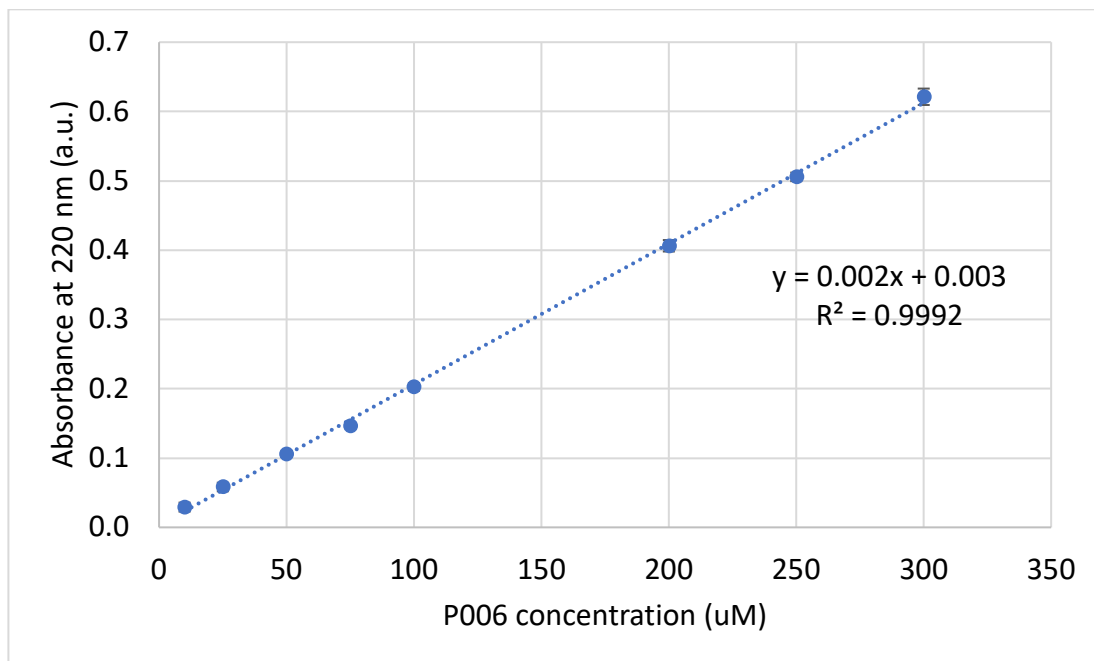


Figure S 39. P006 calibration curve in aq. PBS solution saturated with 1-octanol.

Absorbance detected at 220 nm. Experiment performed in duplicate.

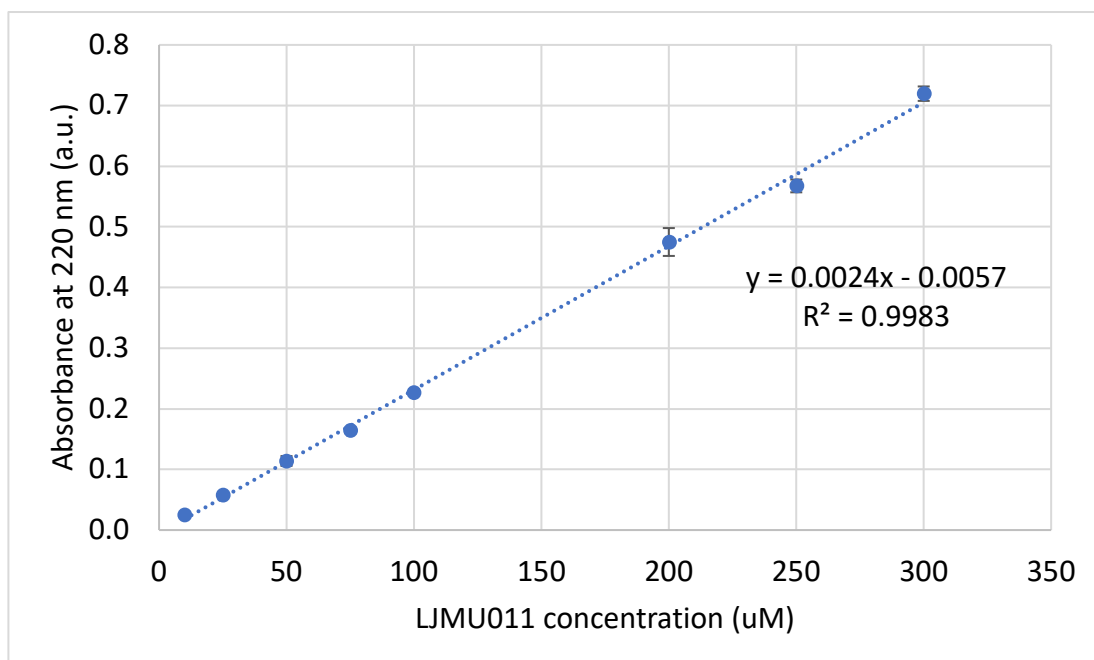


Figure S 40. LJMU011 calibration curve in aq. PBS solution saturated with 1-octanol.

Absorbance detected at 220 nm. Experiment performed in duplicate.

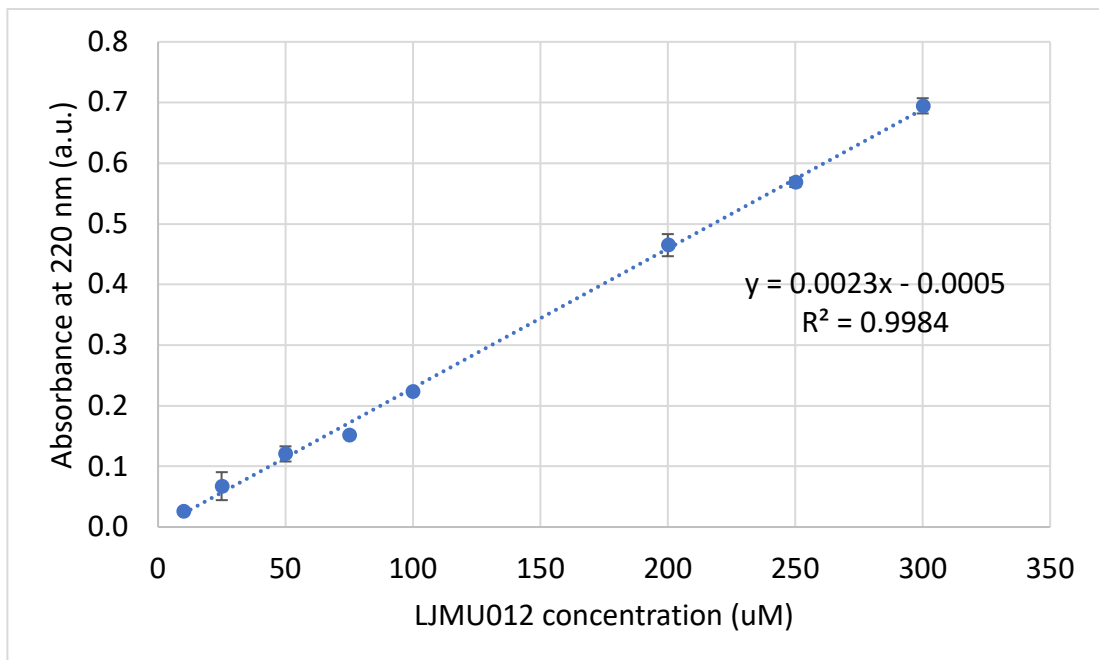


Figure S 41. LJM012 calibration curve in aq. PBS solution saturated with 1-octanol.
Absorbance detected at 220 nm. Experiment performed in duplicate.

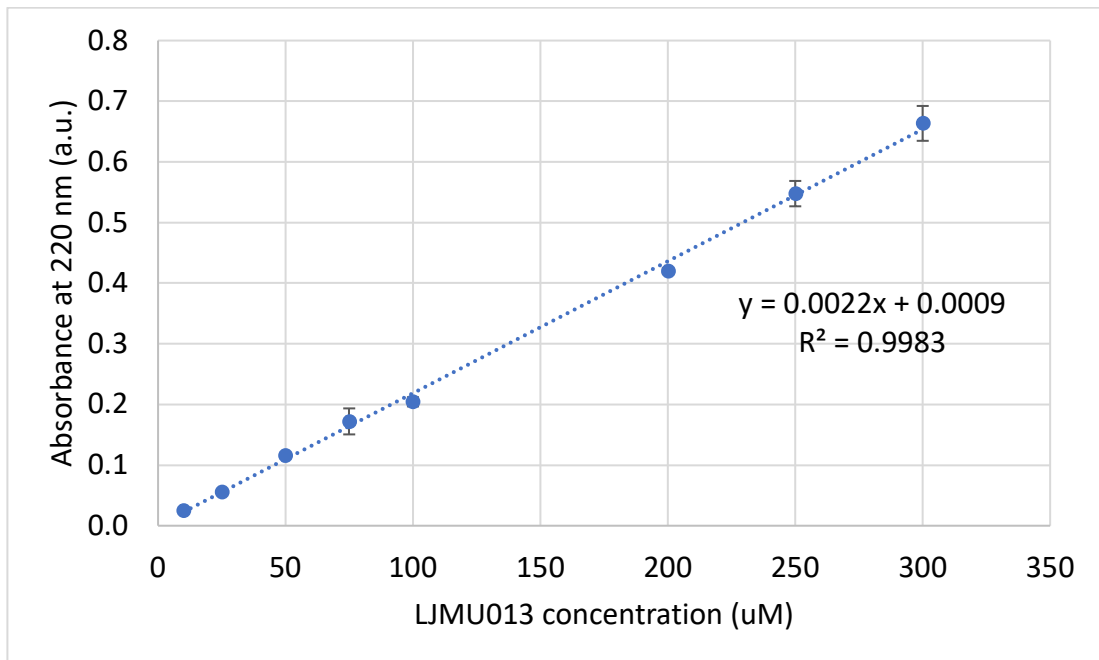


Figure S 42. LJM013 calibration curve in aq. PBS solution saturated with 1-octanol.
Absorbance detected at 220 nm. Experiment performed in duplicate.

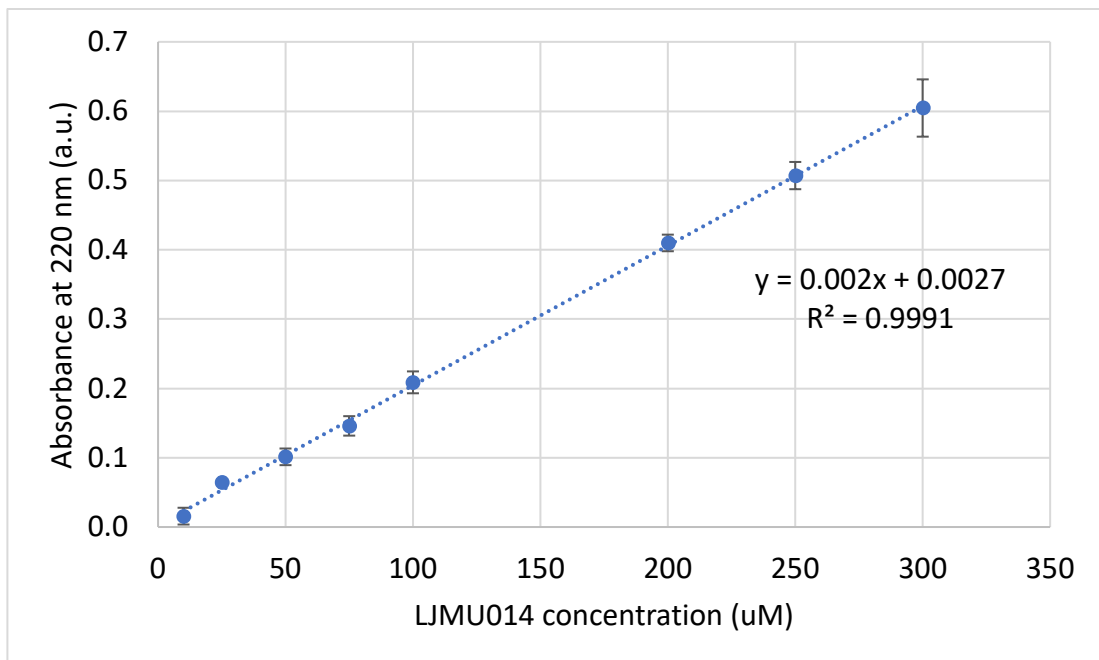


Figure S 43. LJM014 calibration curve in aq. PBS solution saturated with 1-octanol.
Absorbance detected at 220 nm. Experiment performed in duplicate.

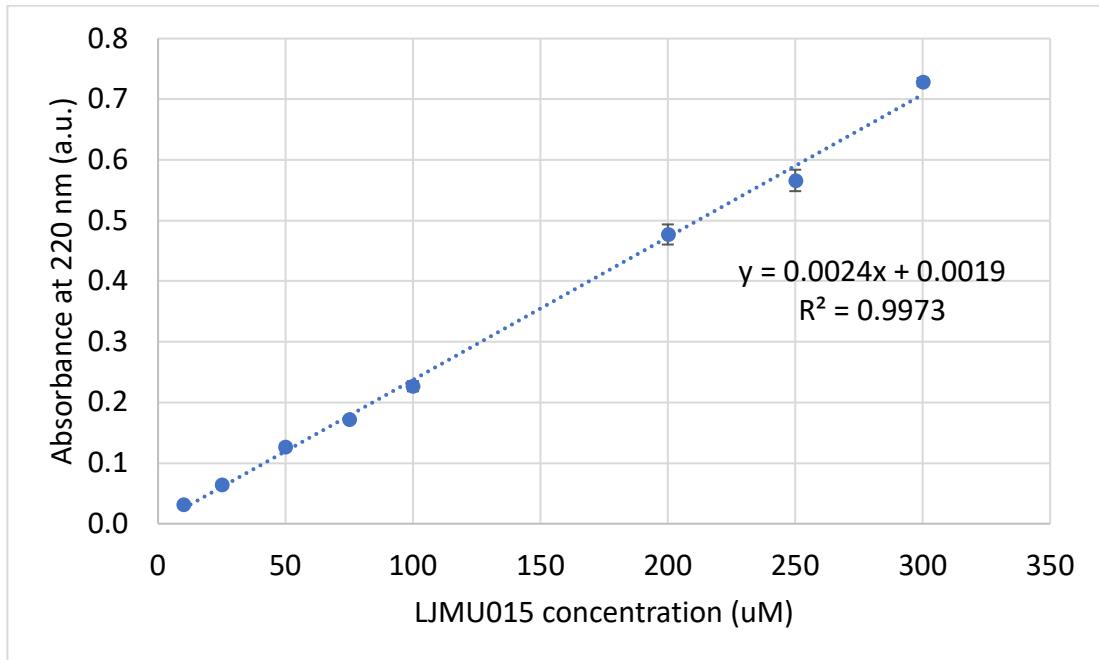


Figure S 44. LJM015 calibration curve in aq. PBS solution saturated with 1-octanol.
Absorbance detected at 220 nm. Experiment performed in duplicate.

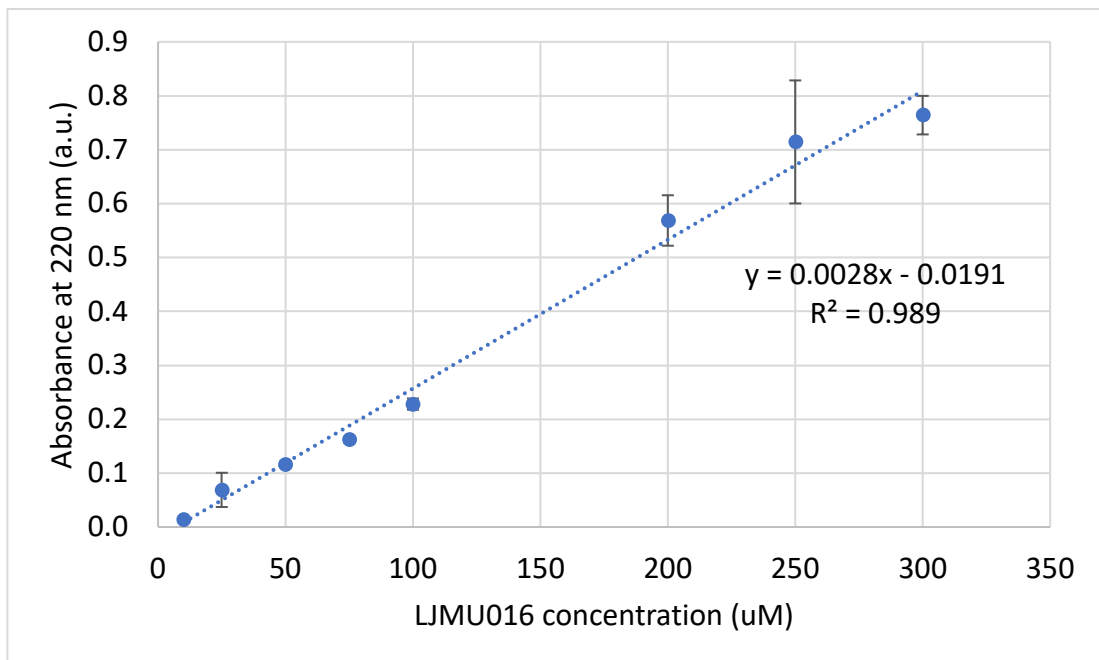


Figure S 45. LJM016 calibration curve in aq. PBS solution saturated with 1-octanol.
Absorbance detected at 220 nm. Experiment performed in duplicate

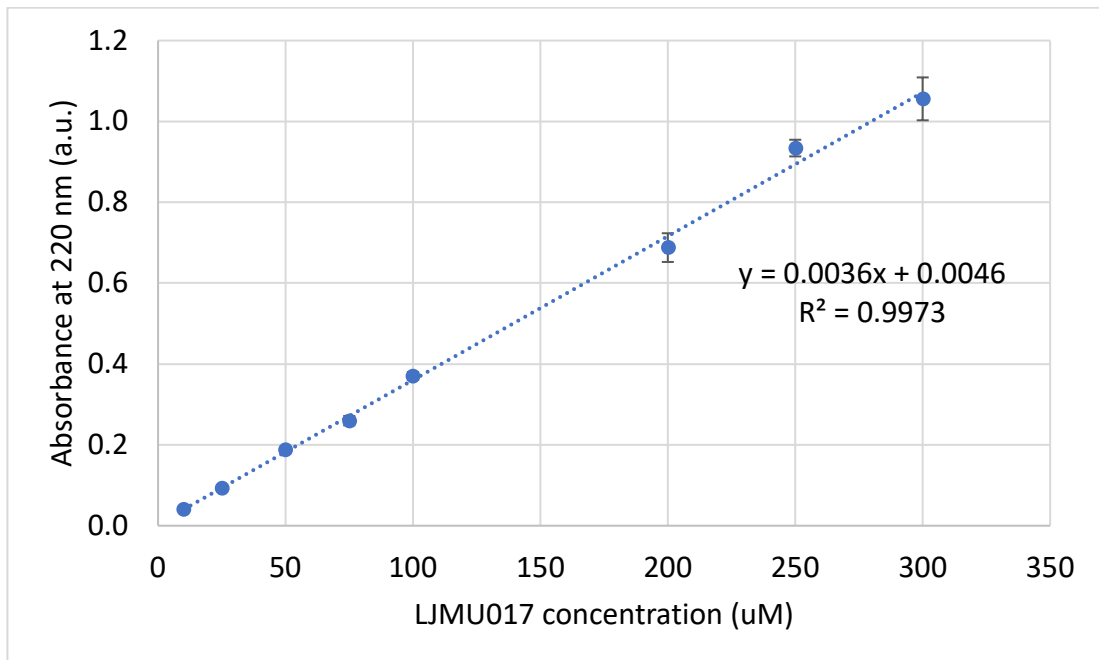


Figure S 46. LJM017 calibration curve in aq. PBS solution saturated with 1-octanol.
Absorbance detected at 220 nm. Experiment performed in duplicate.

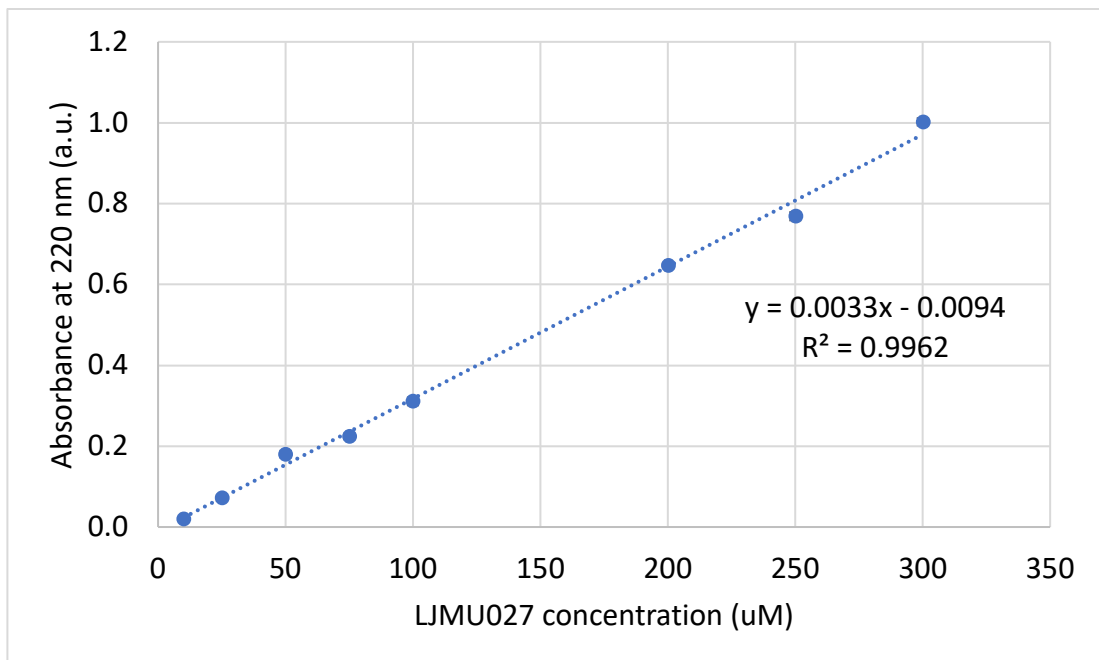


Figure S 47. LJM027 calibration curve in aq. PBS solution saturated with 1-octanol. Absorbance detected at 220 nm. Experiment performed in duplicate.

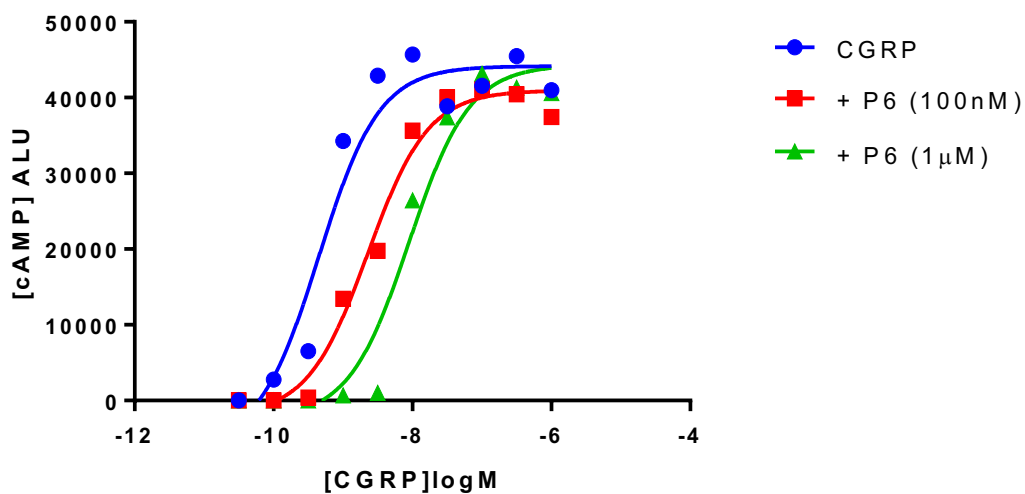
7.1.2.2 LogD and cLogP data

Table S.1. Lipophilicity assessment – full data set. N.P. = experiment non performed.

Entry	RP-HPLC RT (min)	% ACN	Δ RT (min)	Δ % ACN	cLogP (ChemDraw)	miLogP (Molinspiration)	cLogP (Chemicalize)	cLogD, pH 7.4 (Chemicalize)	Experimental LogD, pH 7.4
P006	5.424	34.3	N.A.	N.A.	-1.4278	-2.94	-4.687	-4.740	-3.800
LMU011	5.668	35.3	0.244	1.0	-0.6222	-1.70	-3.058	-3.160	-1.120
LMU012	5.633	35.2	0.209	0.9	-0.6222	-1.70	-3.058	-3.160	-1.864
LMU013	5.850	36.0	0.426	1.7	-0.4703	-1.54	-2.915	-3.020	-1.405
LMU014	6.589	39.0	1.165	4.7	-0.9228	-2.41	-3.973	-4.030	-1.972
LMU015	6.601	39.0	1.177	4.7	-0.9228	-2.41	-3.973	-4.030	-1.676
LMU016	7.735	43.6	2.311	9.3	-0.4178	-1.88	-3.275	-3.710	-0.232
LMU017	8.961	48.5	3.537	14.2	2.5966	-0.83	-0.607	-3.700	-1.200
LMU018	10.015	52.7	4.591	18.4	2.2786	-0.47	-0.036	-3.140	N.P.
LMU019	5.295	33.8	-0.129	-0.5	-0.9316	-3.65	-4.963	-5.020	N.P.
LMU020	5.288	33.8	-0.136	-0.5	-1.1536	-2.52	-5.032	-5.090	N.P.
LMU021	5.435	34.4	0.011	0.1	-0.9316	-2.59	-4.963	-5.020	N.P.

Entry	RP-HPLC RT (min)	% ACN	Δ RT (min)	Δ % ACN	cLogP (ChemDraw)	miLogP (Molinspiration)	cLogP (Chemicalize)	cLogD, pH 7.4 (Chemicalize)	Experimental LogD, pH 7.4
UMU022	5.160	33.3	-0.264	-1.0	-1.1812	-2.63	-5.146	-5.200	N.P.
UMU023	5.453	34.4	0.029	0.1	-0.2848	-3.37	-4.912	-4.970	N.P.
UMU024	5.451	34.4	0.027	0.1	-1.4856	-2.47	-5.145	-5.160	N.P.
UMU025	5.073	32.9	-0.351	-1.4	-2.6533	-4.34	-4.241	-7.230	N.P.
UMU026	5.468	34.5	0.044	0.2	-1.5698	-3.30	-5.103	-5.160	N.P.
UMU027	8.718	47.5	3.294	13.2	2.4536	-1.00	-0.749	-3.850	-0.300

7.1.3 Concentration-response curves (cAMP accumulation assay)



$$EC_{50} \text{ CGRP} = 0.45 \text{ nM}$$

$$EC_{50} \text{ CGRP+P6(100 nM)} = 2.3 \text{ nM}$$

$$EC_{50} \text{ CGRP+P6 (1 μM)} = 9.0 \text{ nM}$$

Figure S 48. Concentration-response curves previously obtained for P006 (experiment carried out by Professor David A. Kendall in 2017 using DiscoverX Eurofins kit and CHO-K1 CALCRL RAMP1 cells). K_b estimates for P006 = 24 nM and 5.3 nM.

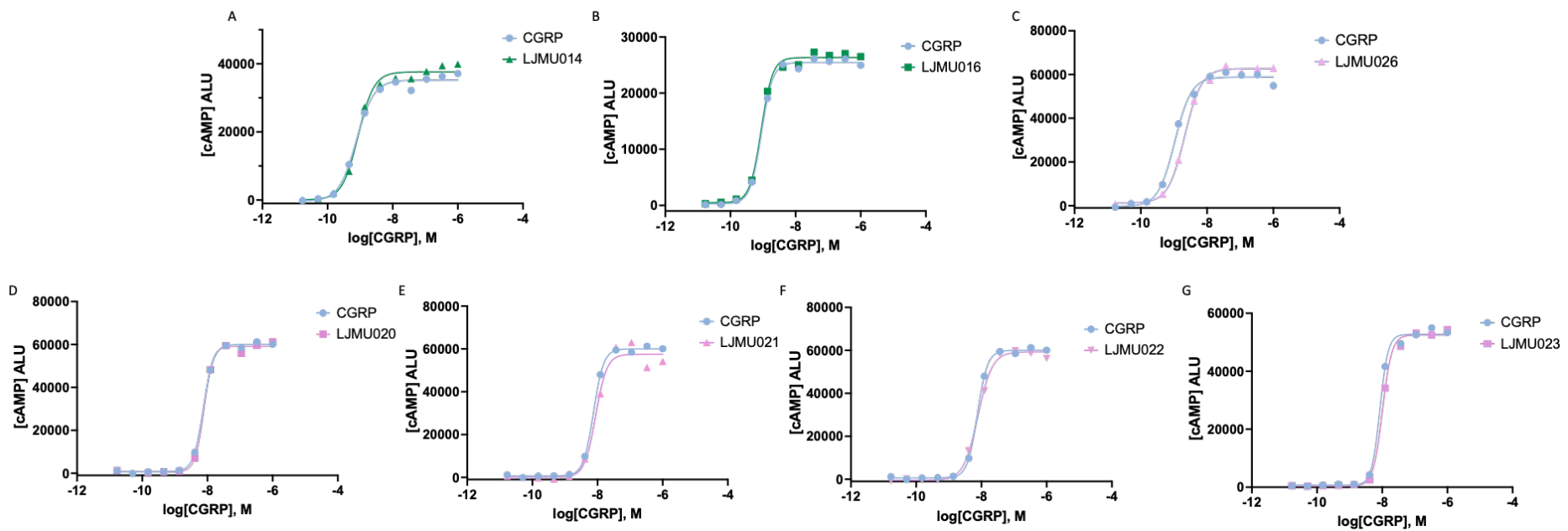


Figure S 49. Representative cAMP concentration-response curves for inactive peptides. From top left to bottom right: LJM014 (A), LJM016 (B), LJM020 (C), LJM021 (D), LJM022 (E), LJM023 (F).

7.2 Chapter 4 – supporting information

7.2.1 Calibration curves for serum stability study

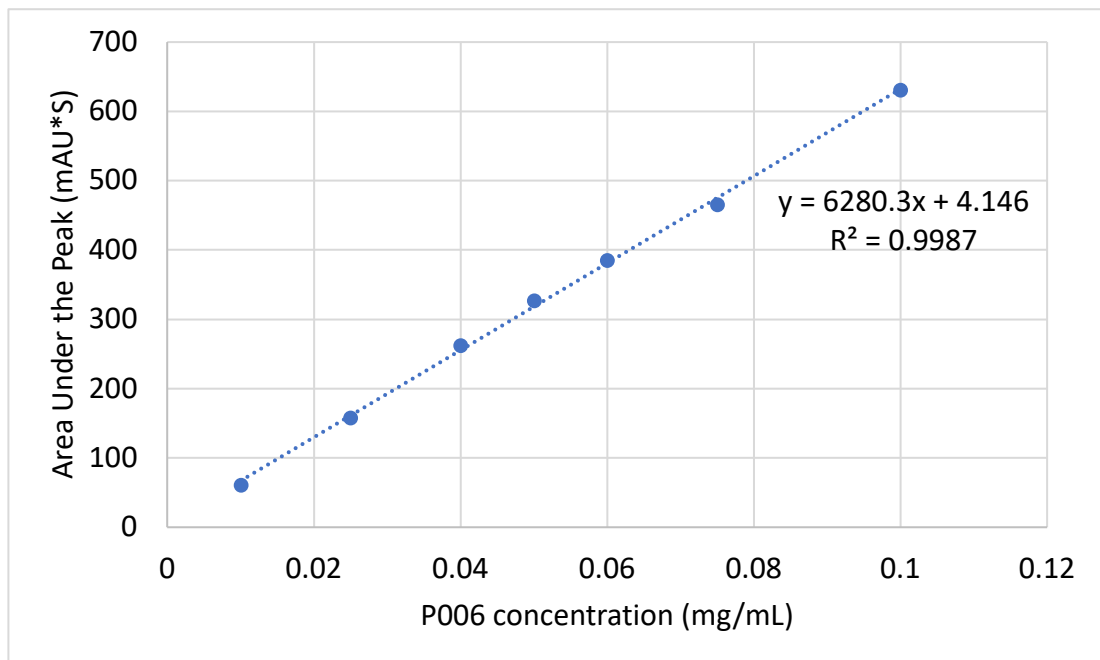


Figure S 50. P006 calibration curve in serum after protein precipitation with TCA.

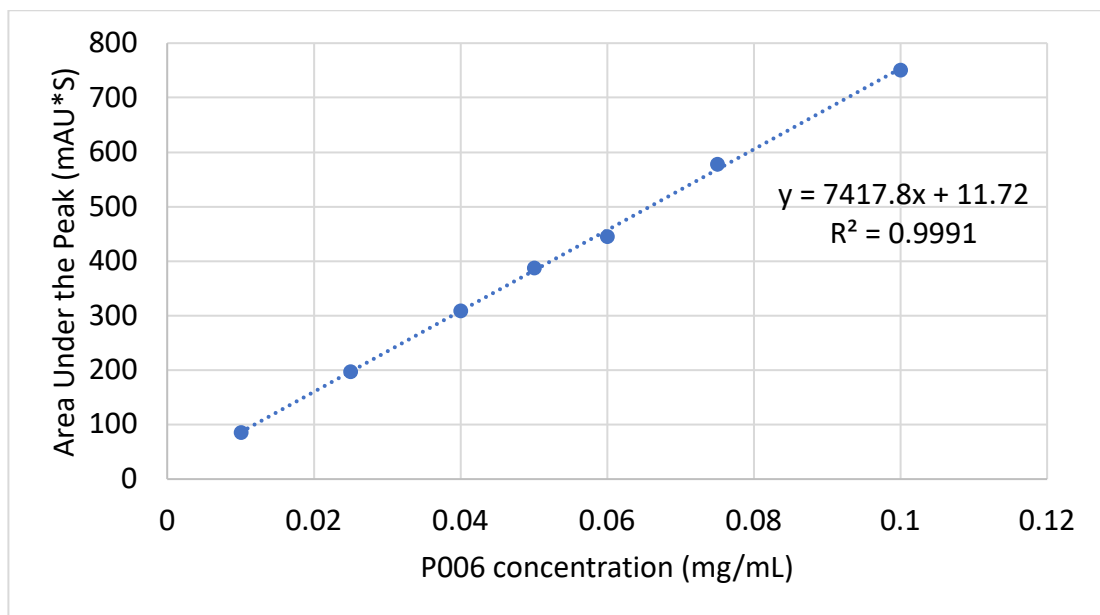


Figure S 51. P006 calibration curve in serum after protein precipitation with MeOH.

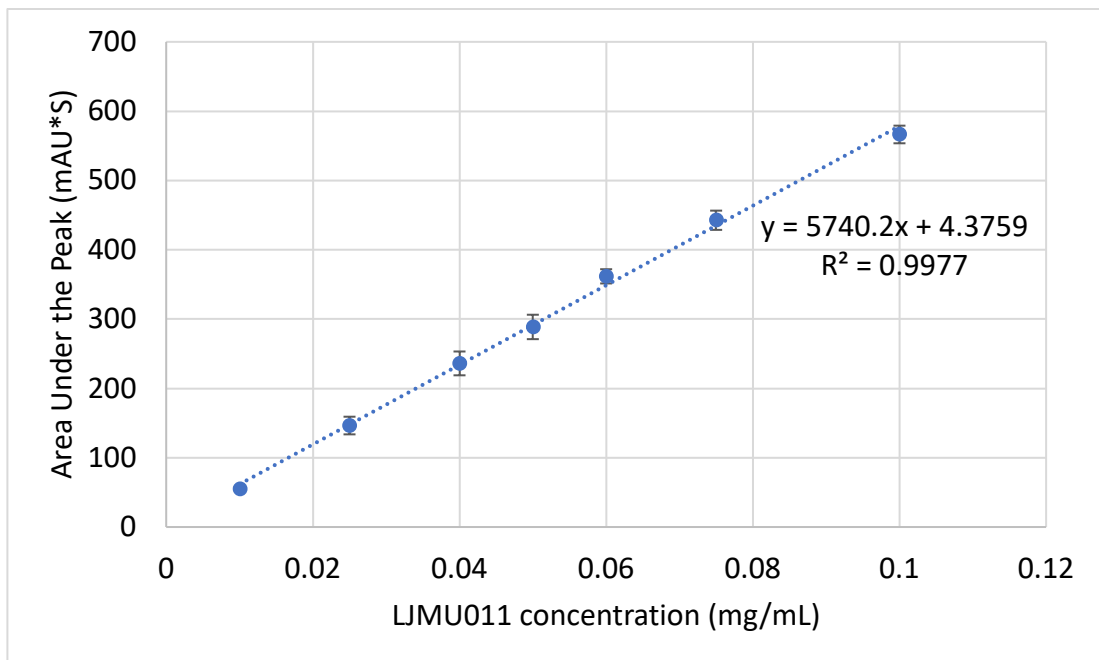


Figure S 52. LJM011 calibration curve in serum after protein precipitation with TCA.
Experiment performed in duplicate.

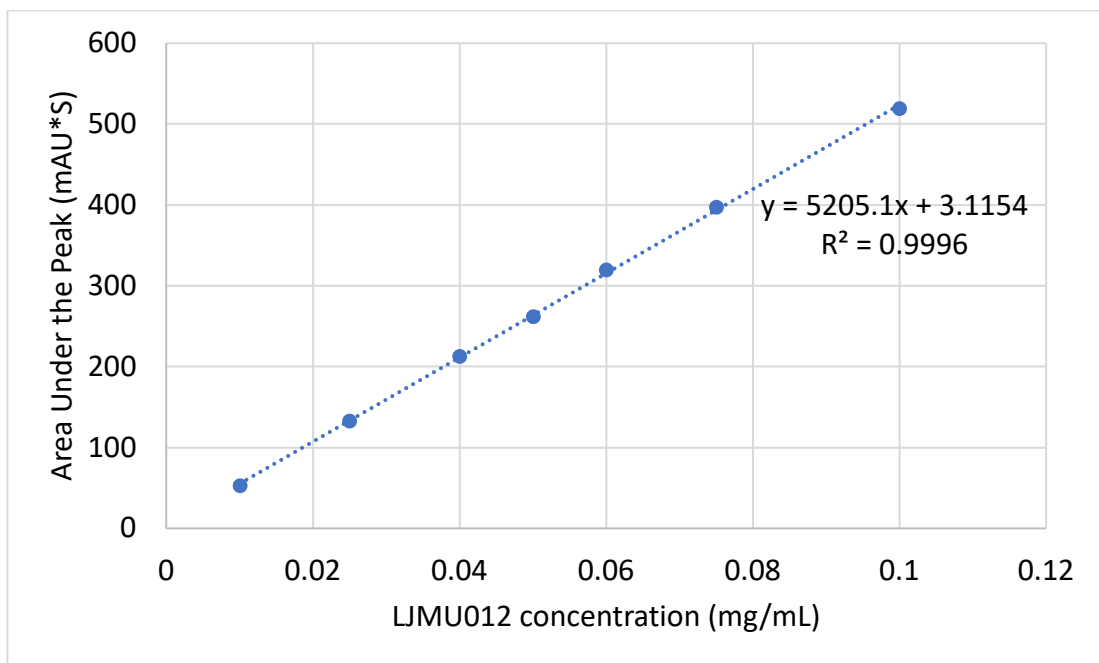


Figure S 53. LJM012 calibration curve in serum after protein precipitation with TCA.
Experiment performed in duplicate.

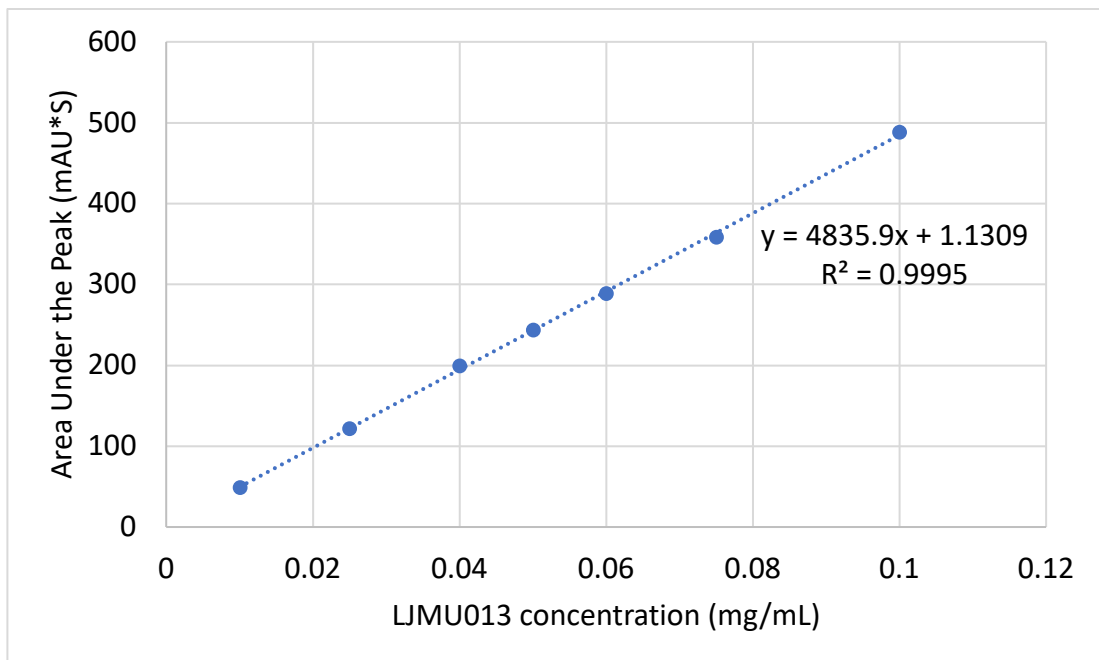


Figure S 54. LJM013 calibration curve in serum after protein precipitation with TCA.

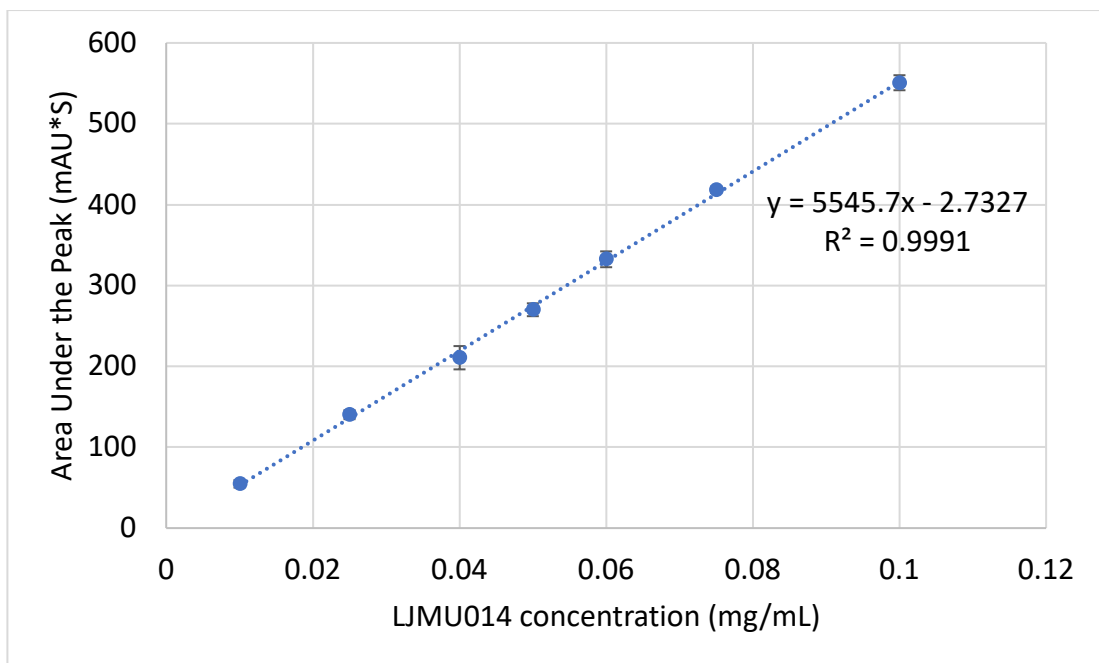


Figure S 55. LJM014 calibration curve in serum after protein precipitation with TCA.
Experiment performed in duplicate.

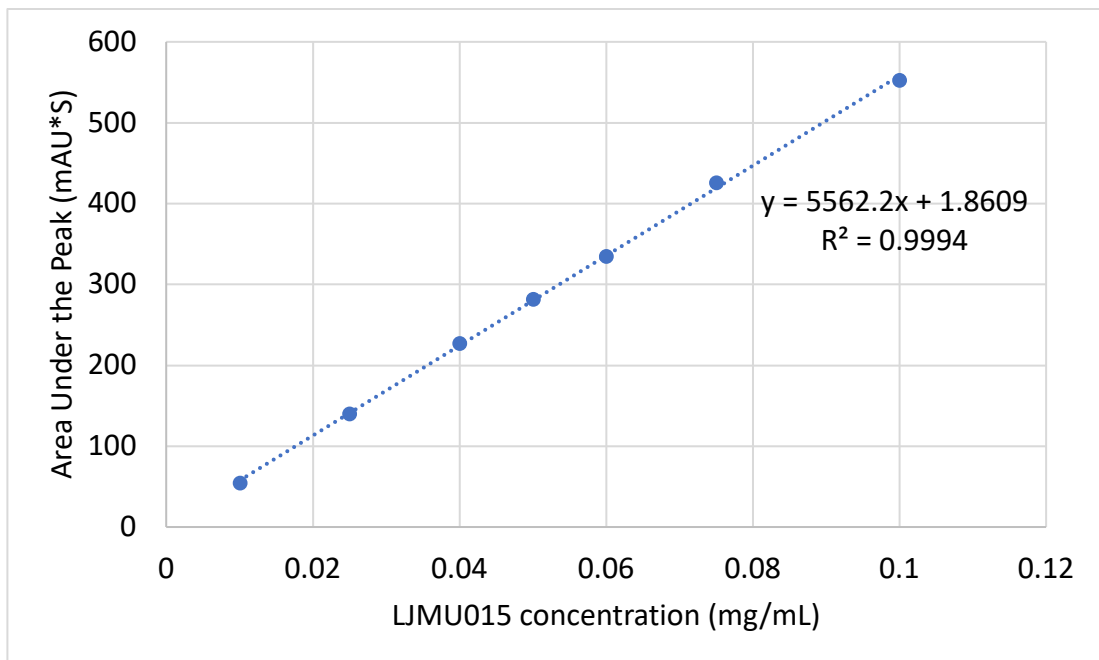


Figure S 56. LJM015 calibration curve in serum after protein precipitation with TCA.
Experiment performed in duplicate.

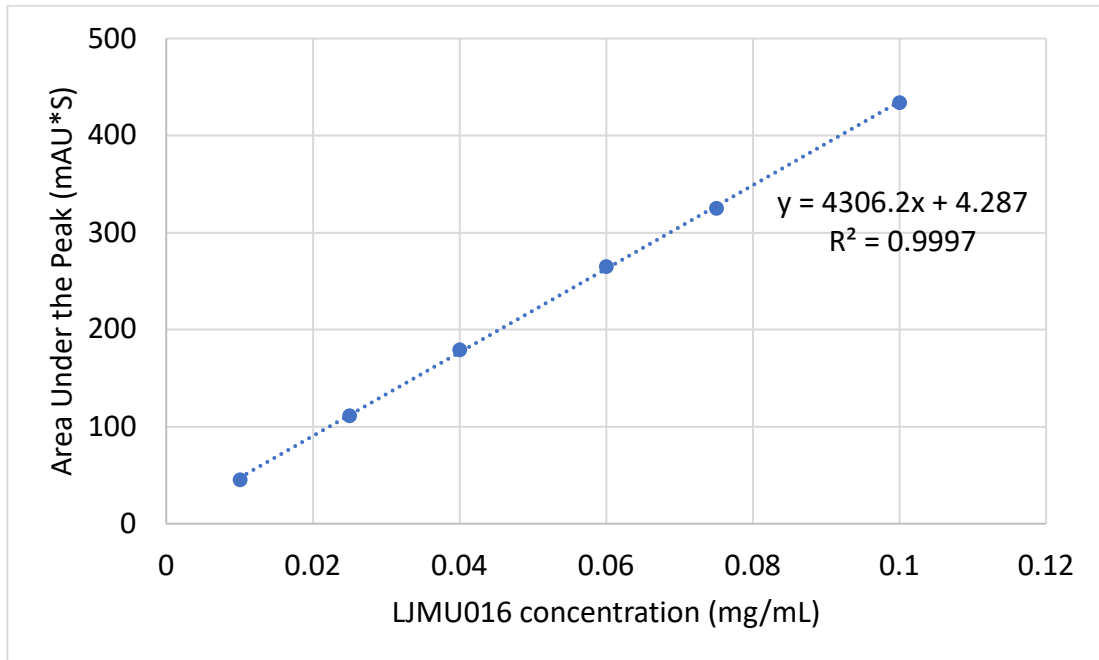


Figure S 57. LJM016 calibration curve in serum after protein precipitation with TCA.

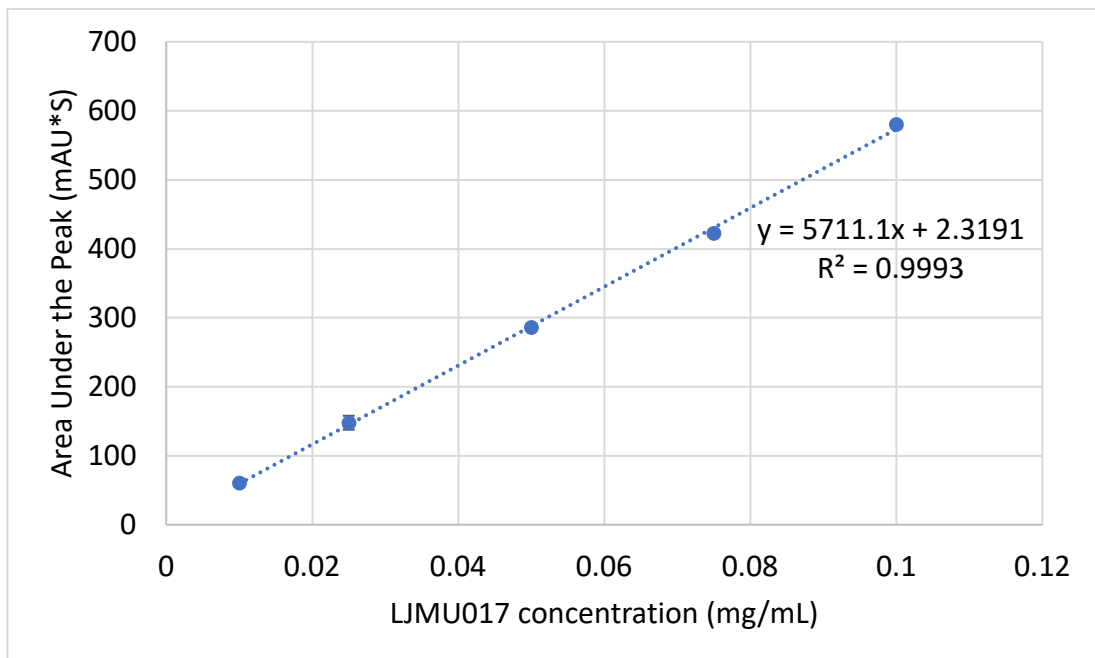


Figure S 58. LJM017 calibration curve in H_2O .

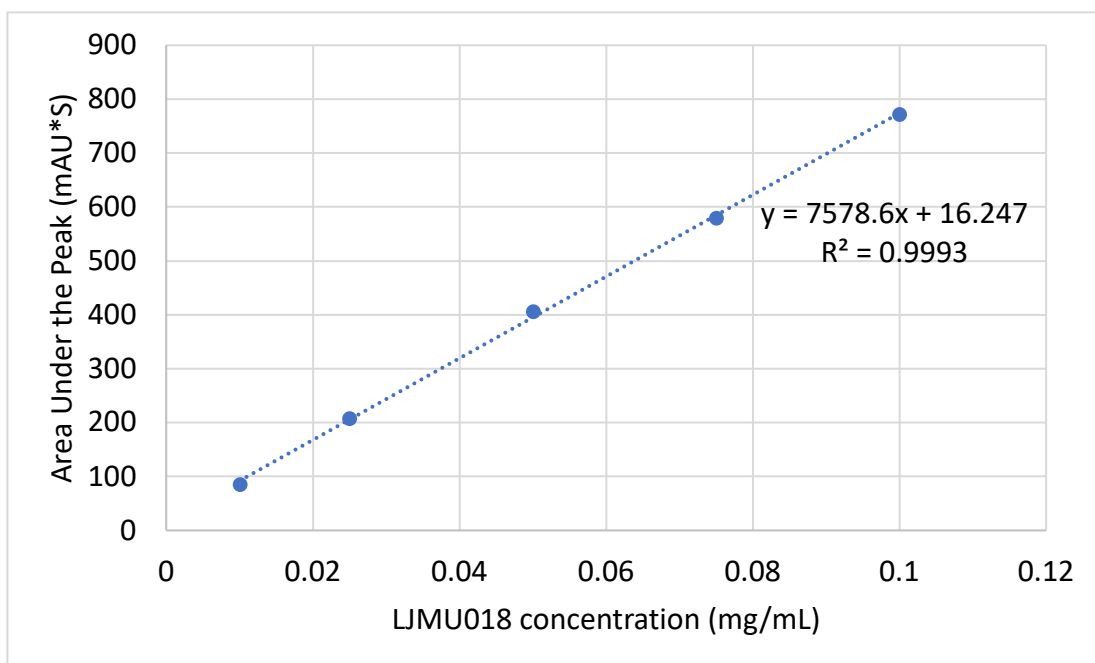


Figure S 59. LJM018 calibration curve in H_2O .

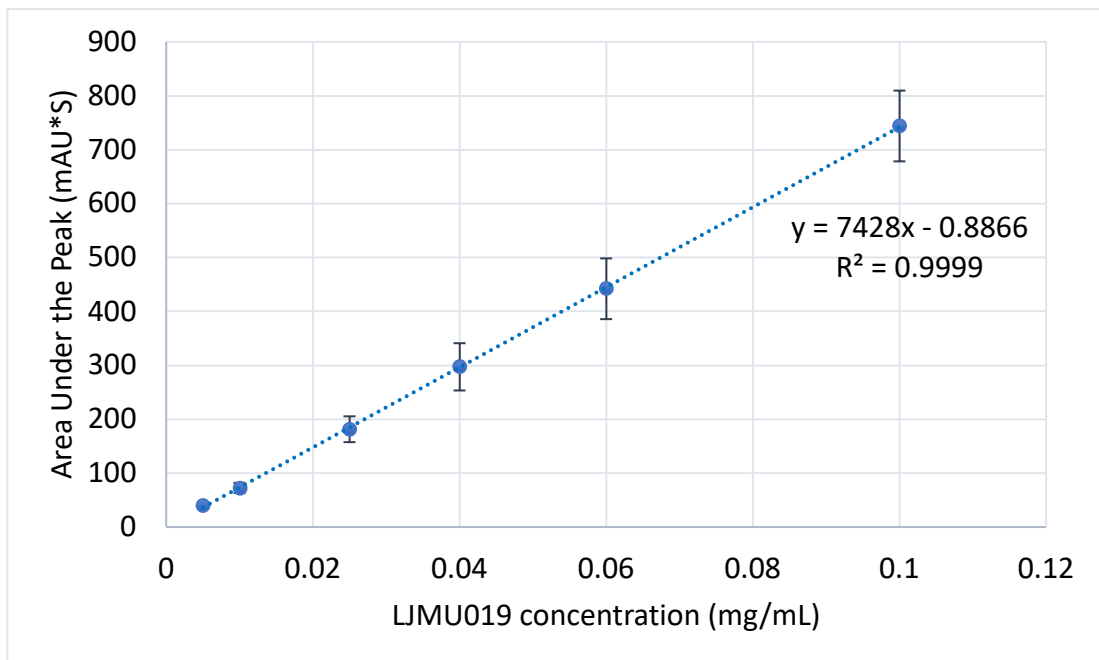


Figure S 60. LJM019 calibration curve in serum after protein precipitation with TCA.
Experiment performed in triplicate.

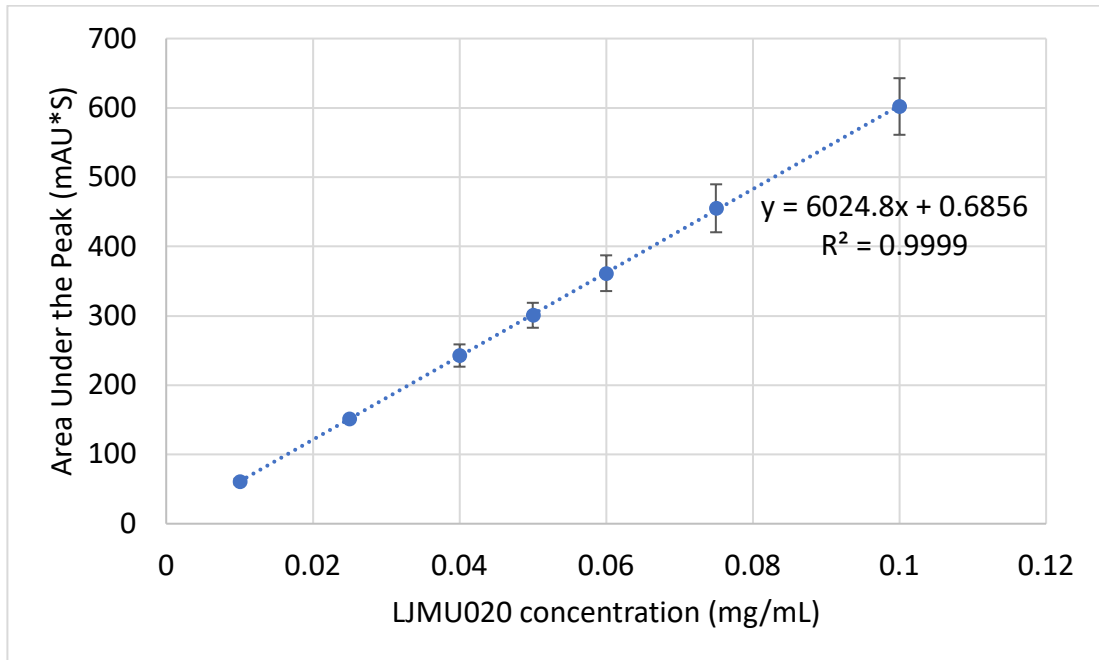


Figure S 61. LJM020 calibration curve in serum after protein precipitation with TCA.
Experiment performed in triplicate.

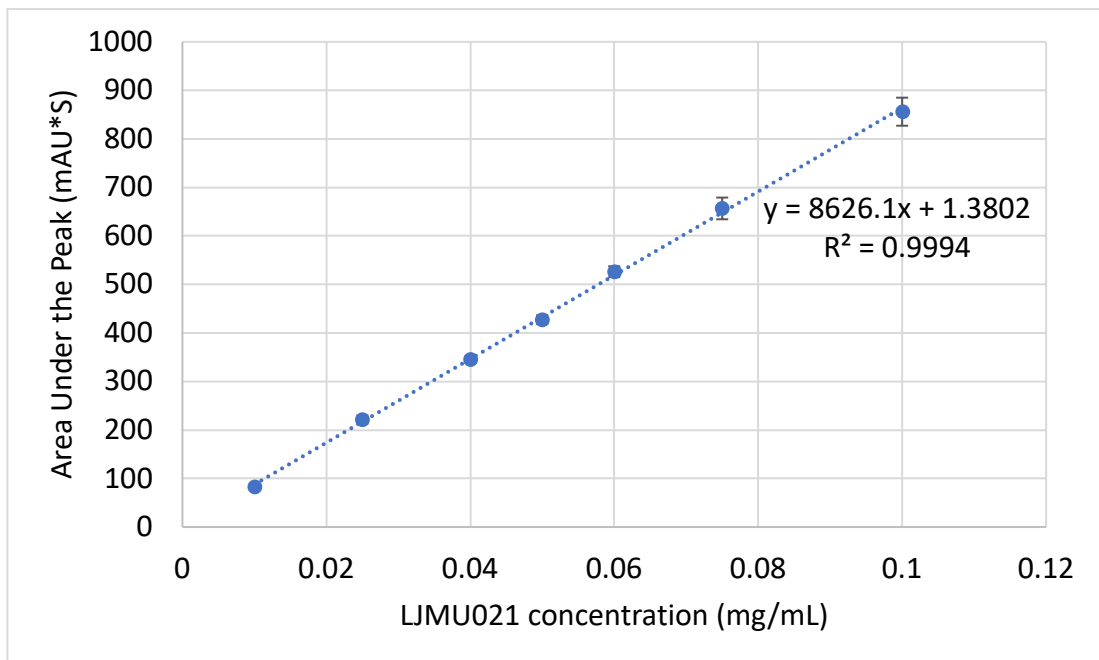


Figure S 62. LJM021 calibration curve in serum after protein precipitation with TCA.
Experiment performed in duplicate.

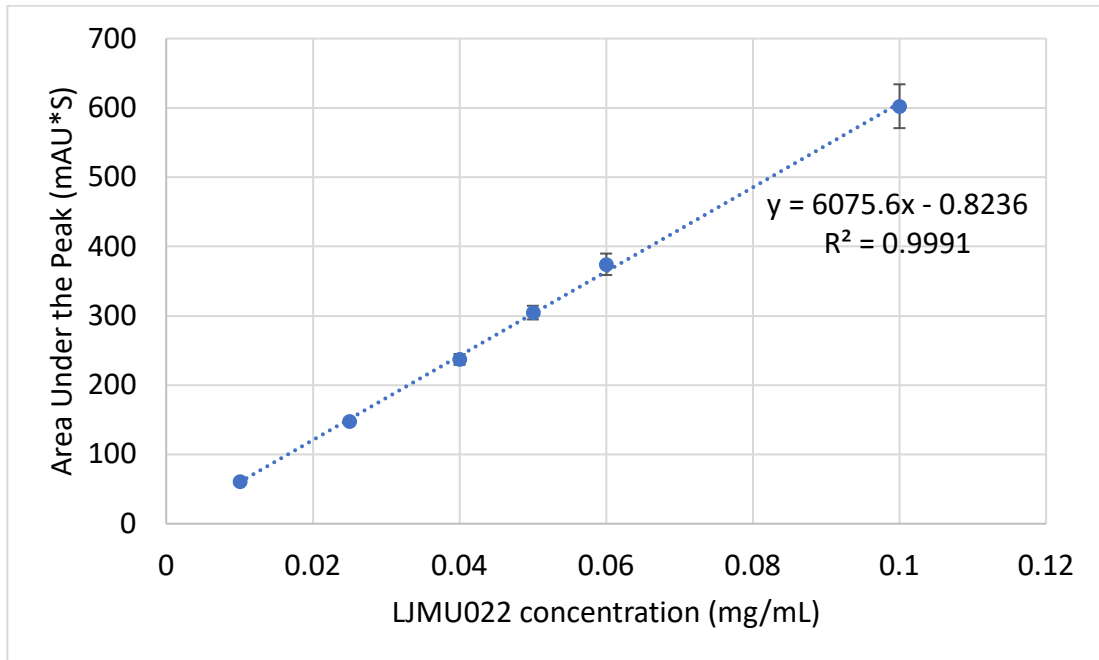


Figure S 63. LJM022 calibration curve in serum after protein precipitation with TCA.
Experiment performed in duplicate.

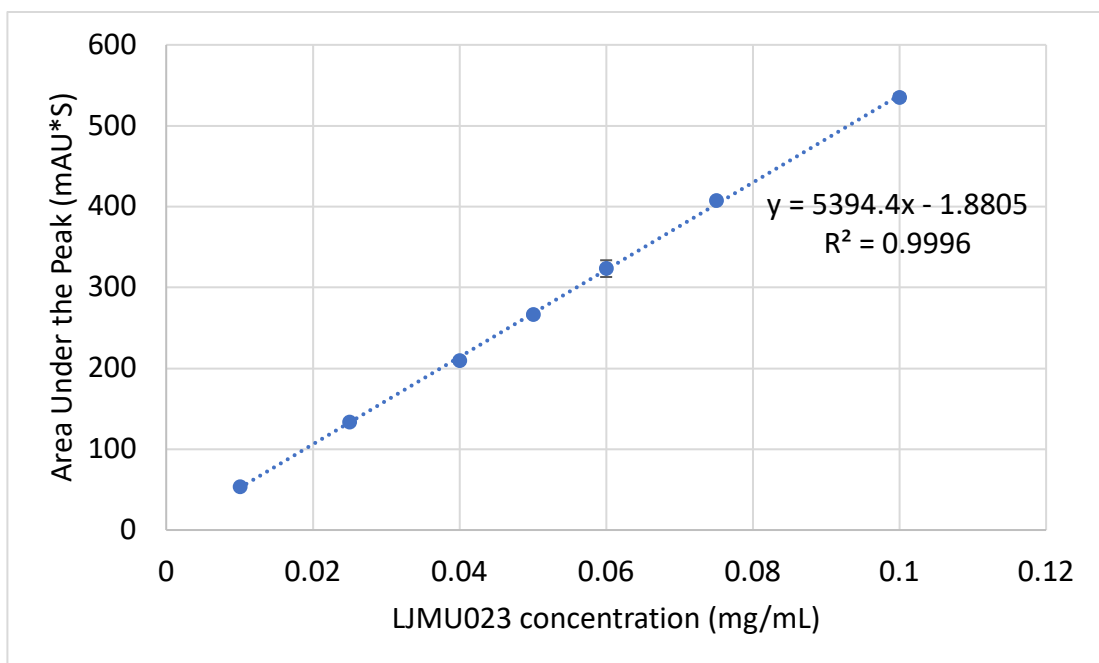


Figure S 64. LJM023 calibration curve in serum after protein precipitation with TCA.
Experiment performed in duplicate.

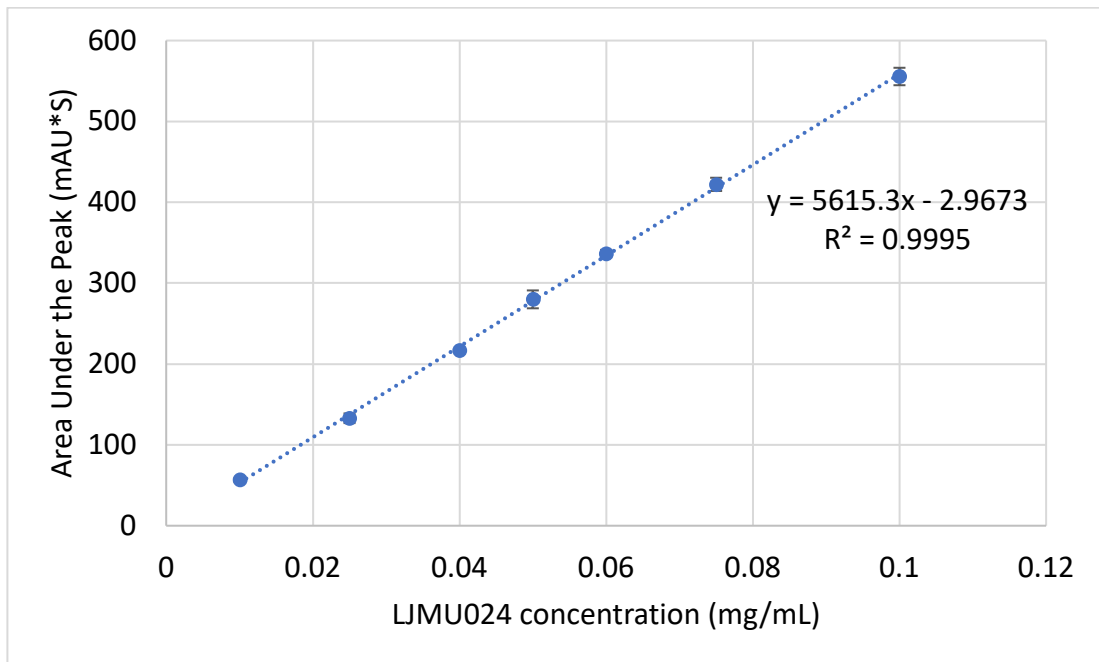


Figure S 65. LJM024 calibration curve in serum after protein precipitation with TCA.
Experiment performed in duplicate.

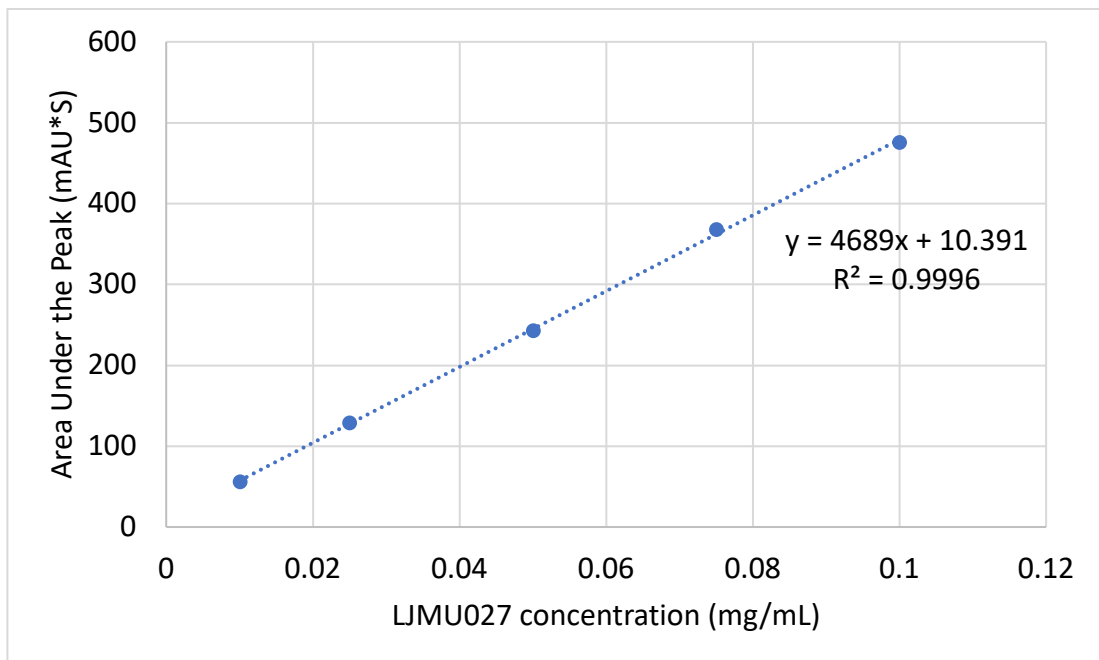


Figure S 66. LJM027 calibration curve in H_2O .

7.2.2 Stability in human serum – full dataset

Table S.2. Stability in human serum. Full dataset expressed as percentage of intact peptide compared to 0 min sample (taken as 100%).

	Detected intact peptide (%)			
	15 min	30 min	45 min	60 min
P006	61.02 ± 1.43	32.55 ± 2.39	14.95 ± 1.72	4.11 ± 0.55
LJMU011	69.89 ± 1.39	33.93 ± 2.72	14.56 ± 2.27	5.16 ± 1.02
LJMU012	62.92 ± 3.61	30.94 ± 2.63	11.98 ± 1.90	2.82 ± 1.24
LJMU013	63.57 ± 5.16	33.95 ± 4.20	19.36 ± 3.87	3.57 ± 3.34
LJMU014	60.79 ± 3.85	29.99 ± 3.04	15.25 ± 1.44	9.45 ± 1.79
LJMU015	55.68 ± 3.50	34.60 ± 2.60	18.18 ± 3.94	7.05 ± 0.62
LJMU016	69.81 ± 4.13	48.34 ± 3.14	36.48 ± 2.00	32.78 ± 0.72
LJMU017	96.60 ± 3.70	90.40 ± 5.10	90.10 ± 6.80	85.50 ± 4.40
LJMU018	89.95 ± 5.47	87.22 ± 2.79	79.51 ± 8.57	74.95 ± 2.04
LJMU019	64.24 ± 1.04	35.85 ± 1.16	17.06 ± 5.88	4.44 ± 1.68
LJMU020	61.82 ± 5.29	30.52 ± 7.27	16.18 ± 3.52	4.05 ± 1.68
LJMU021	64.20 ± 1.50	35.56 ± 0.31	16.52 ± 1.50	6.69 ± 1.24
LJMU022	68.45 ± 6.22	45.63 ± 3.33	24.50 ± 0.88	13.01 ± 0.32
LJMU023	64.18 ± 2.79	38.37 ± 2.53	21.20 ± 4.61	10.38 ± 3.47
LJMU024	70.73 ± 2.79	52.84 ± 1.70	42.77 ± 1.73	38.04 ± 2.21
LJMU027	101.09 ± 0.68	100.33 ± 0.78	100.50 ± 0.76	94.33 ± 3.27

7.2.3 First-order reaction plot $\ln[\text{peptide}]$ versus time

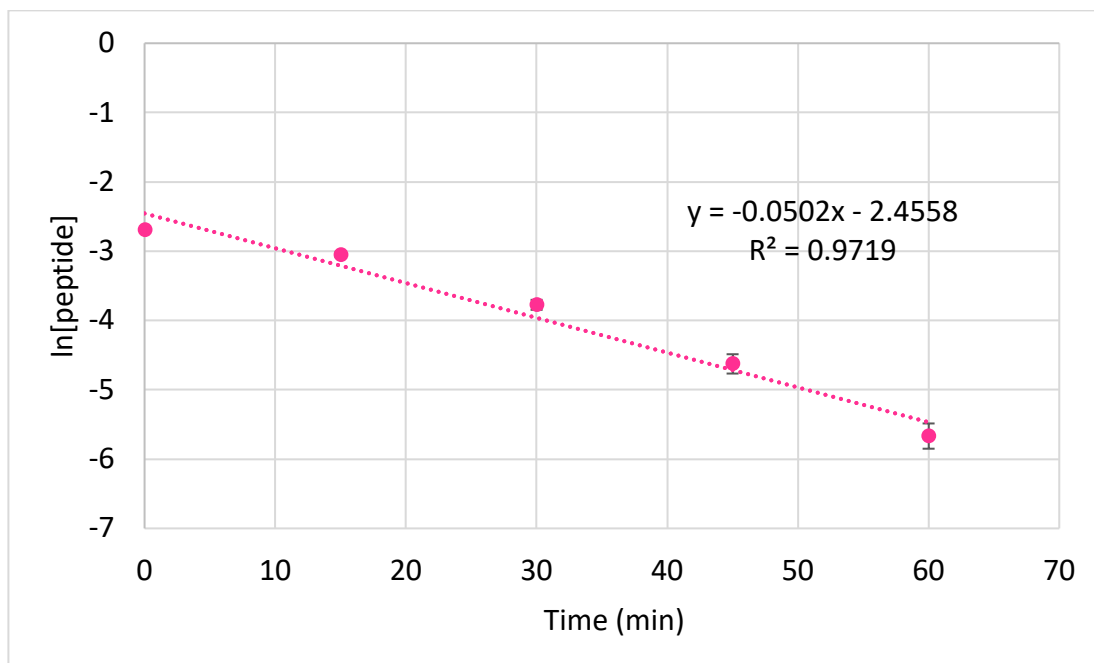


Figure S 67. First-order reaction plot $\ln[\text{LJMU011}]$ versus time (min) to determine rate constant.

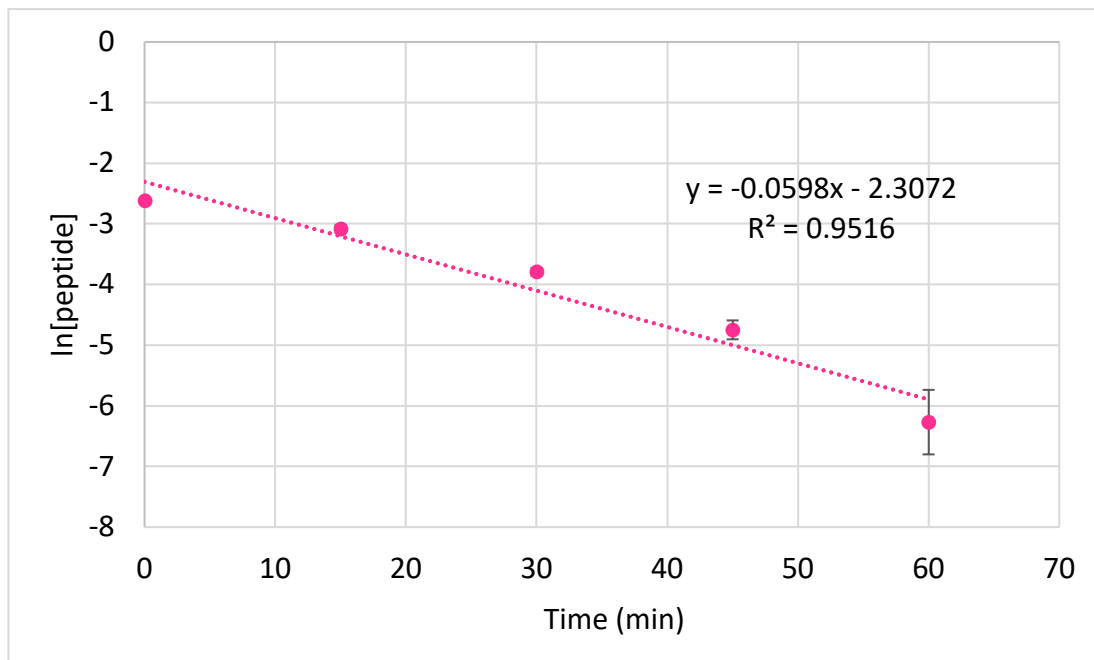


Figure S 68. First-order reaction plot $\ln[\text{LJMU012}]$ versus time (min) to determine rate constant.

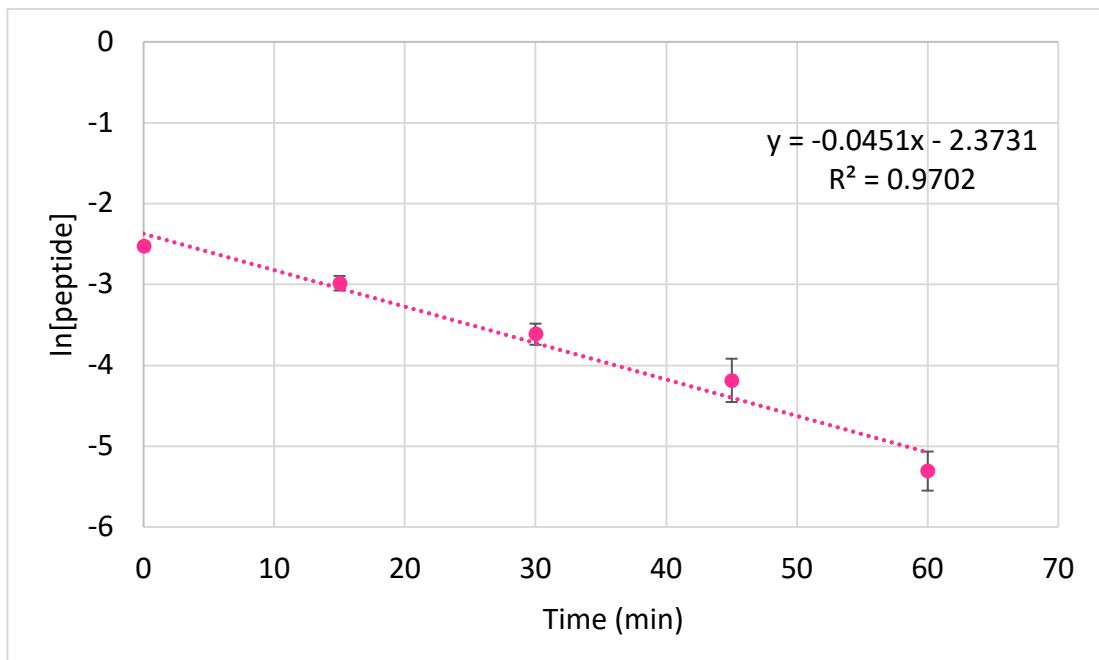


Figure S 69. First-order reaction plot $\ln[\text{LJM}013]$ versus time (min) to determine rate constant.

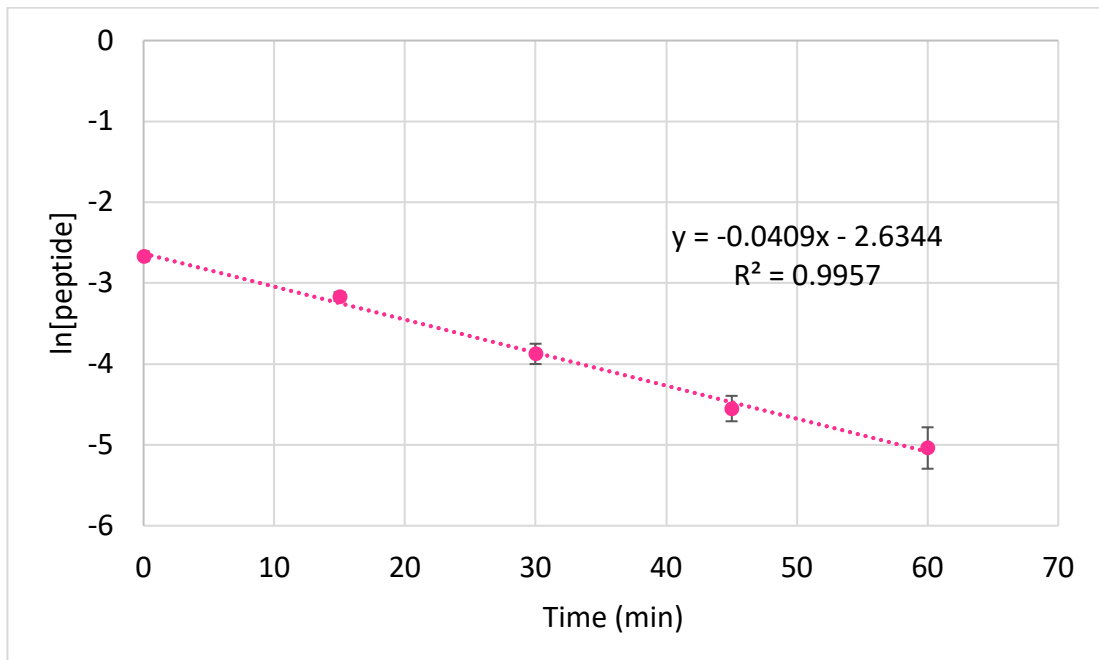


Figure S 70. First-order reaction plot $\ln[\text{LJM}014]$ versus time (min) to determine rate constant.

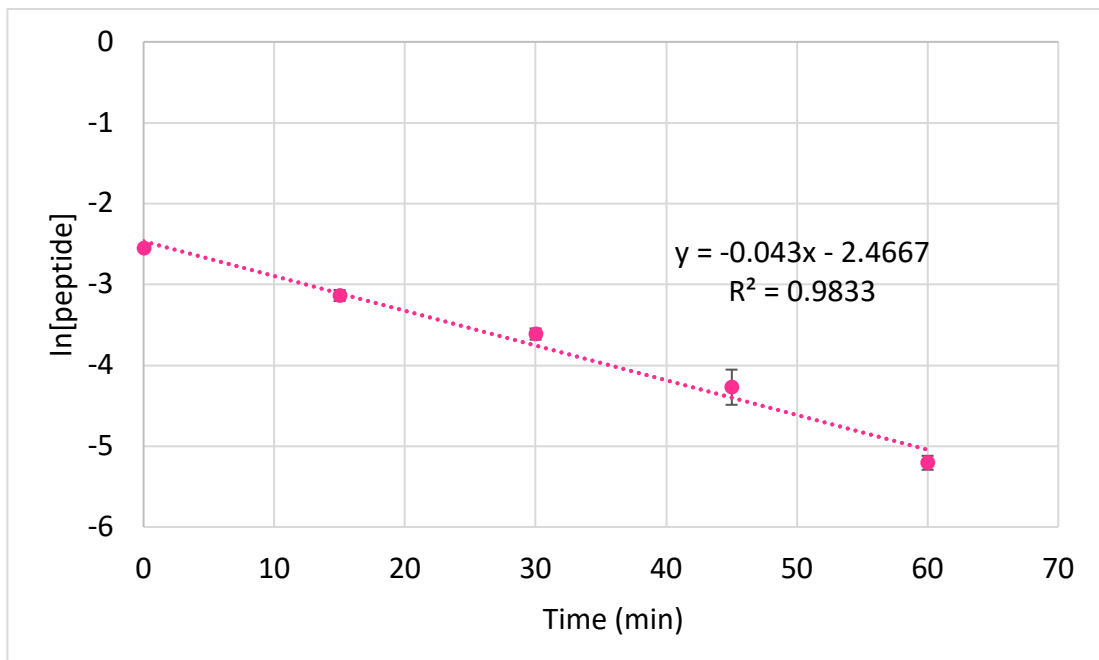


Figure S 71. First-order reaction plot $\ln[\text{LJM}015]$ versus time (min) to determine rate constant.

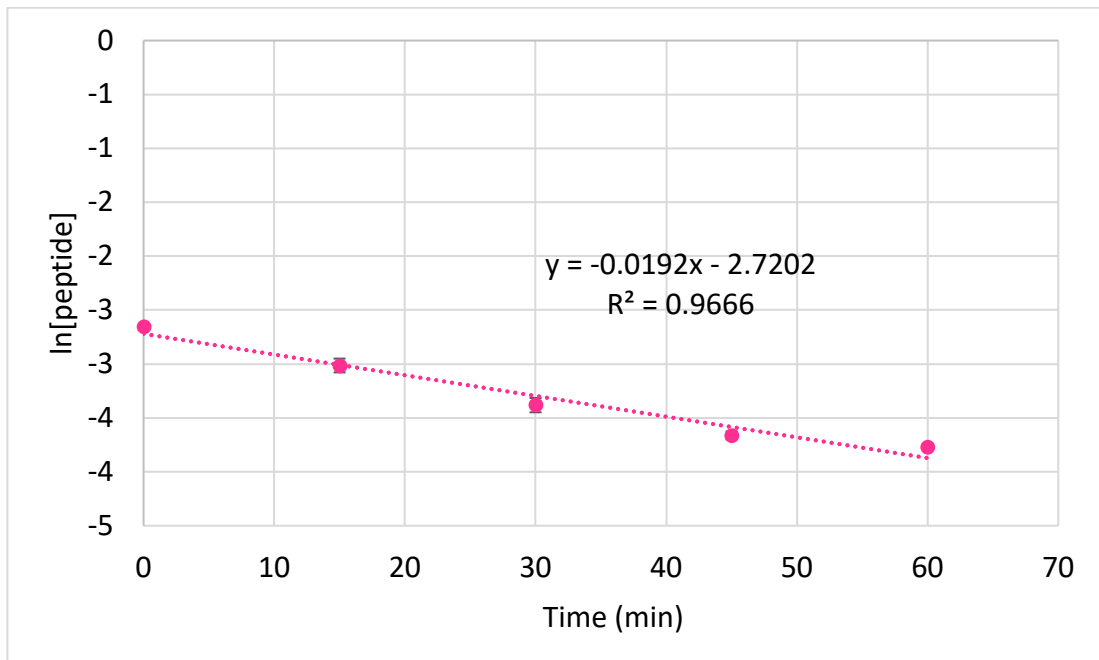


Figure S 72. First-order reaction plot $\ln[\text{LJM}016]$ versus time (min) to determine rate constant.

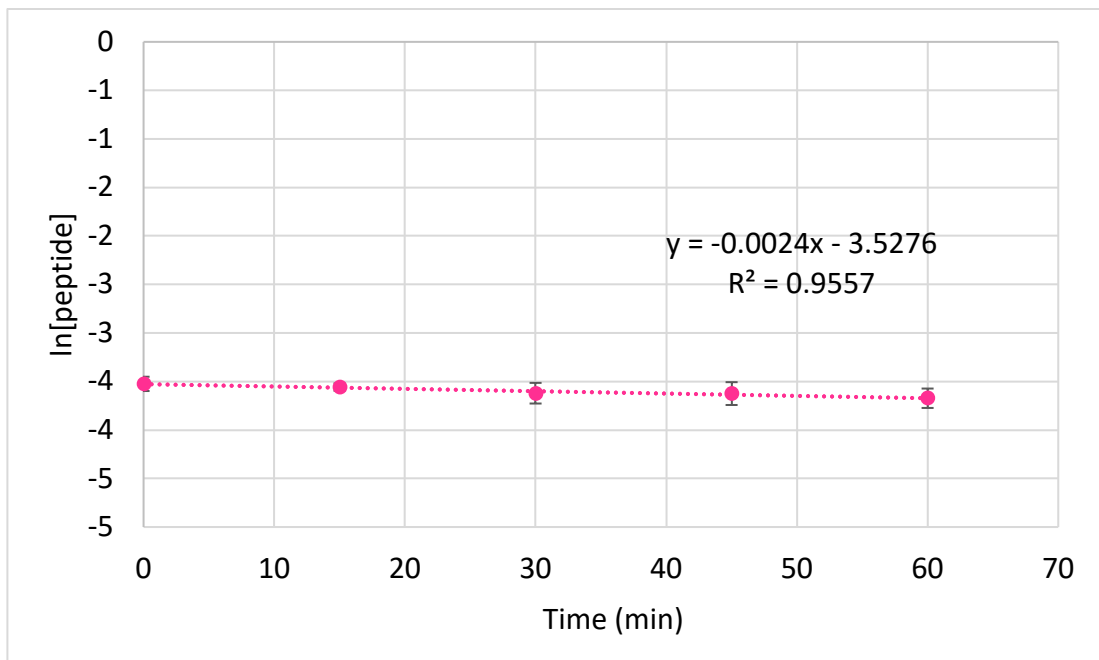


Figure S 73. First-order reaction plot $\ln[\text{LJM}017]$ versus time (min) to determine rate constant.

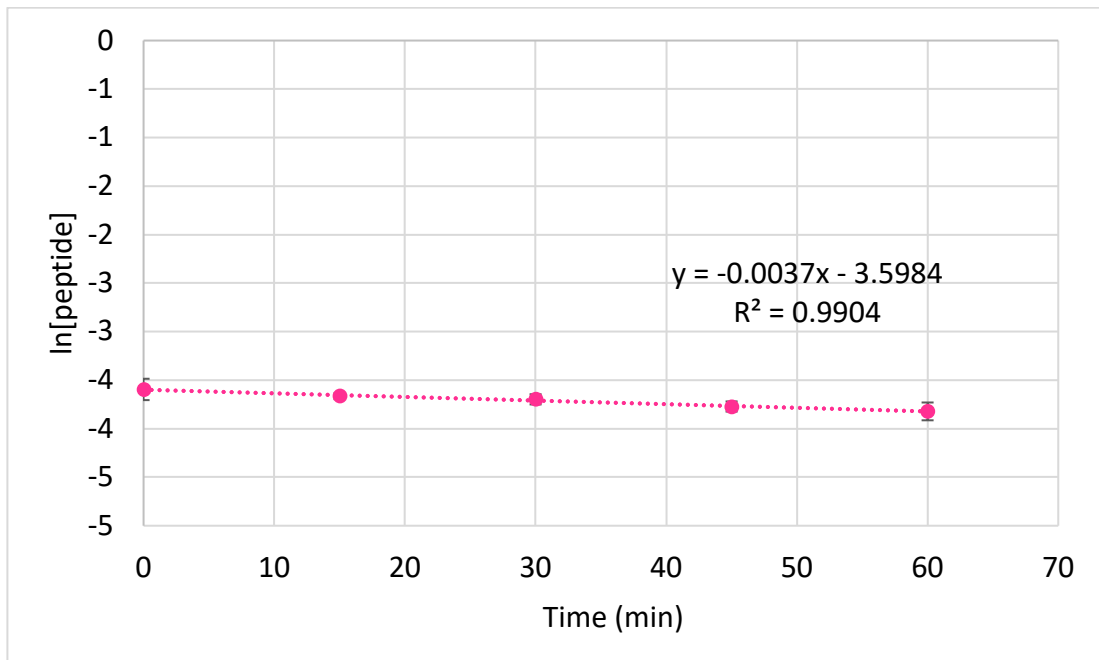


Figure S 74. First-order reaction plot $\ln[\text{LJM}018]$ versus time (min) to determine rate constant.

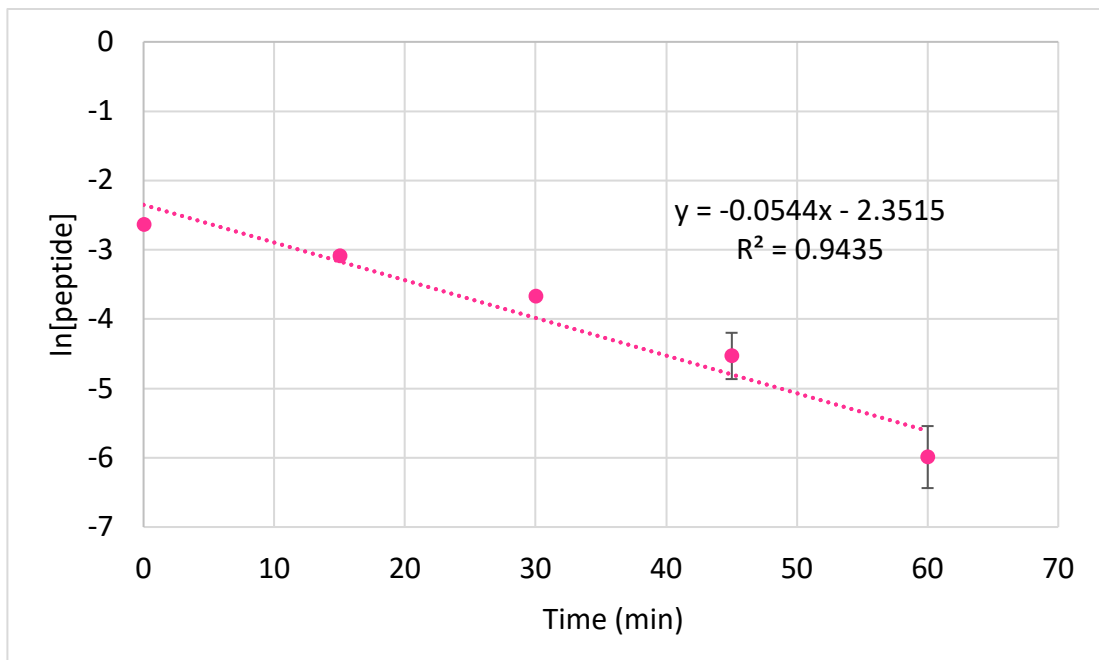


Figure S 75. First-order reaction plot $\ln[\text{LJM}019]$ versus time (min) to determine rate constant.

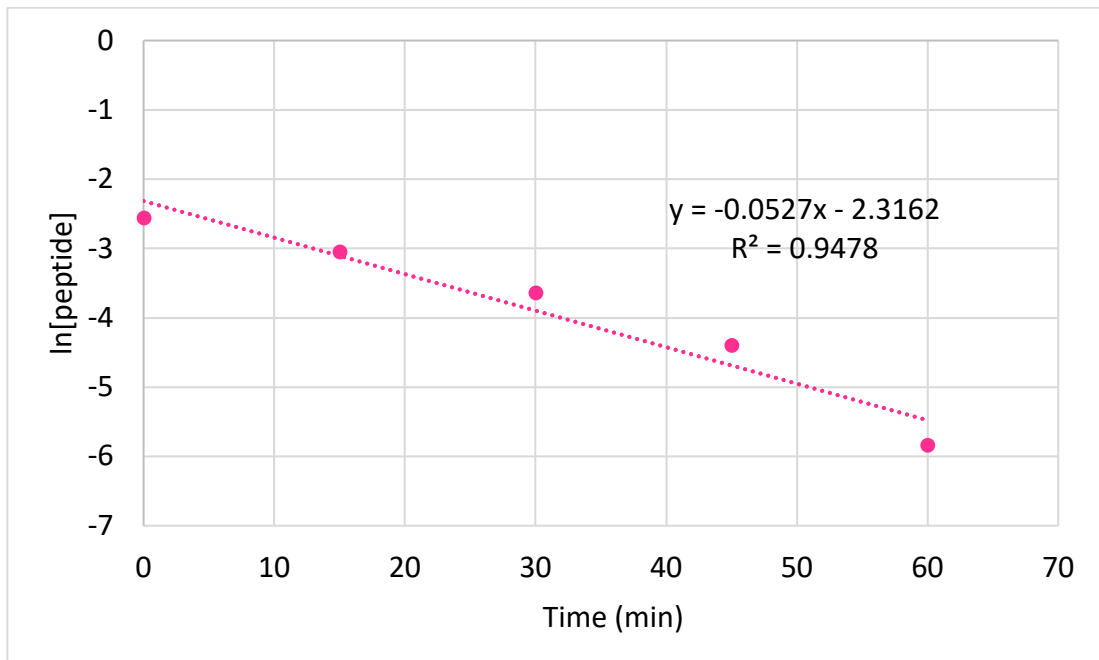


Figure S 76. First-order reaction plot $\ln[\text{LJM}020]$ versus time (min) to determine rate constant.

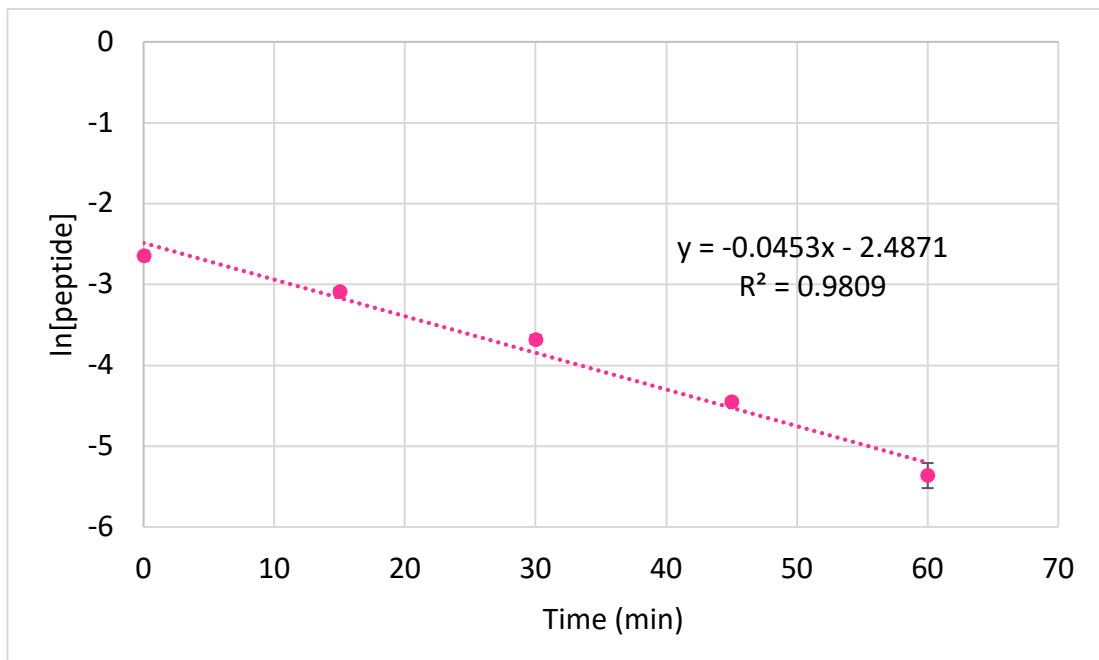


Figure S 77. First-order reaction plot $\ln[\text{LJM}021]$ versus time (min) to determine rate constant.

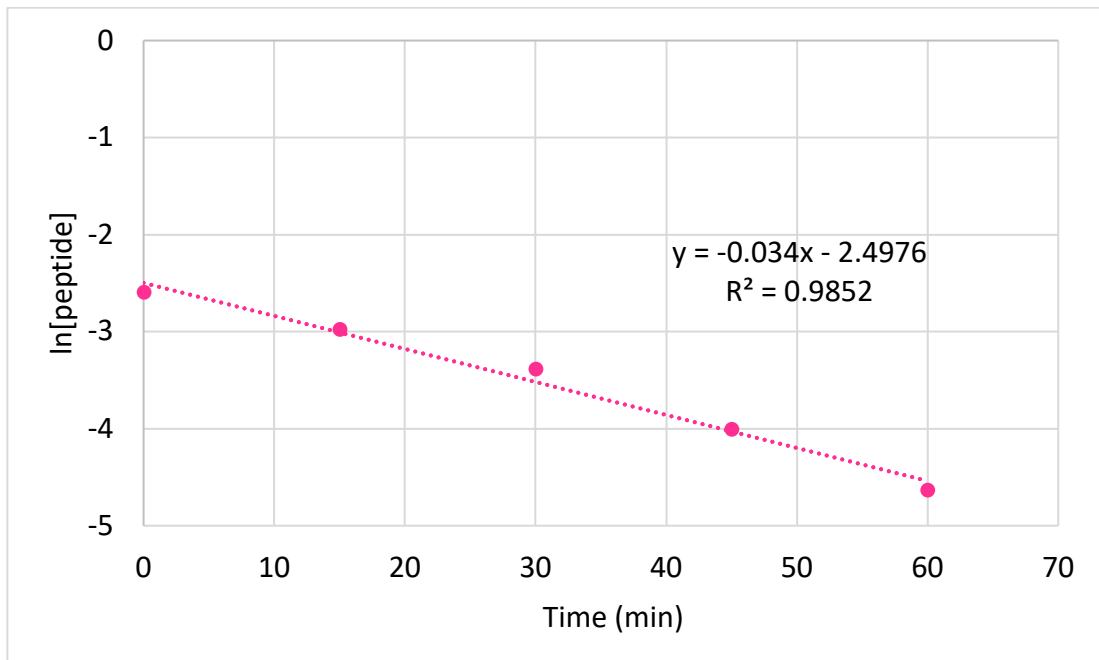


Figure S 78. First-order reaction plot $\ln[\text{LJM}022]$ versus time (min) to determine rate constant.

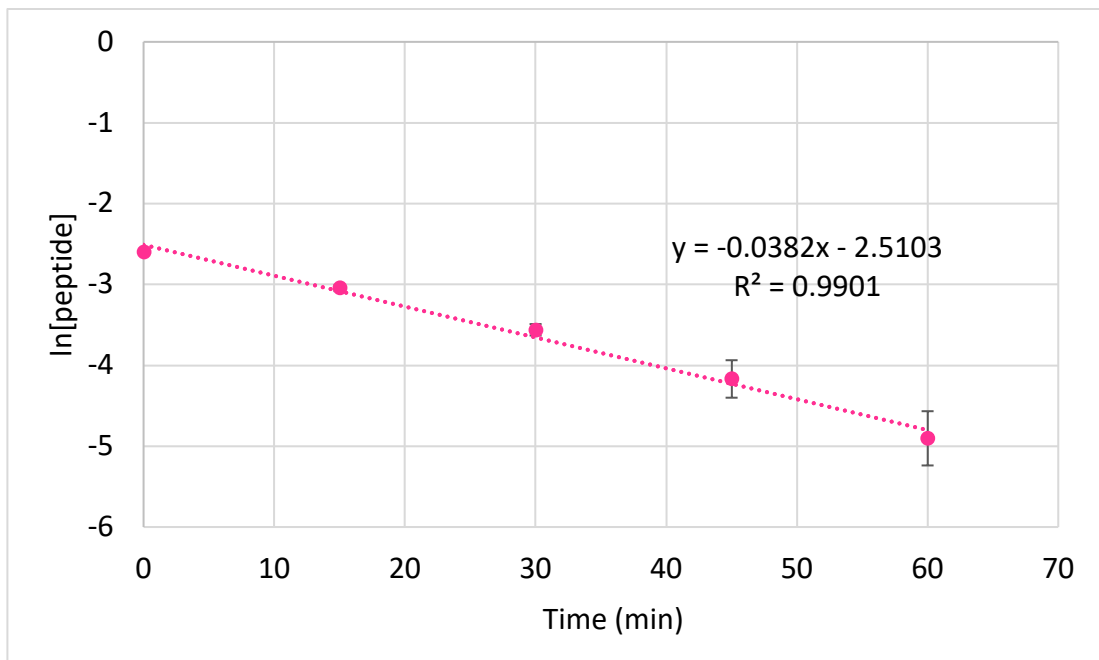


Figure S 79. First-order reaction plot $\ln[\text{LJM}023]$ versus time (min) to determine rate constant.

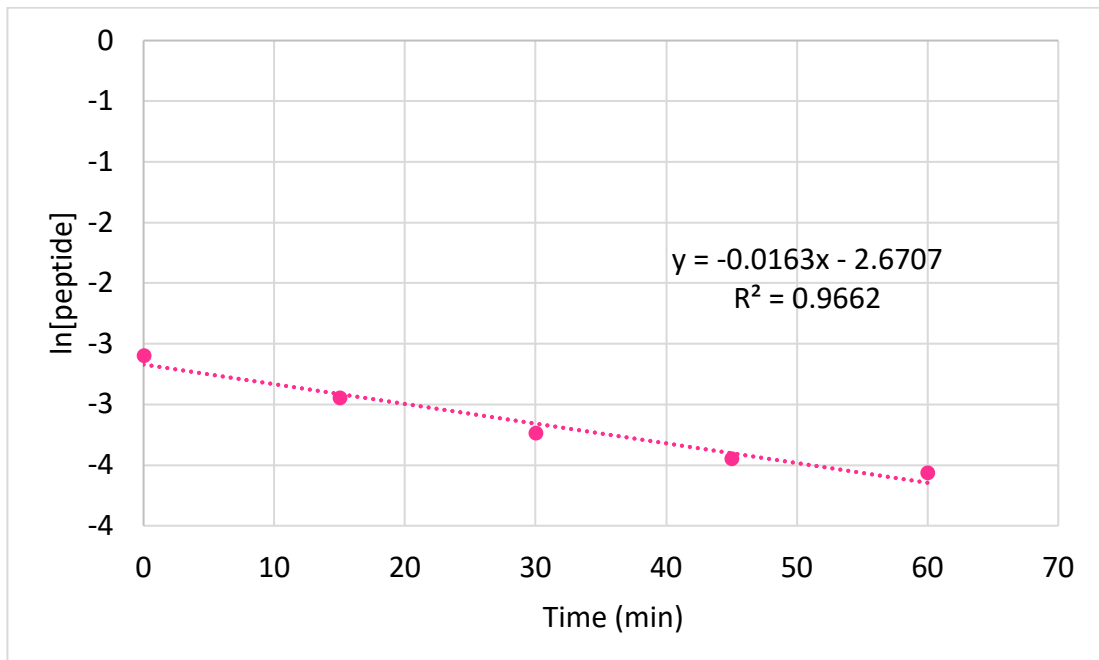


Figure S 80. First-order reaction plot $\ln[\text{LJM}024]$ versus time (min) to determine rate constant

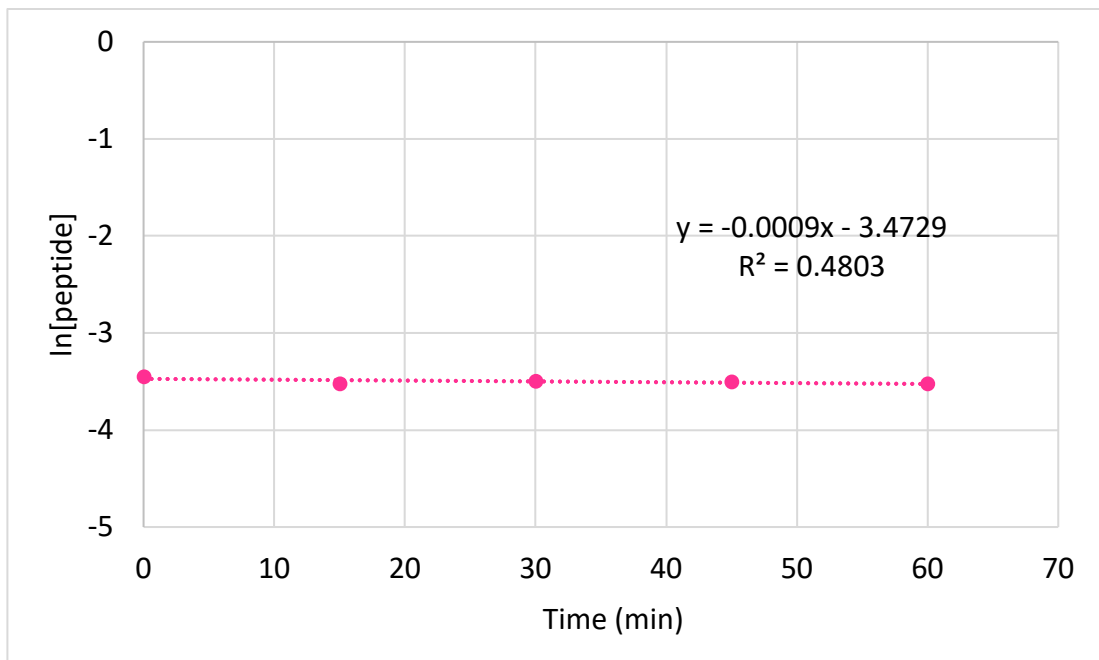


Figure S 81. First-order reaction plot $\ln[\text{LJMU027}]$ versus time (min) to determine rate constant.

7.2.4 Metabolite ID – stability study in human serum

7.2.4.1 P006 – parent and metabolite identification after 60 min incubation

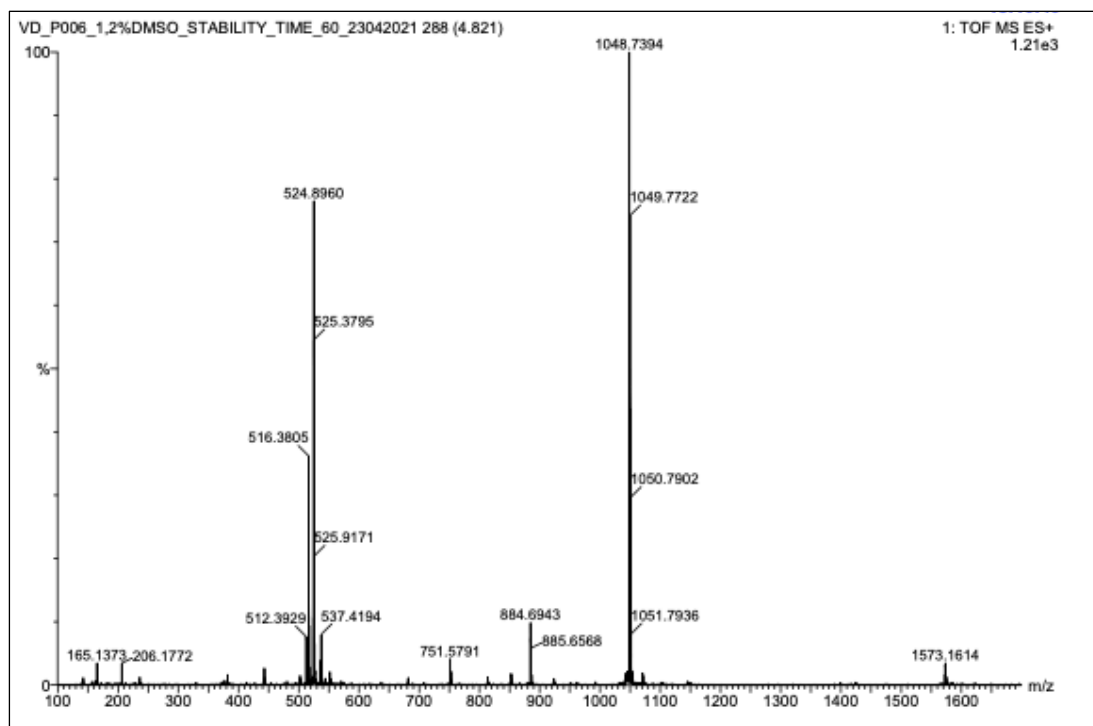


Figure S 82. LC-MS spectrum of parent peptide detected after 60 min incubation in diluted human serum.

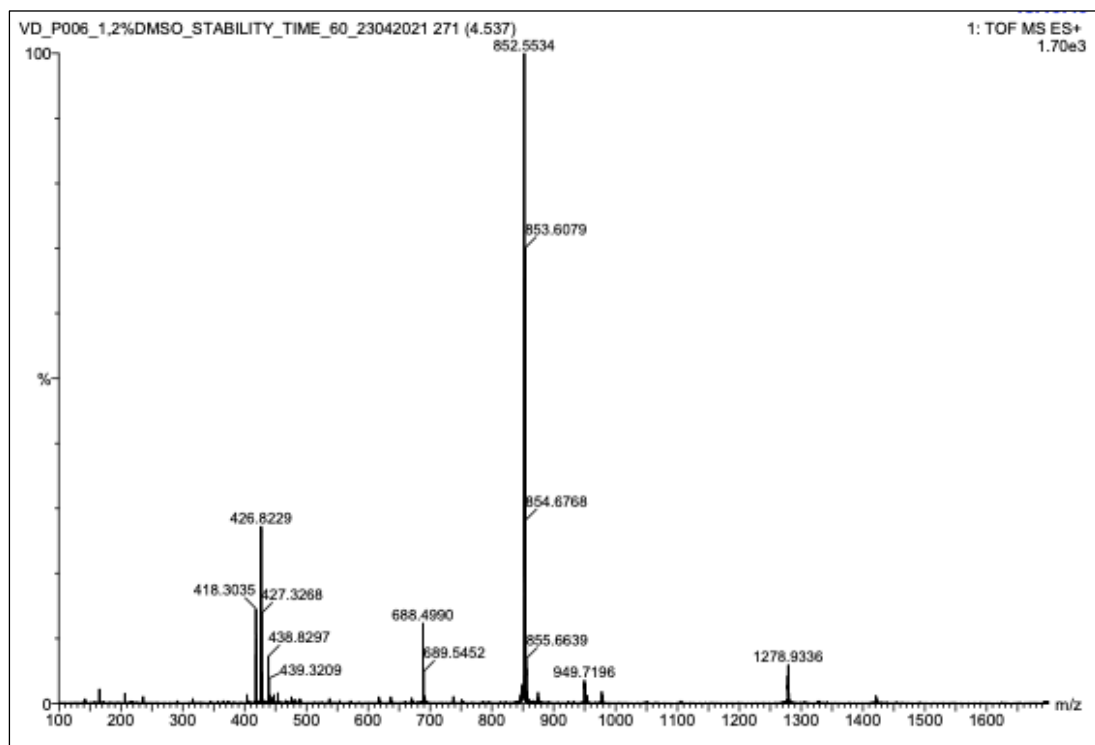


Figure S 83. LC-MS spectrum of main metabolite detected after 60 min incubation in human serum.

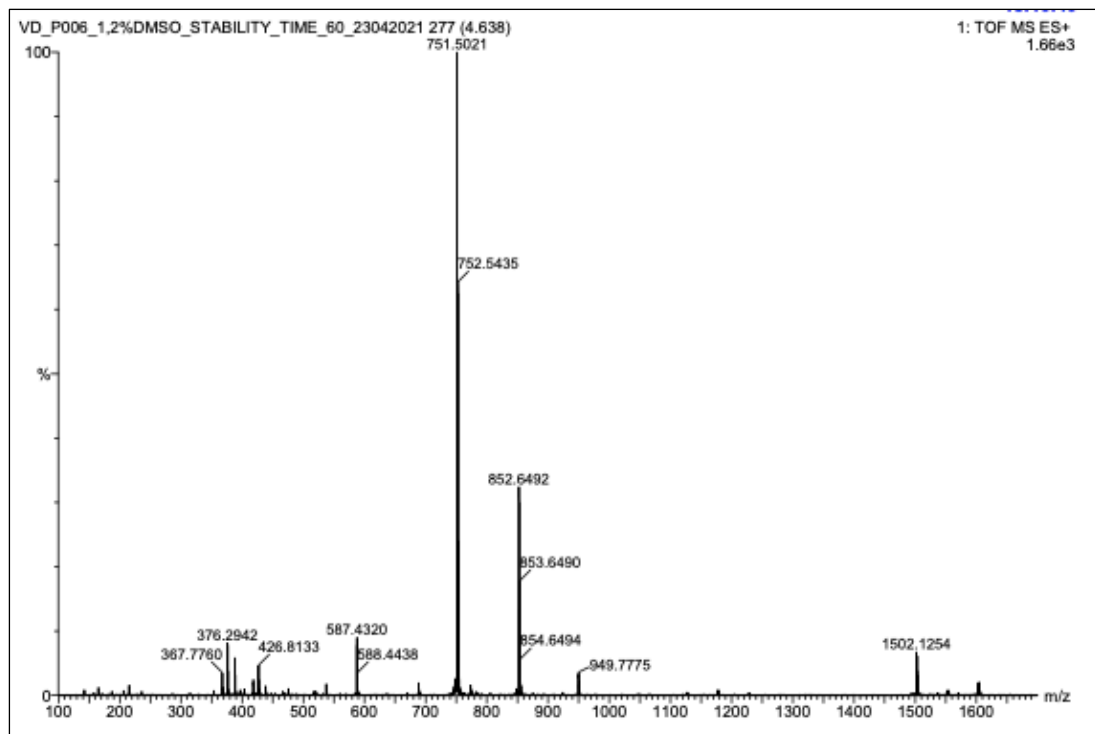


Figure S 84. LC-MS spectrum of minor metabolite detected after 60 min incubation in human serum.

7.2.4.2 LJMU011 – parent and metabolite identification after 60 min incubation

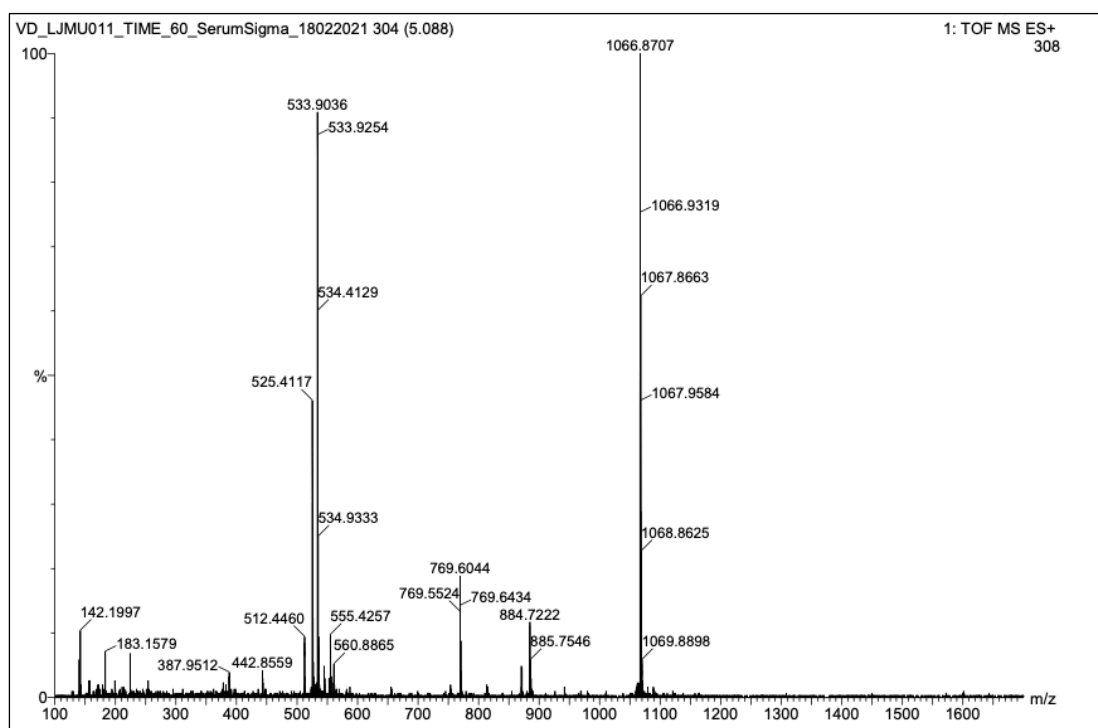


Figure S 85. LC-MS spectrum of parent peptide detected after 60 min incubation in diluted human serum.

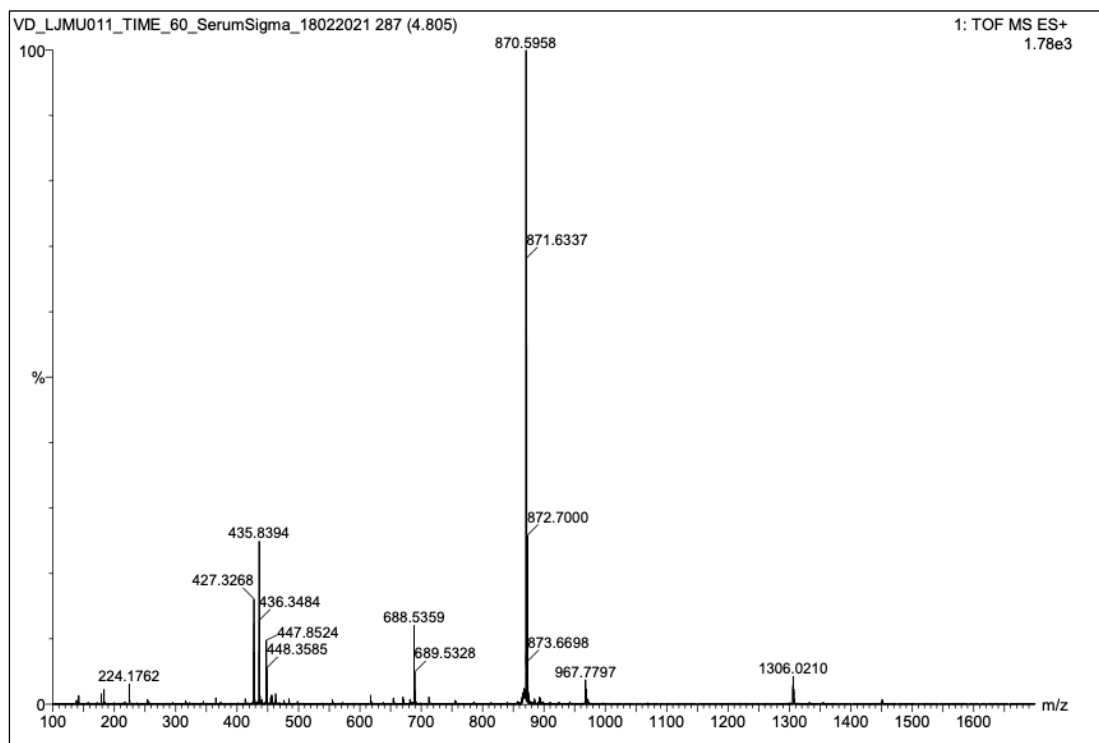


Figure S 86. LC-MS spectrum of main metabolite detected after 60 min incubation in human serum.

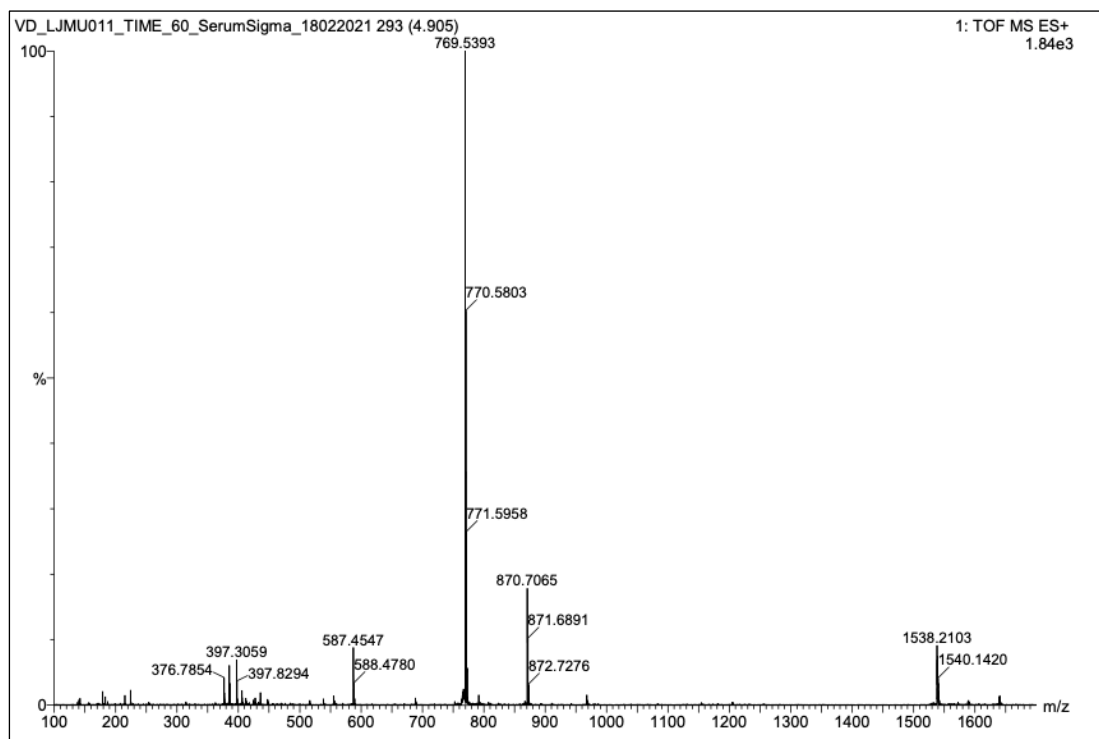


Figure S 87. LC-MS spectrum of minor metabolite detected after 60 min incubation in human serum.

7.2.4.3 LJMU012 – parent and metabolite identification after 60 min incubation

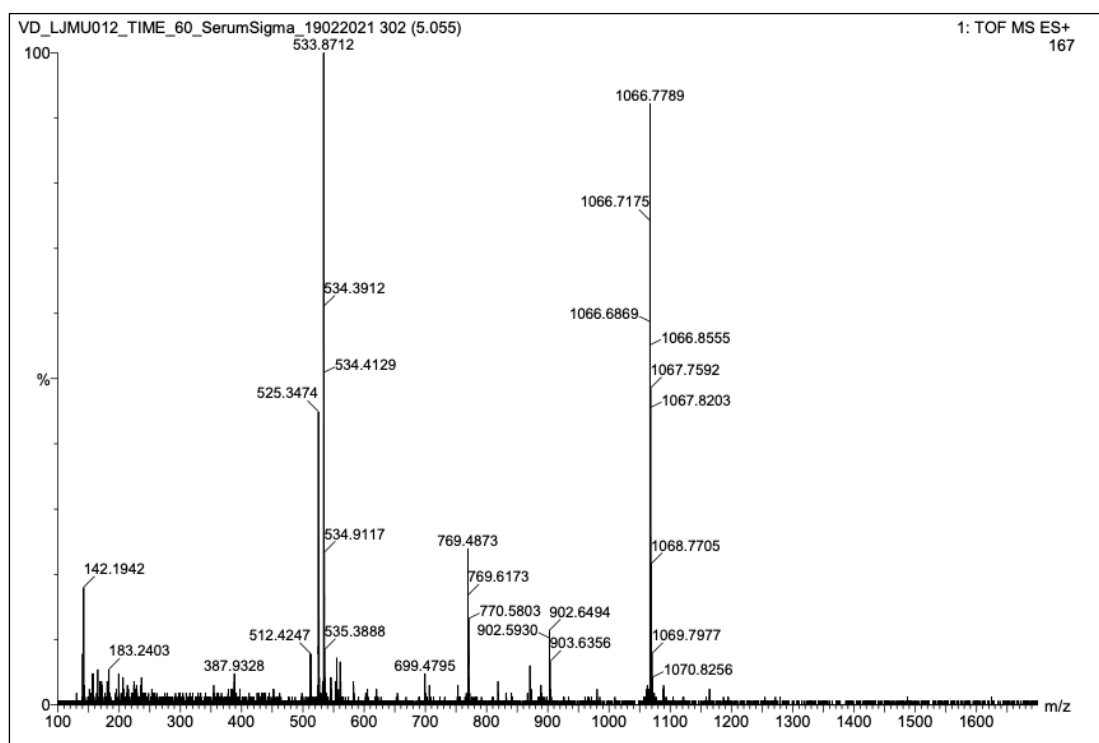


Figure S 88. LC-MS spectrum of parent peptide detected after 60 min incubation in diluted human serum.

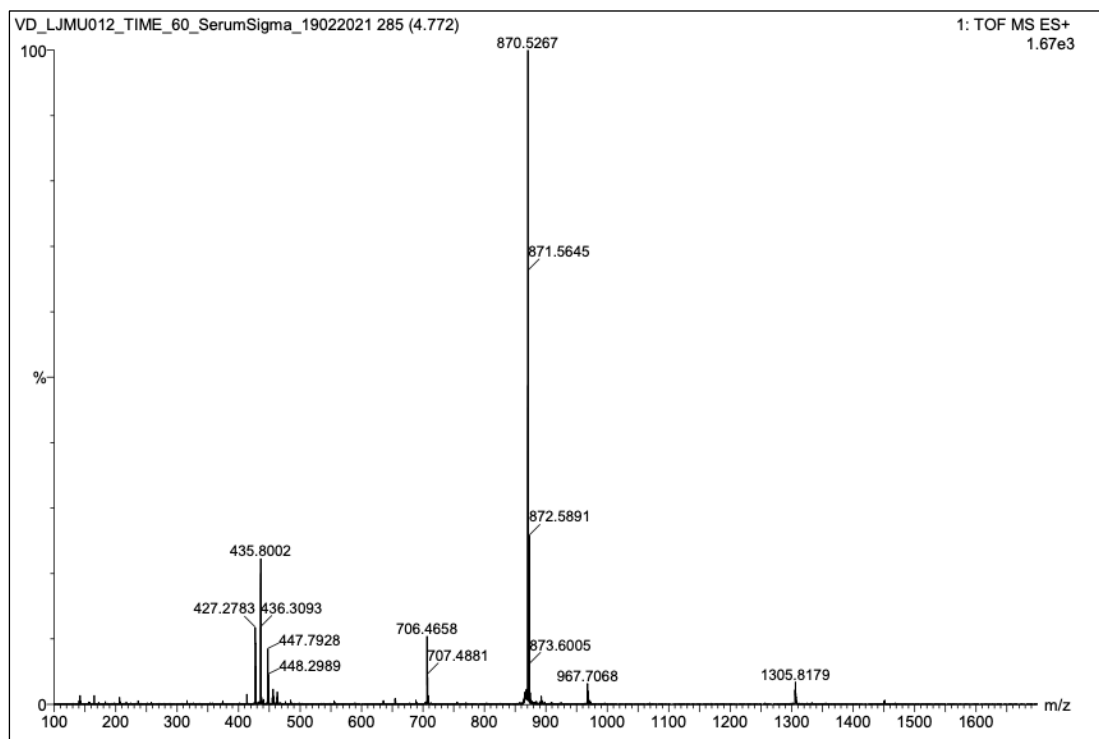


Figure S 89. LC-MS spectrum of main metabolite detected after 60 min incubation in human serum.

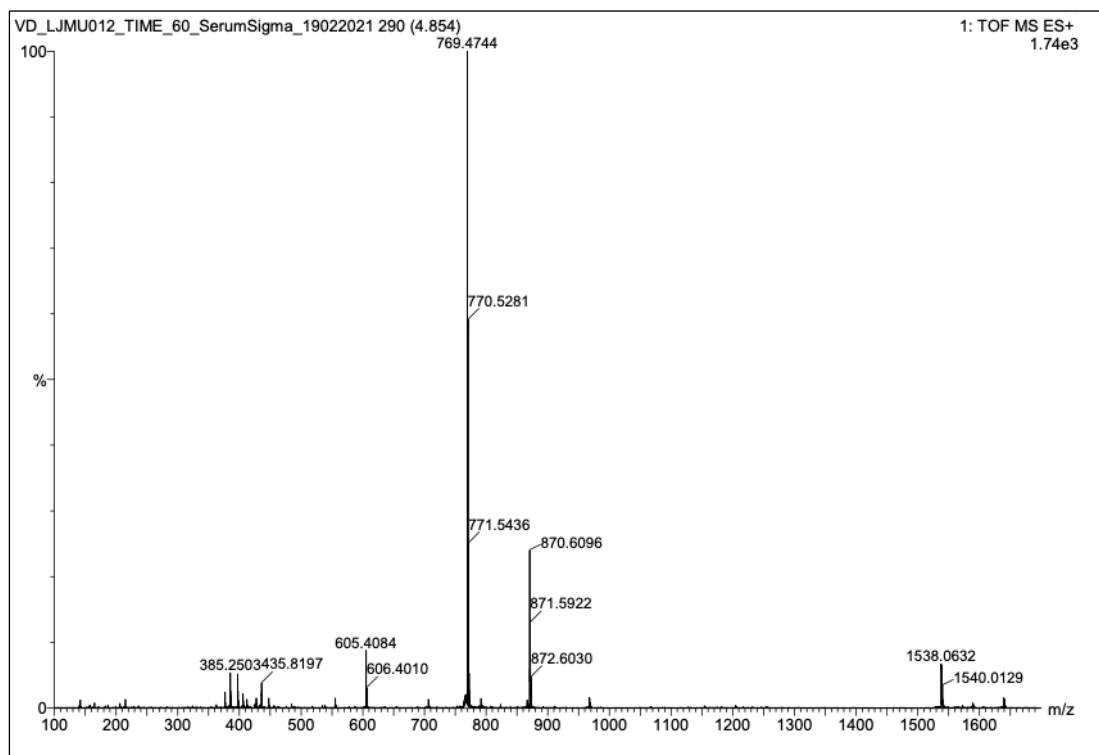


Figure S 90. LC-MS spectrum of minor metabolite detected after 60 min incubation in human serum.

7.2.4.4 LJMU013 – parent and metabolite identification after 60 min incubation

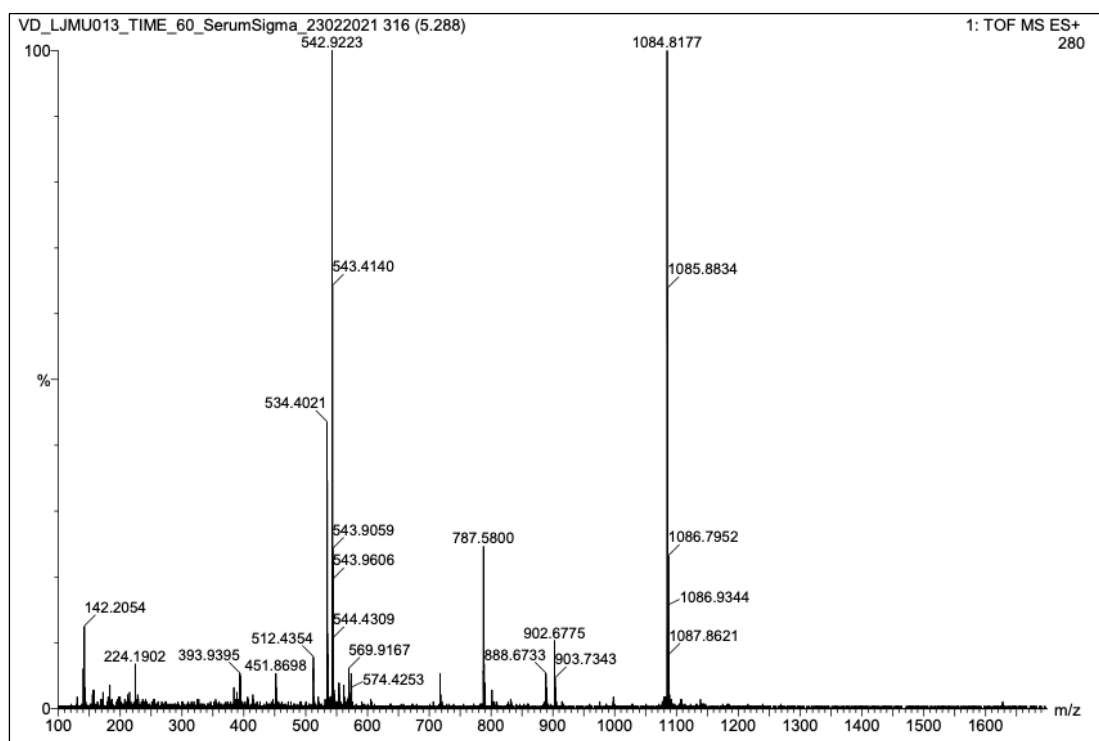


Figure S 91. LC-MS spectrum of parent peptide detected after 60 min incubation in diluted human serum.

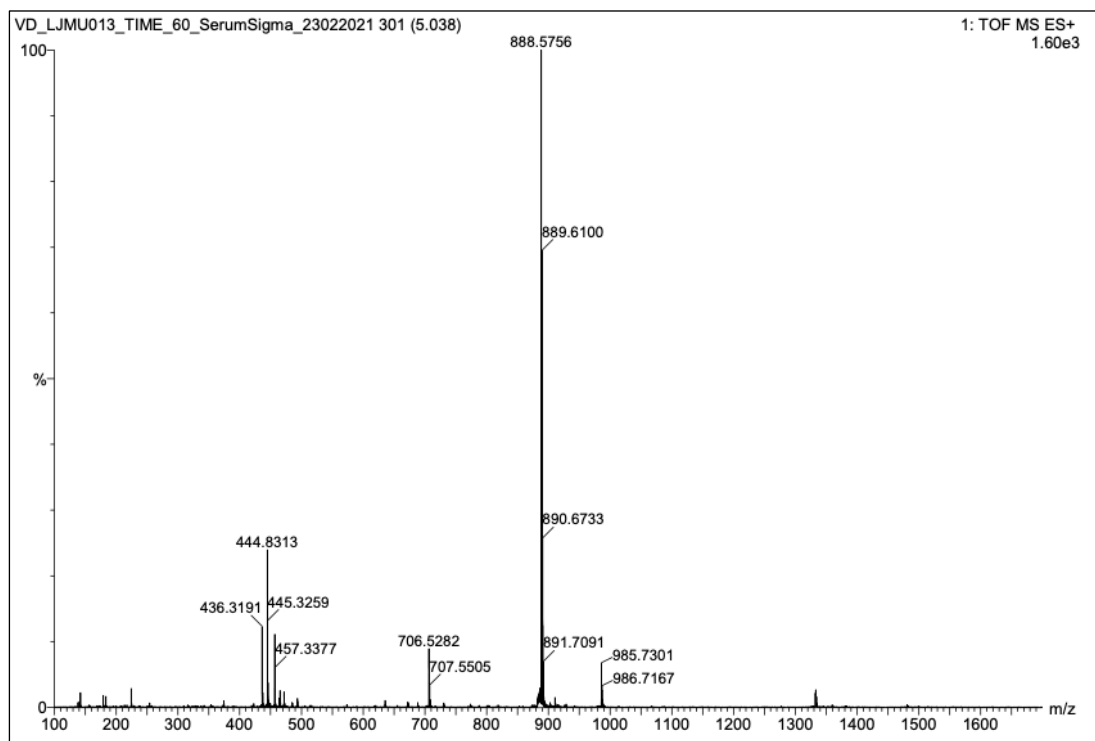


Figure S 92. LC-MS spectrum of main metabolite detected after 60 min incubation in human serum.

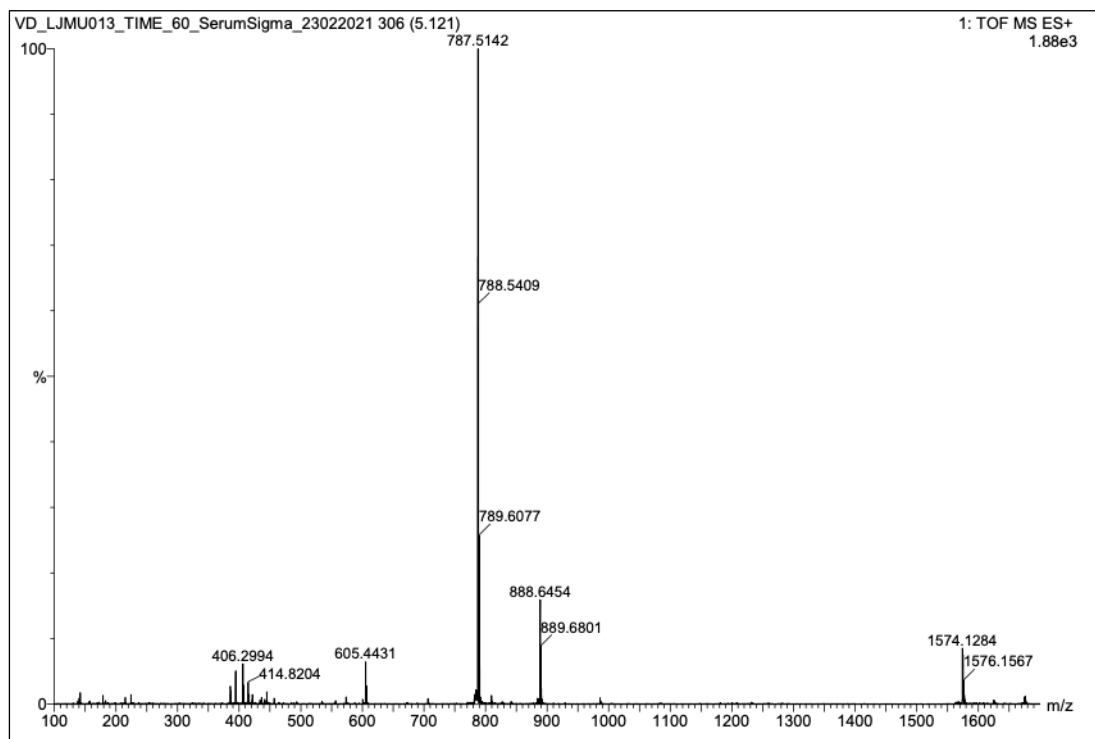


Figure S 93. LC-MS spectrum of minor metabolite detected after 60 min incubation in human serum.

7.2.4.5 LJMU014 – parent and metabolite identification after 60 min incubation

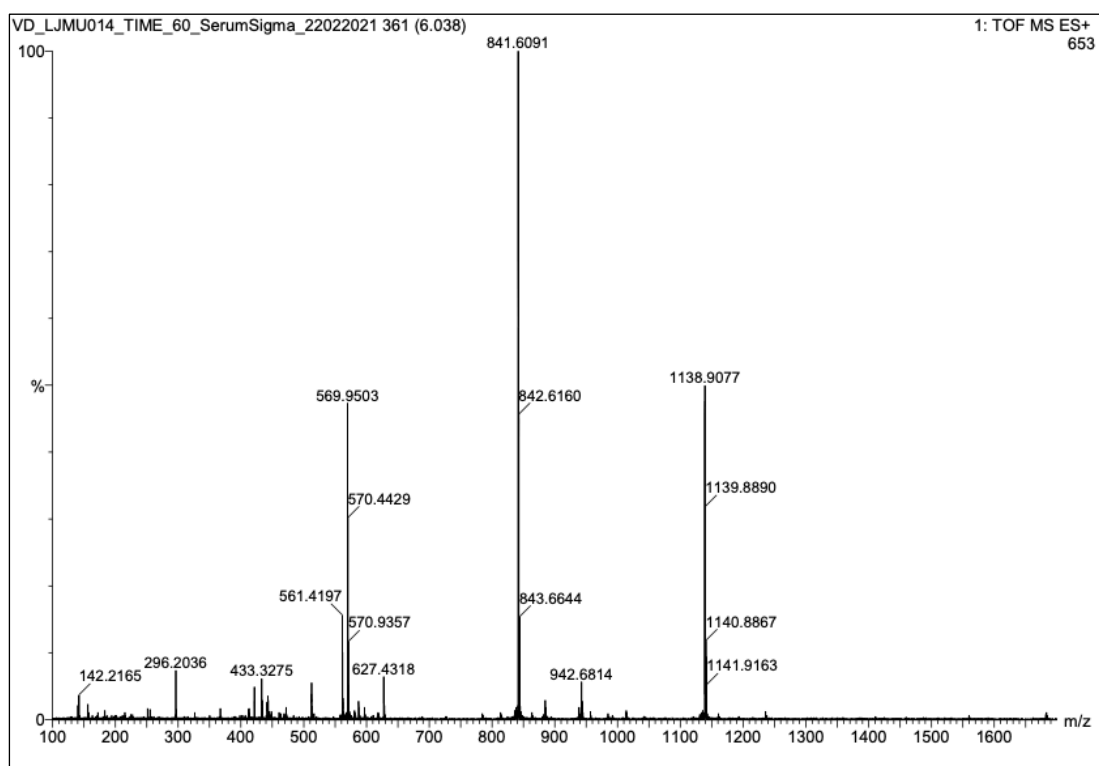


Figure S 94. LC-MS spectrum of parent peptide detected after 60 min incubation in diluted human serum.

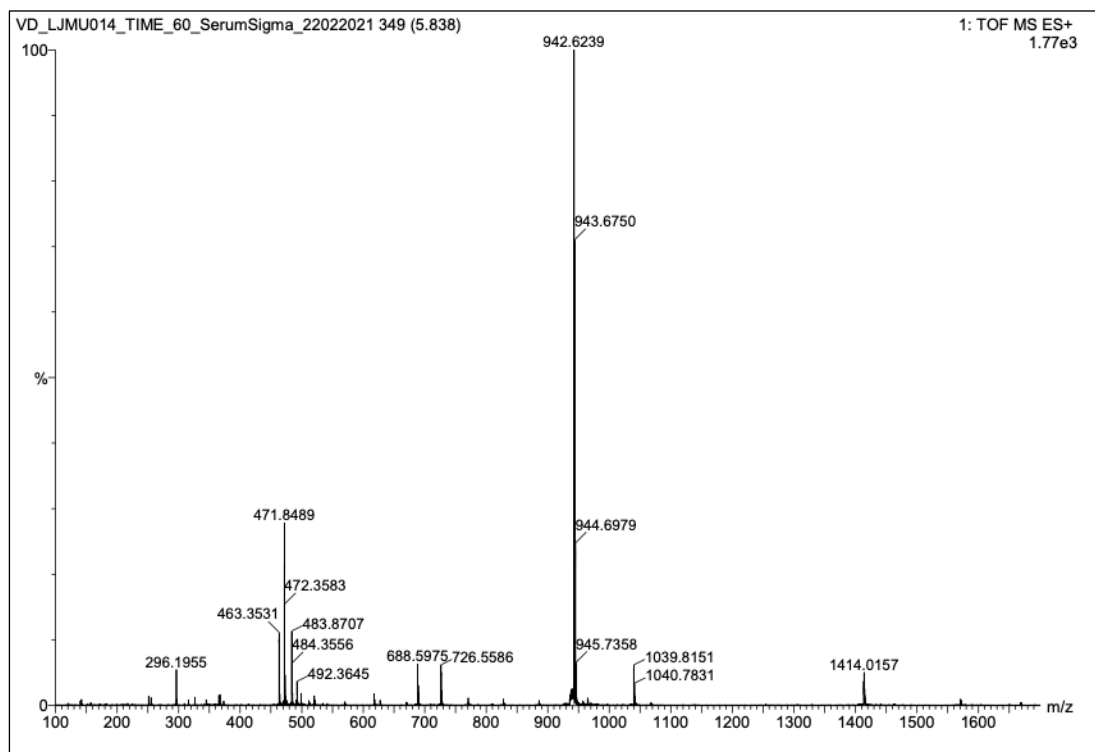


Figure S 95. LC-MS spectrum of main metabolite detected after 60 min incubation in human serum.

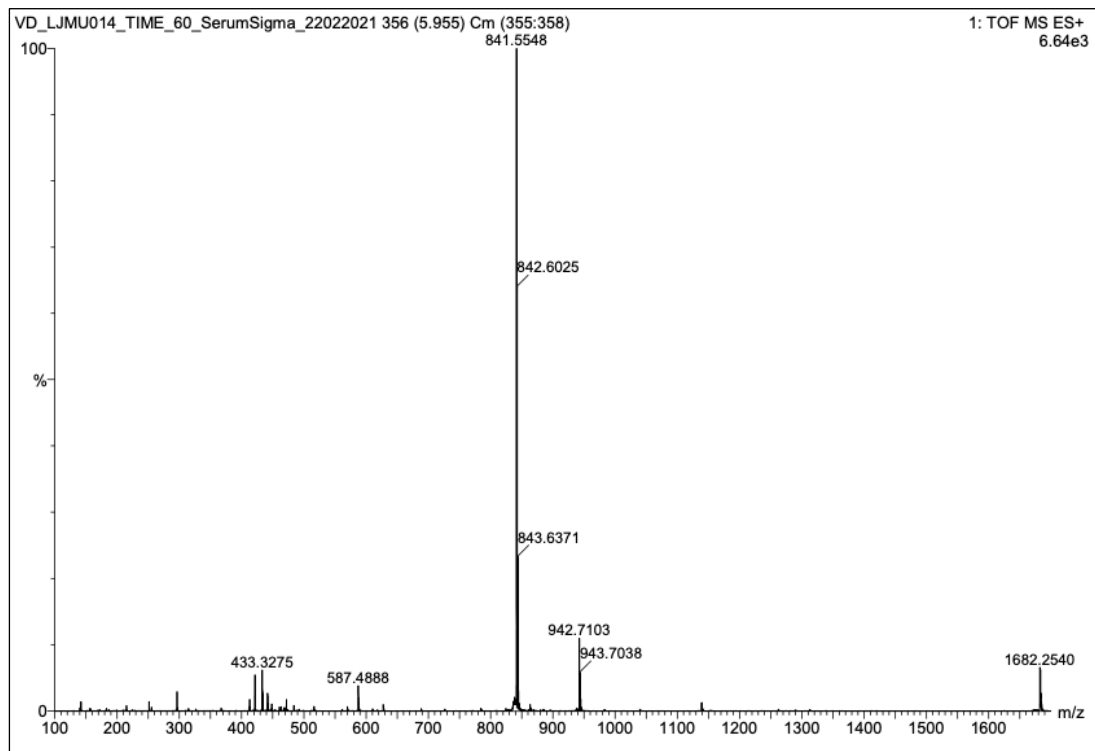


Figure S 96. LC-MS spectrum of minor metabolite detected after 60 min incubation in human serum.

7.2.4.6 LJM015 – parent and metabolite identification after 60 min incubation

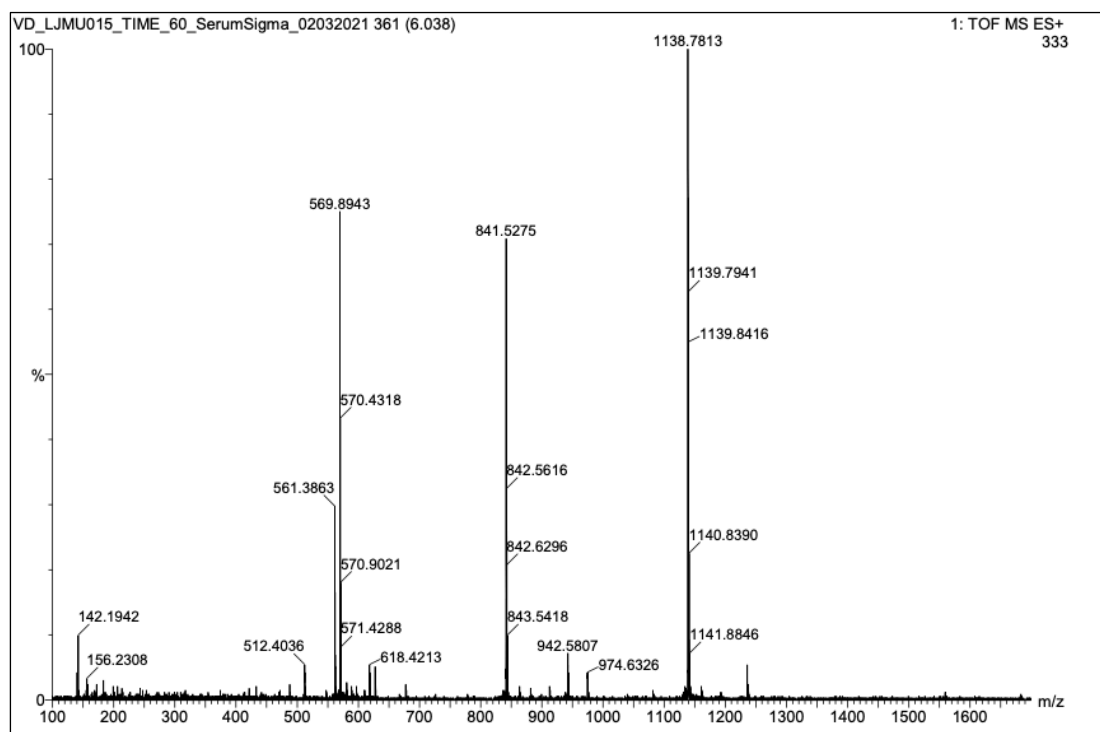


Figure S 97. LC-MS spectrum of parent peptide detected after 60 min incubation in diluted human serum.

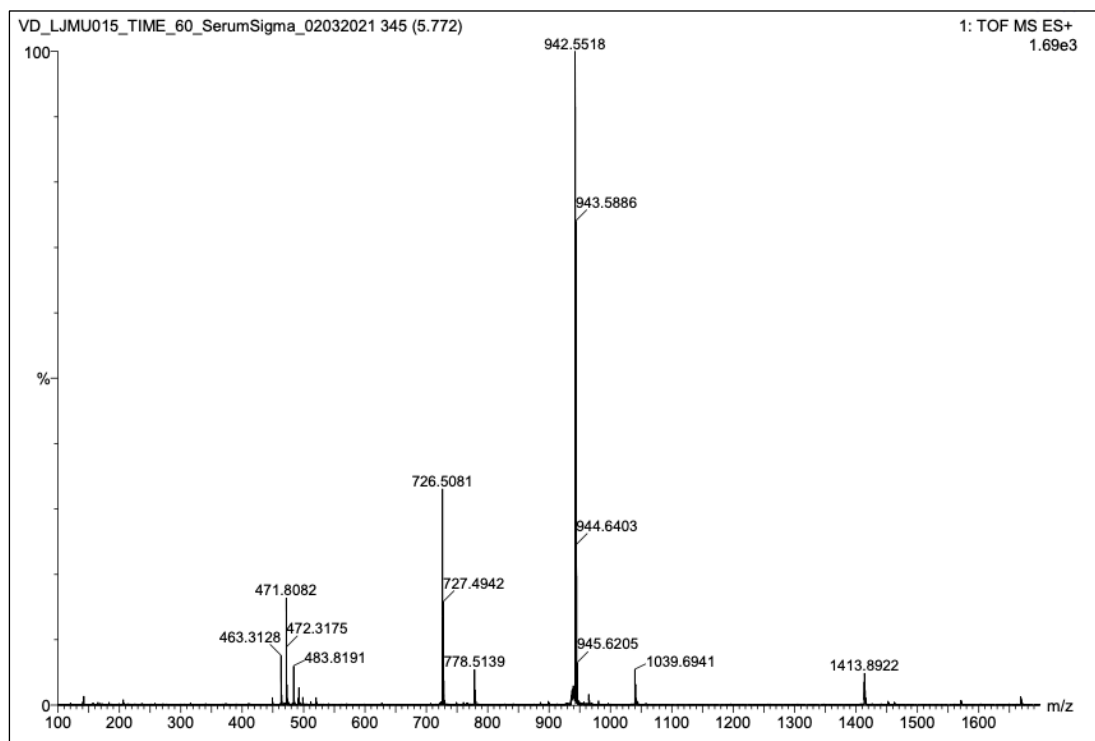


Figure S 98. LC-MS spectrum of main metabolite detected after 60 min incubation in human serum.

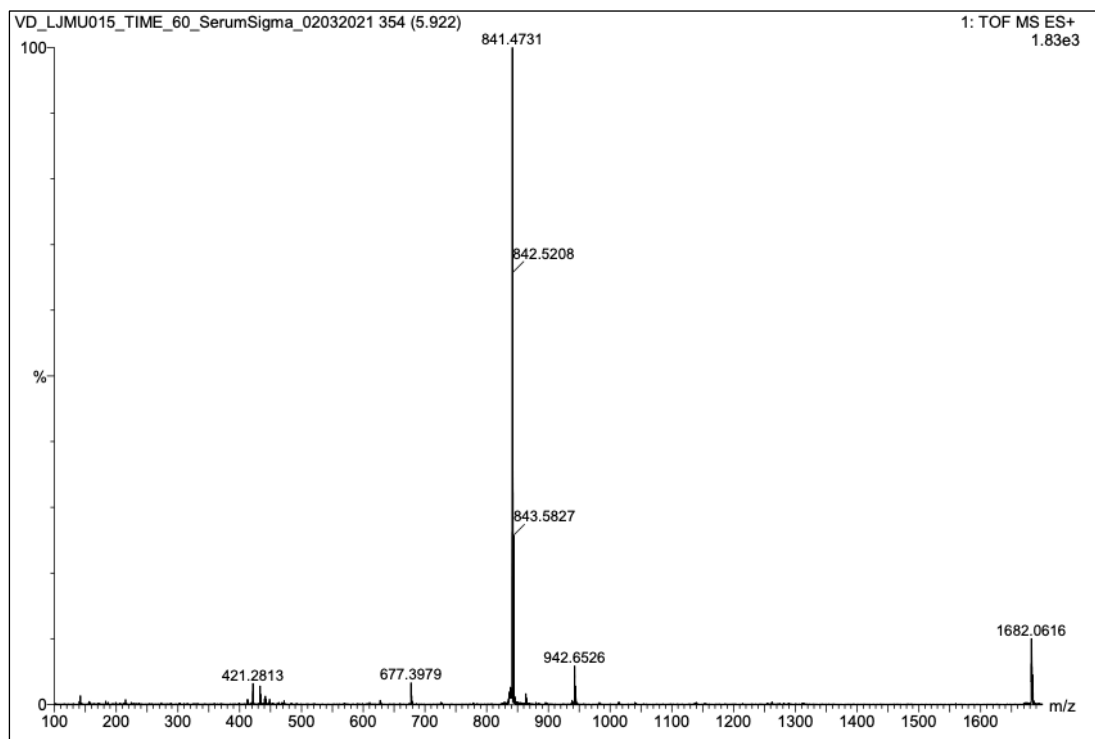


Figure S 99. LC-MS spectrum of minor metabolite detected after 60 min incubation in human serum.

7.2.4.7 LJM016 – parent and metabolite identification after 60 min incubation

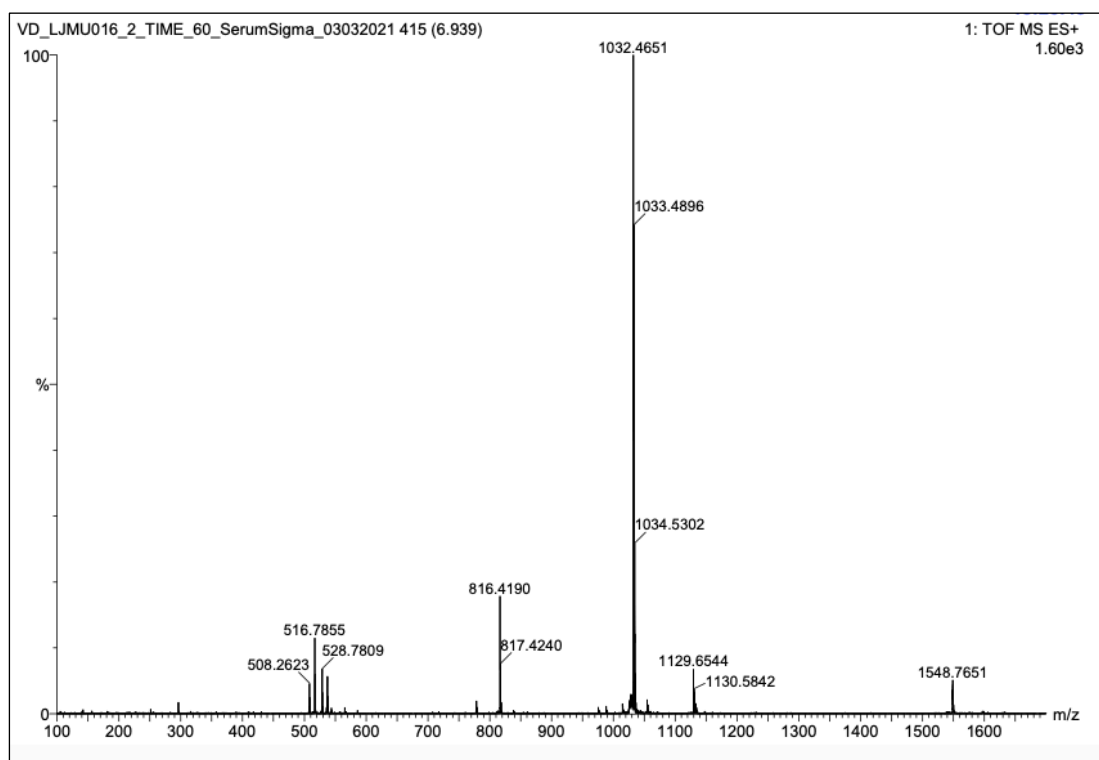


Figure S 100. LC-MS spectrum of main metabolite detected after 60 min incubation in human serum.

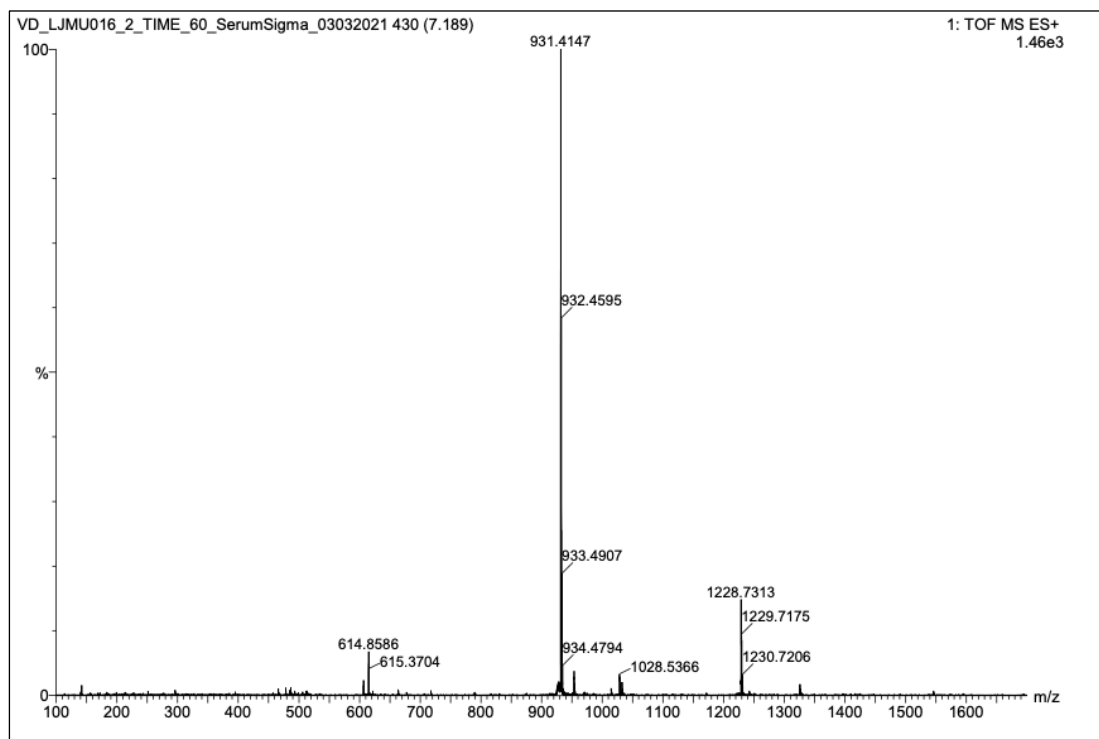


Figure S 101. LC-MS spectrum of minor metabolite detected after 60 min incubation in human serum.

7.2.4.8 LJMU017 – parent and metabolite identification after 60 min incubation

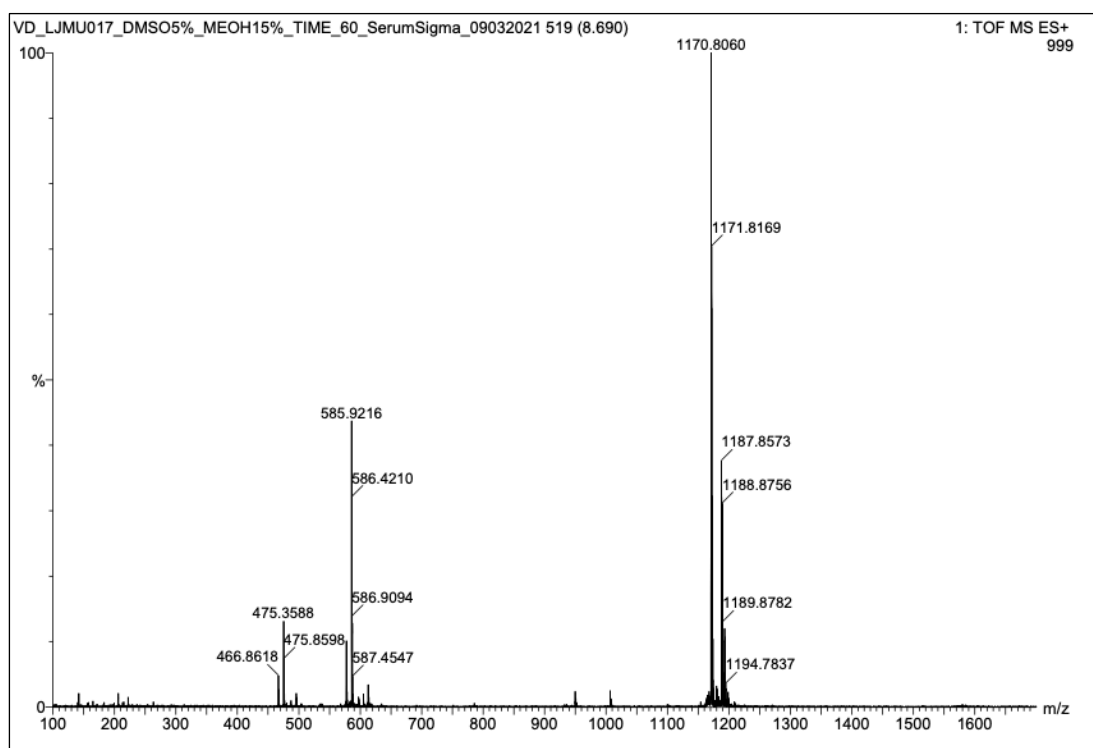


Figure S 102. LC-MS spectrum of parent peptide detected after 60 min incubation in diluted human serum.

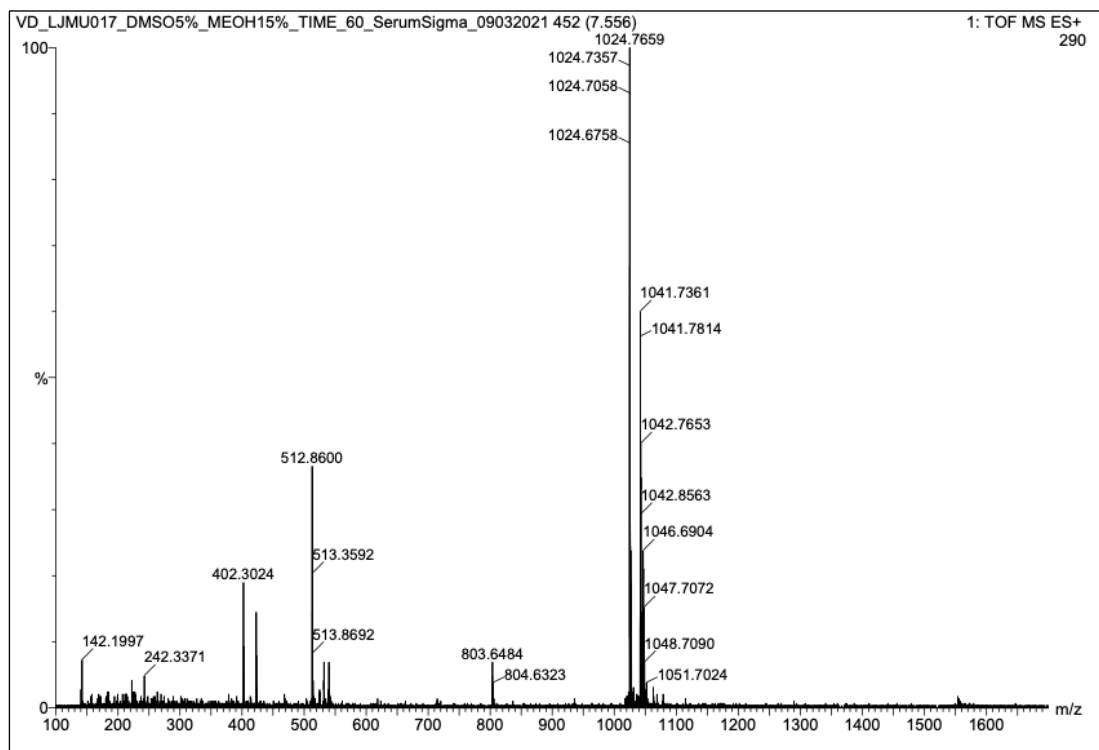


Figure S 103. LC-MS spectrum of main metabolite detected after 60 min incubation in human serum.

7.2.4.9 LJMU018 – parent and metabolite identification after 60 min incubation

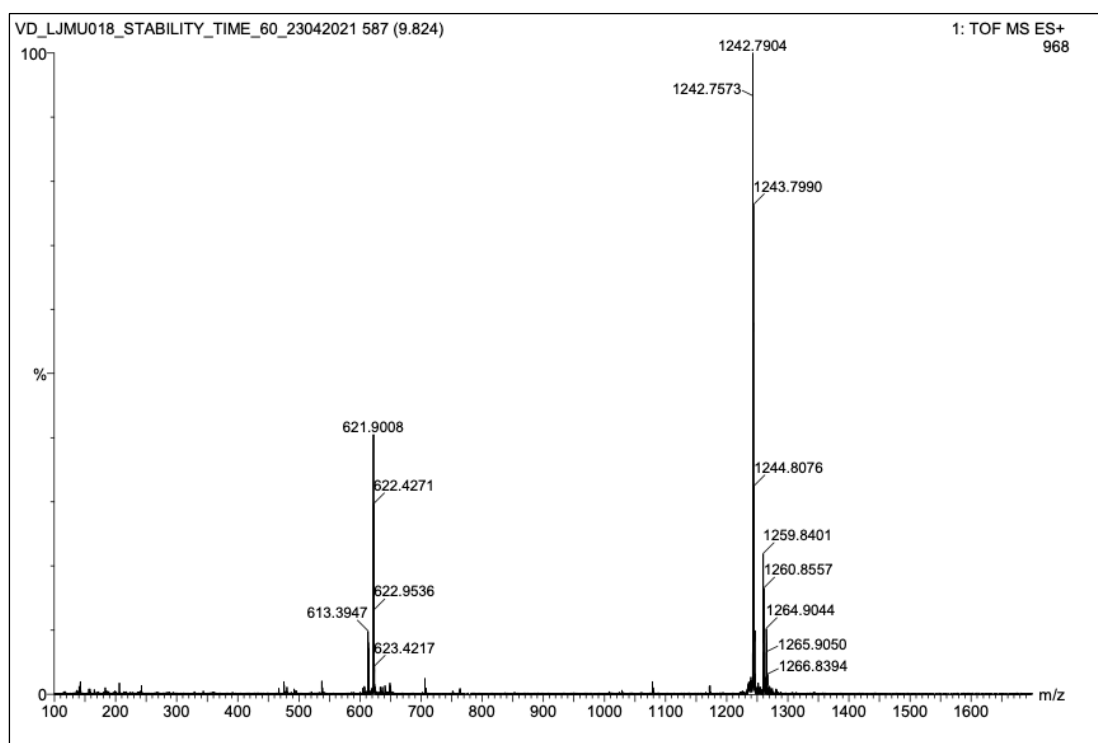


Figure S 104. LC-MS spectrum of parent peptide detected after 60 min incubation in diluted human serum.

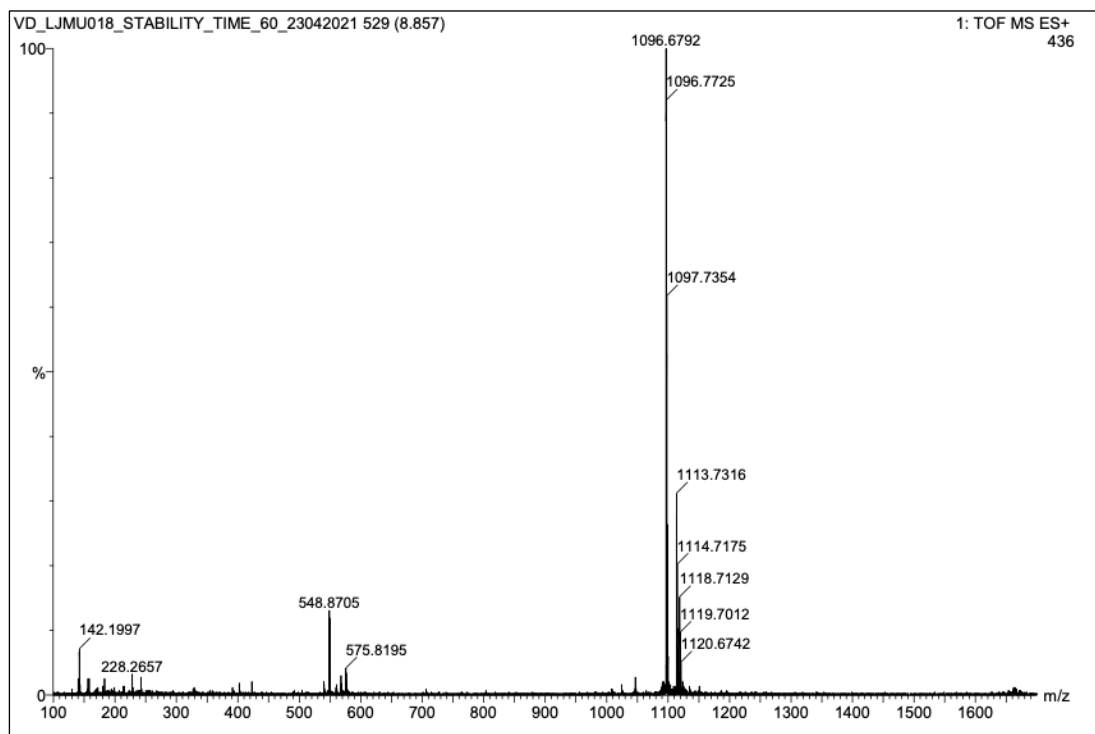


Figure S 105. LC-MS spectrum of main metabolite detected after 60 min incubation in human serum.

7.2.4.10 LJMU019 – parent and metabolite identification after 60 min incubation

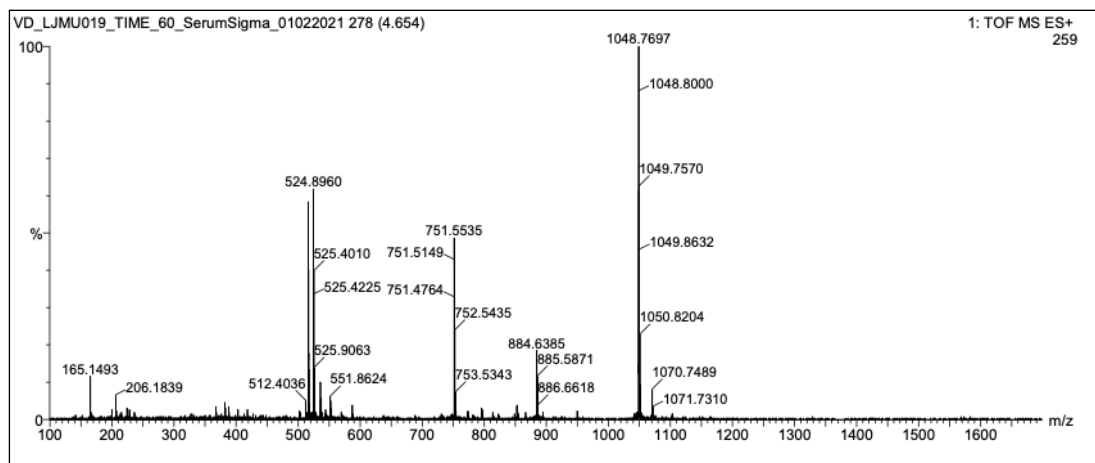


Figure S 106. LC-MS spectrum of parent peptide detected after 60 min incubation in diluted human serum.

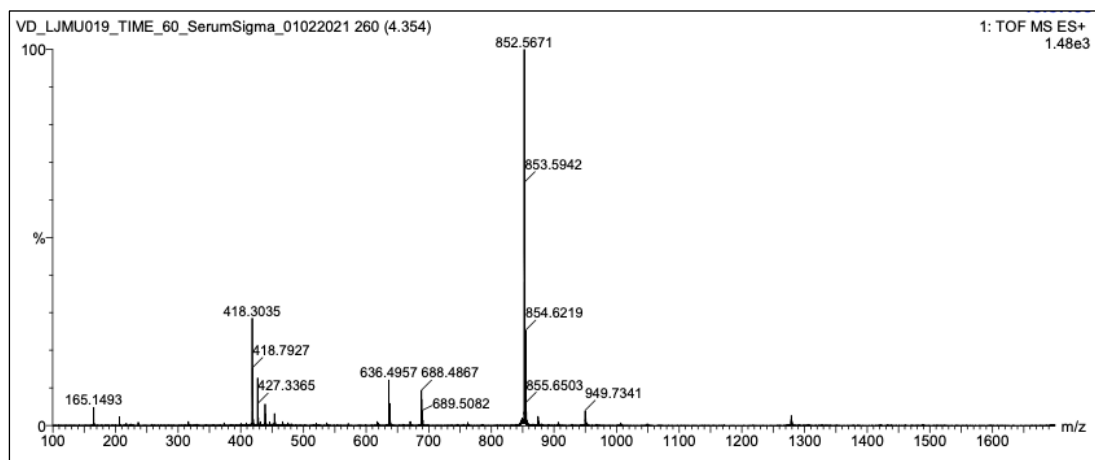


Figure S 107. LC-MS spectrum of main metabolite detected after 60 min incubation in human serum.

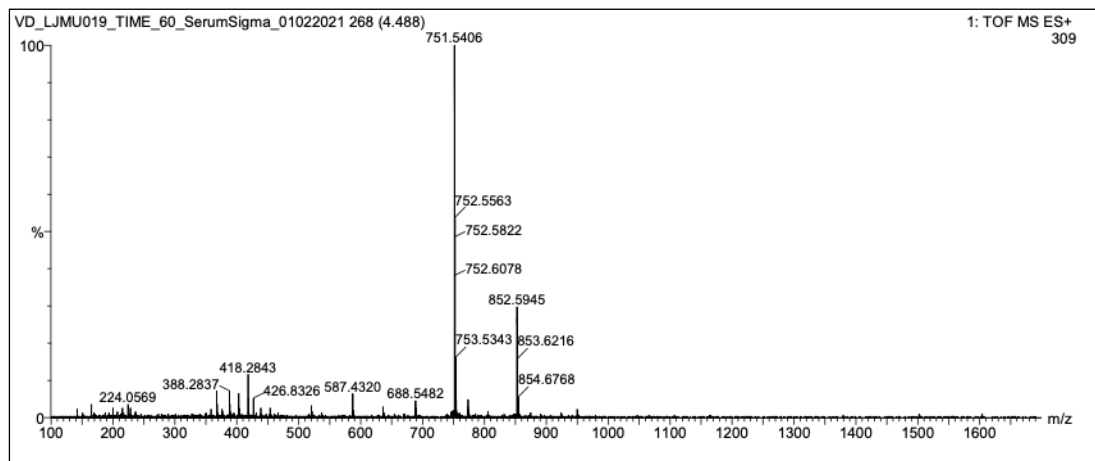


Figure S 108. LC-MS spectrum of minor metabolite detected after 60 min incubation in human serum.

7.2.4.11 LJMU020 – parent and metabolite identification after 60 min incubation

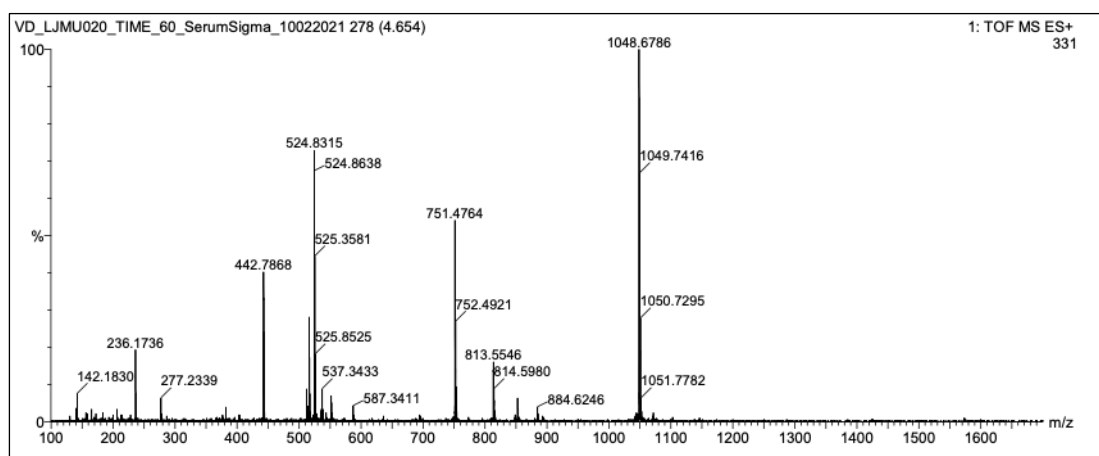


Figure S 109. LC-MS spectrum of parent peptide detected after 60 min incubation in diluted human serum.

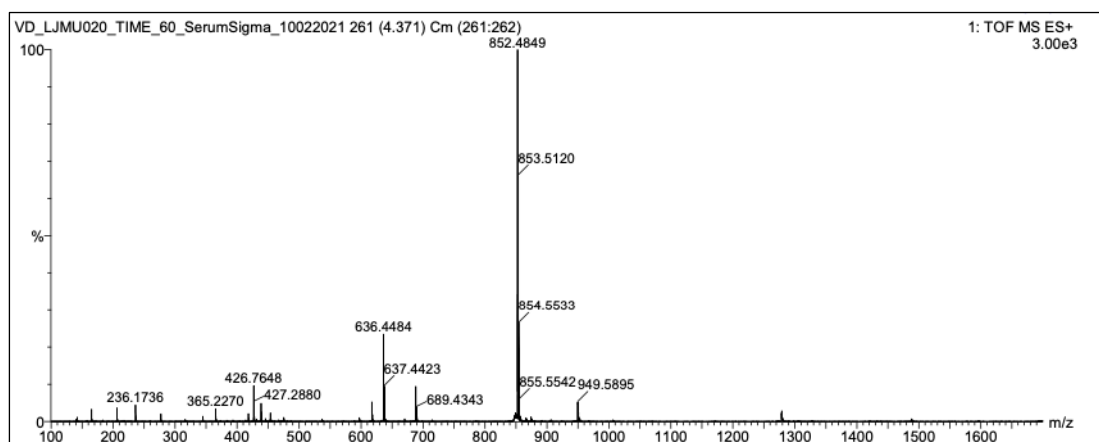


Figure S 110. LC-MS spectrum of main metabolite detected after 60 min incubation in human serum.

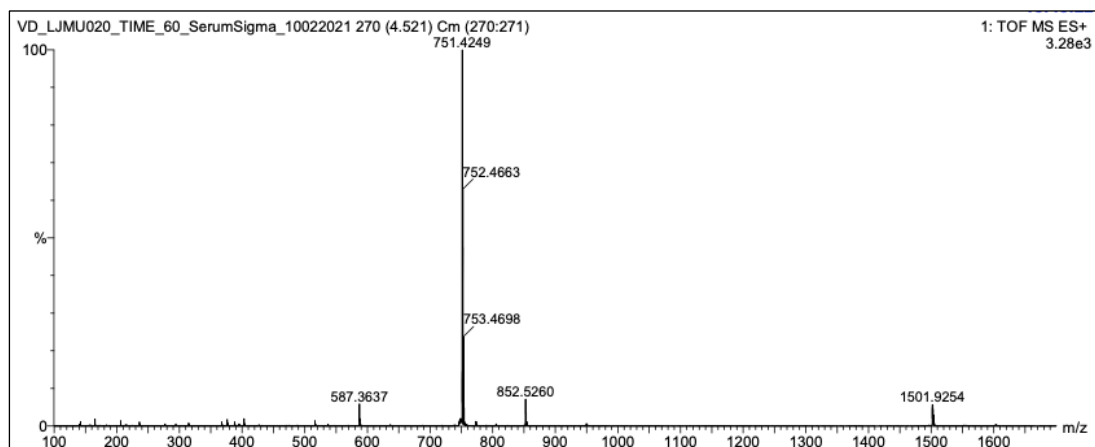


Figure S 111. LC-MS spectrum of minor metabolite detected after 60 min incubation in human serum.

7.2.4.12 LJMU021 – parent and metabolite identification after 60 min incubation

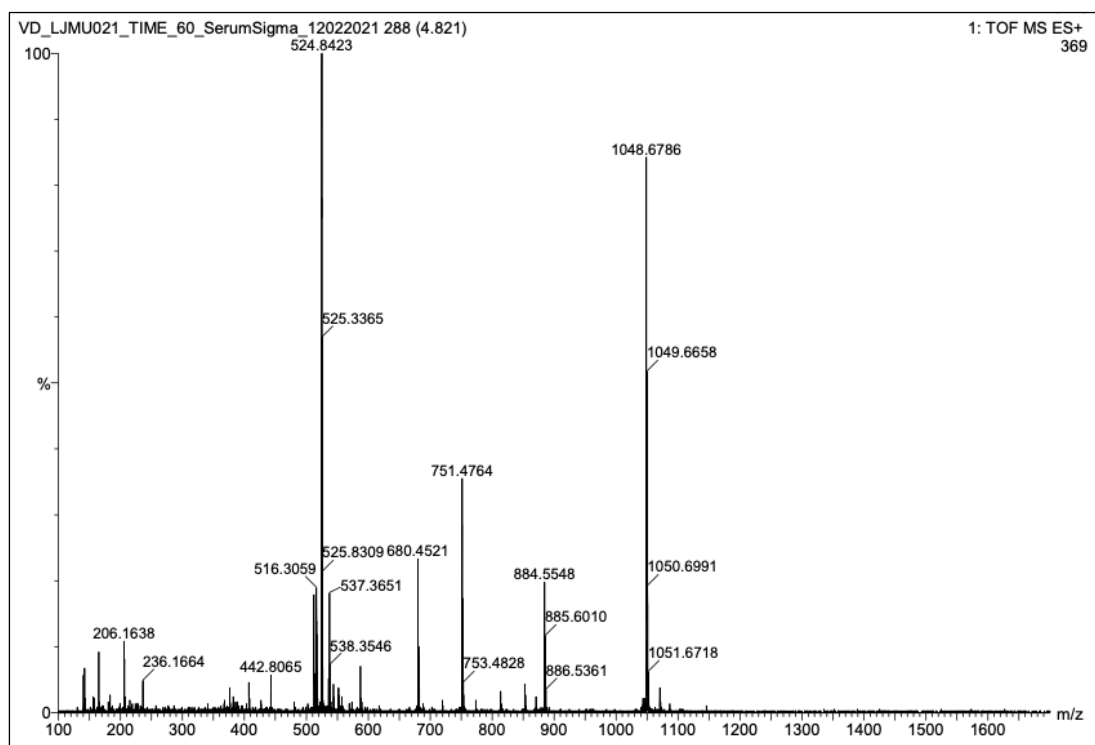


Figure S 112. LC-MS spectrum of parent peptide detected after 60 min incubation in diluted human serum.

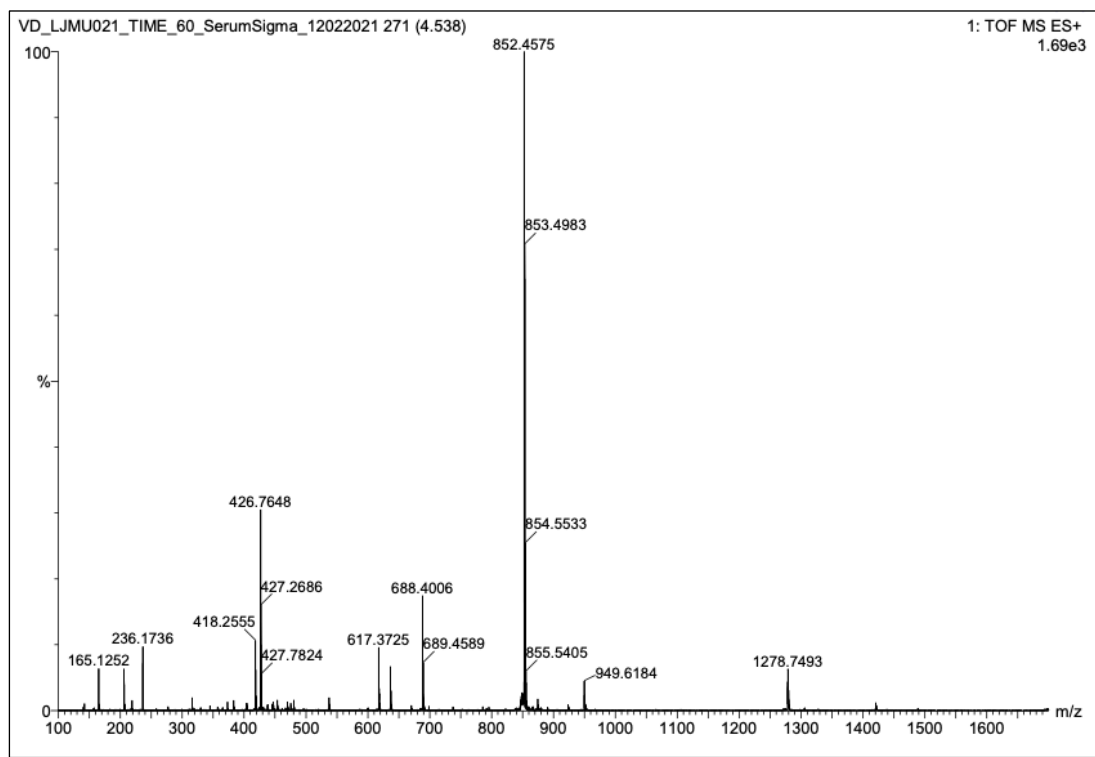


Figure S 113. LC-MS spectrum of main metabolite detected after 60 min incubation in human serum.

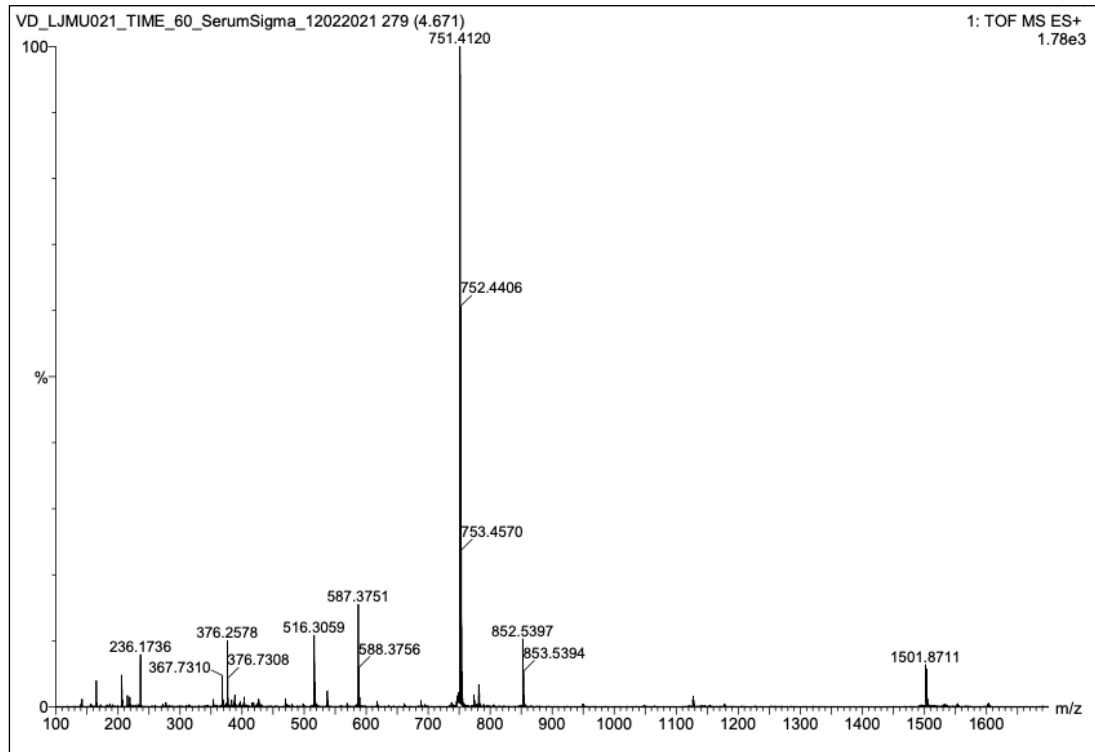


Figure S 114. LC-MS spectrum of minor metabolite detected after 60 min incubation in human serum.

7.2.4.13 LJMU022 – parent and metabolite identification after 60 min incubation

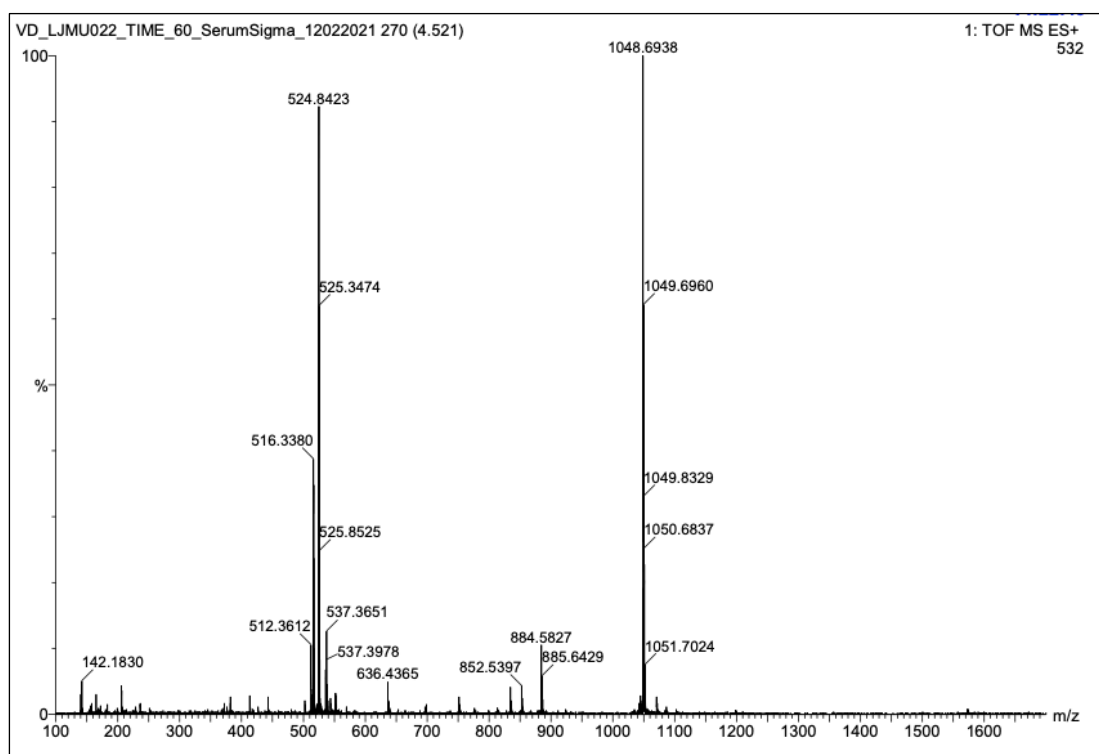


Figure S 115. LC-MS spectrum of parent peptide detected after 60 min incubation in diluted human serum.

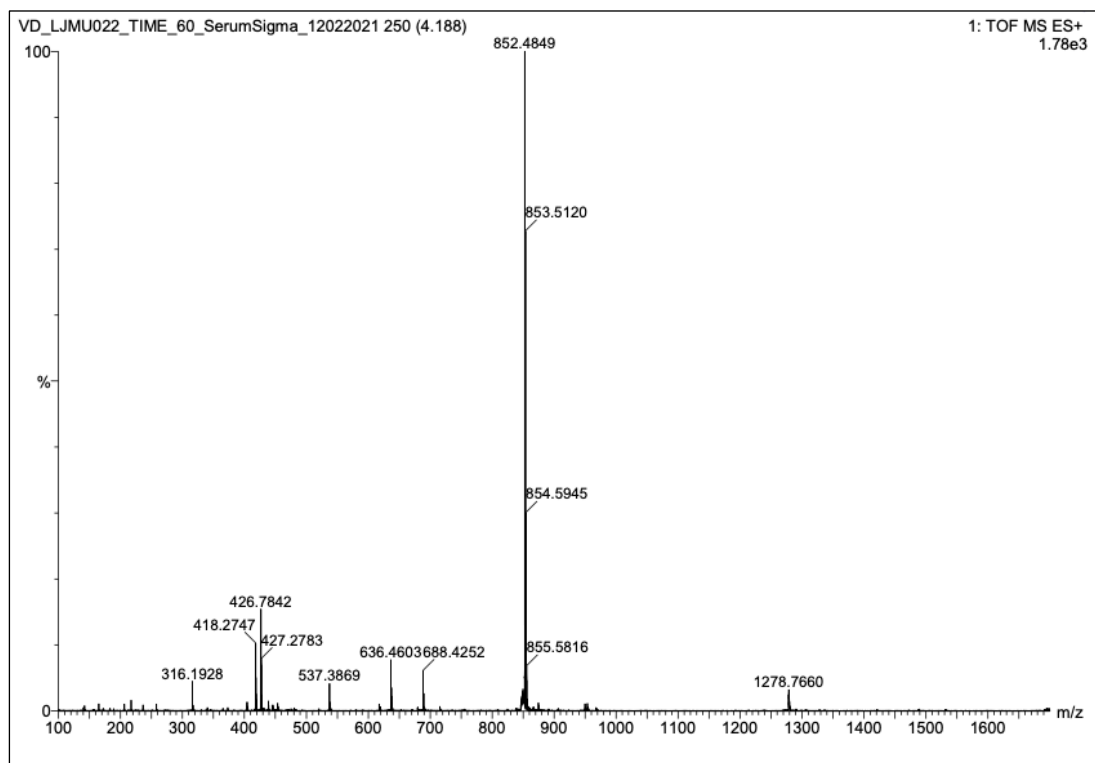


Figure S 116. LC-MS spectrum of main metabolite detected after 60 min incubation in human serum.

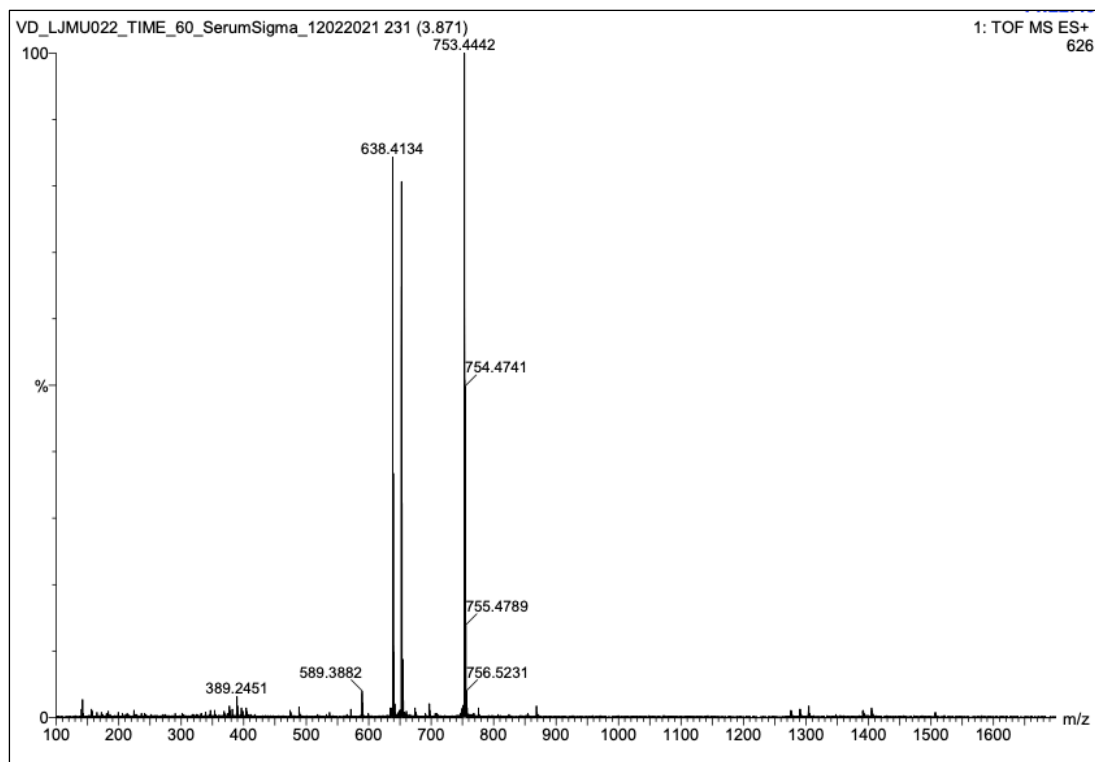


Figure S 117. LC-MS spectrum of minor metabolite detected after 60 min incubation in human serum.

7.2.4.14 LJMU023 – parent and metabolite identification after 60 min incubation

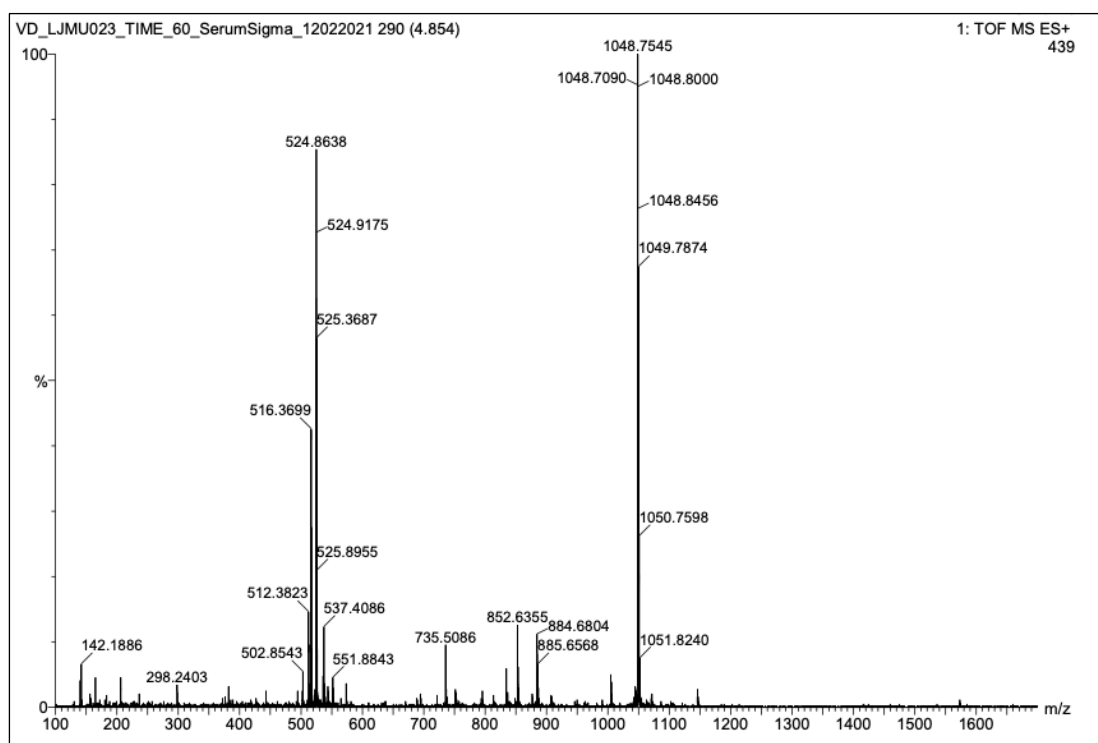


Figure S 118. LC-MS spectrum of parent peptide detected after 60 min incubation in diluted human serum.

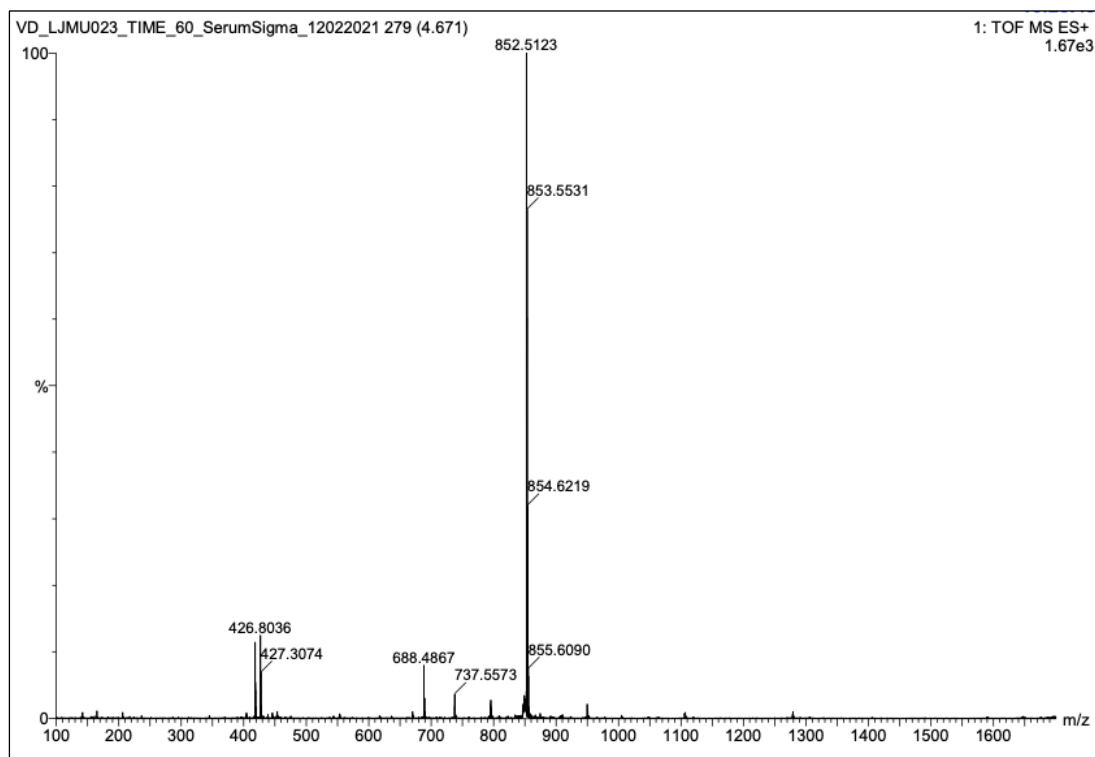


Figure S 119. LC-MS spectrum of main metabolite detected after 60 min incubation in human serum.

7.2.4.15 LJMU024 – parent and metabolite identification after 60 min incubation

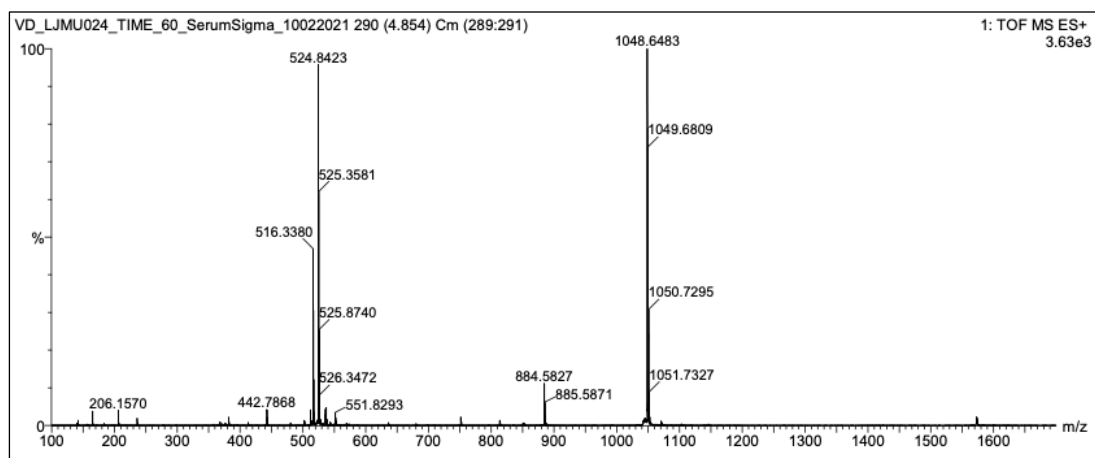


Figure S 120. LC-MS spectrum of parent peptide detected after 60 min incubation in diluted human serum.

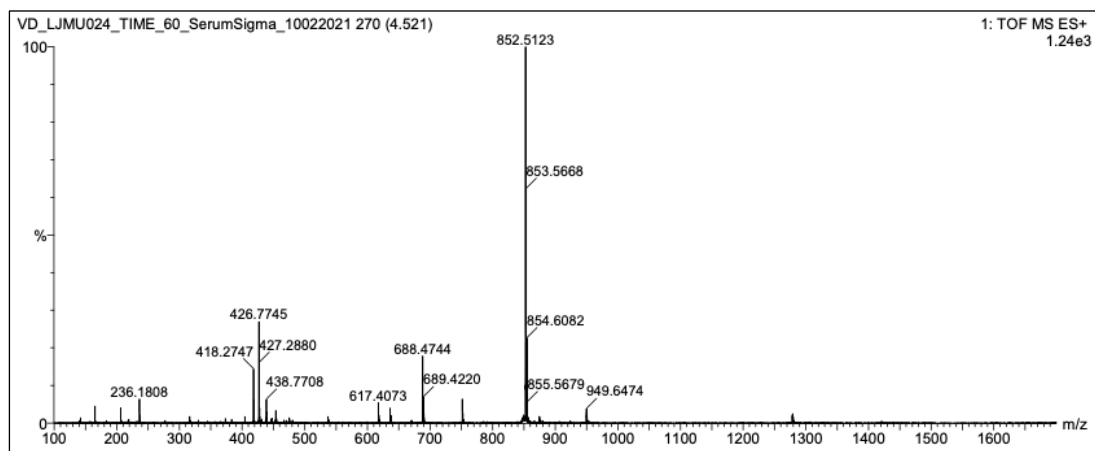


Figure S 121. LC-MS spectrum of main metabolite detected after 60 min incubation in human serum.

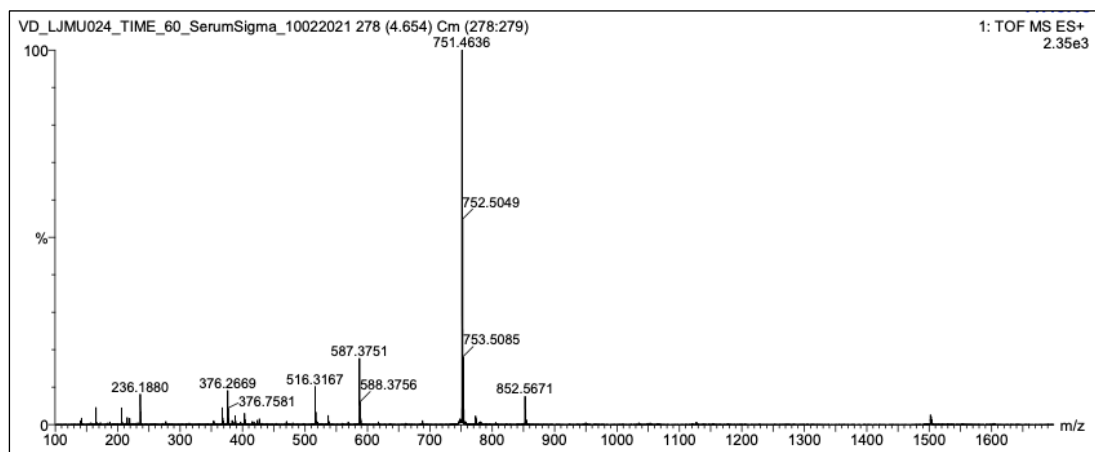


Figure S 122. LC-MS spectrum of minor metabolite detected after 60 min incubation in human serum.

7.2.4.16 LJMU027 – parent and metabolite identification after 60 min incubation

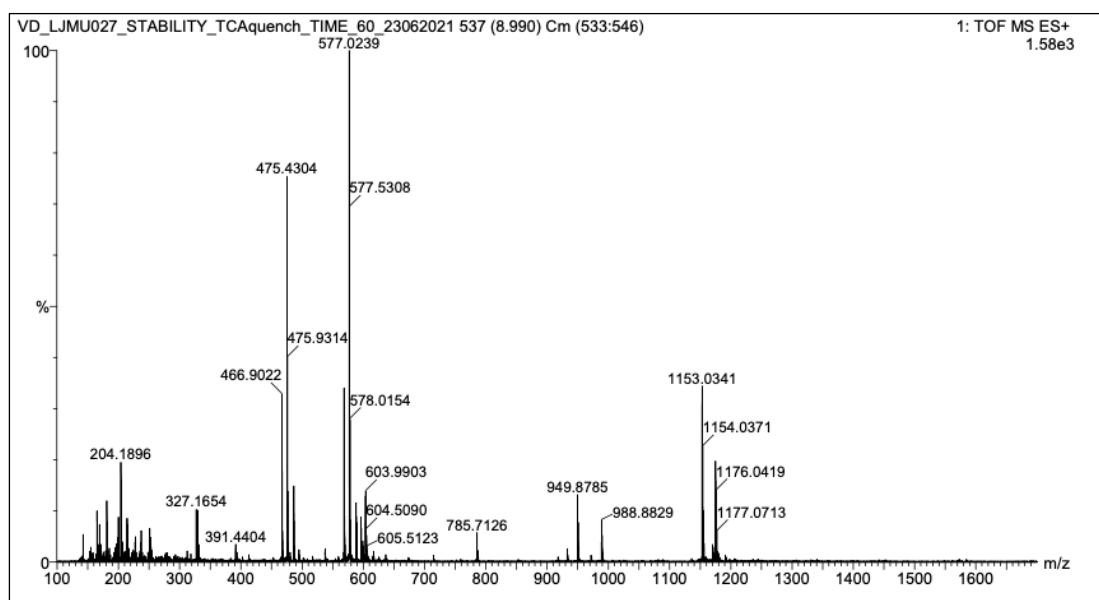


Figure S 123. LC-MS spectrum of parent peptide detected after 60 min incubation in diluted human serum.

7.2.5 Calibration curves for plasma protein binding and physicochemical stability studies

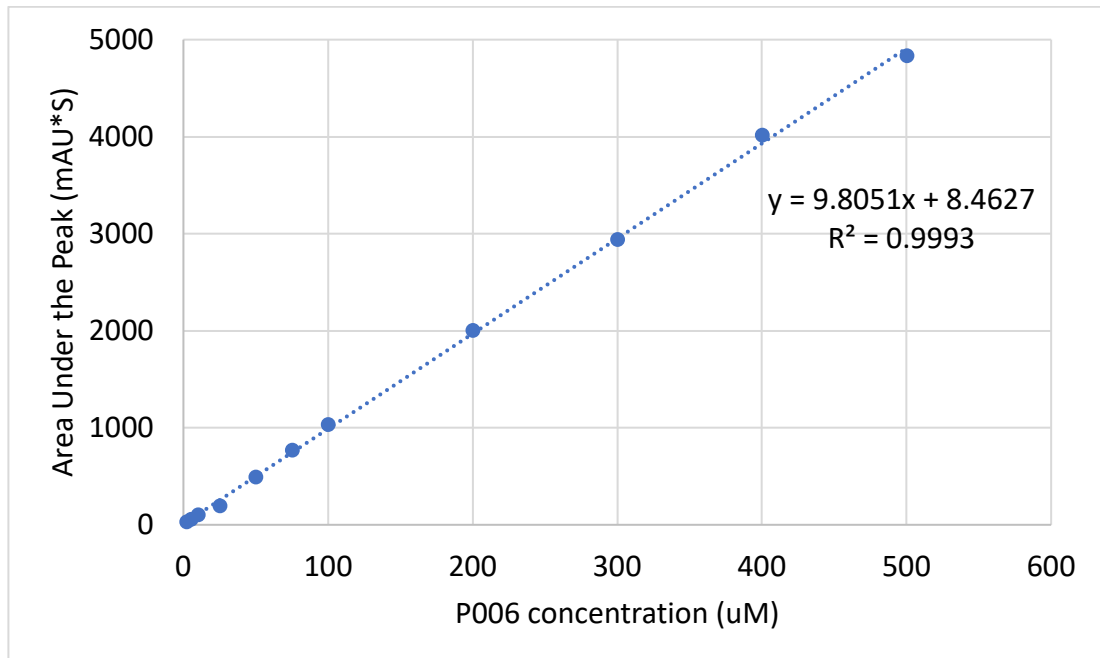


Figure S 124. P006 calibration curve in PBS aq. solution (5 % DMSO).

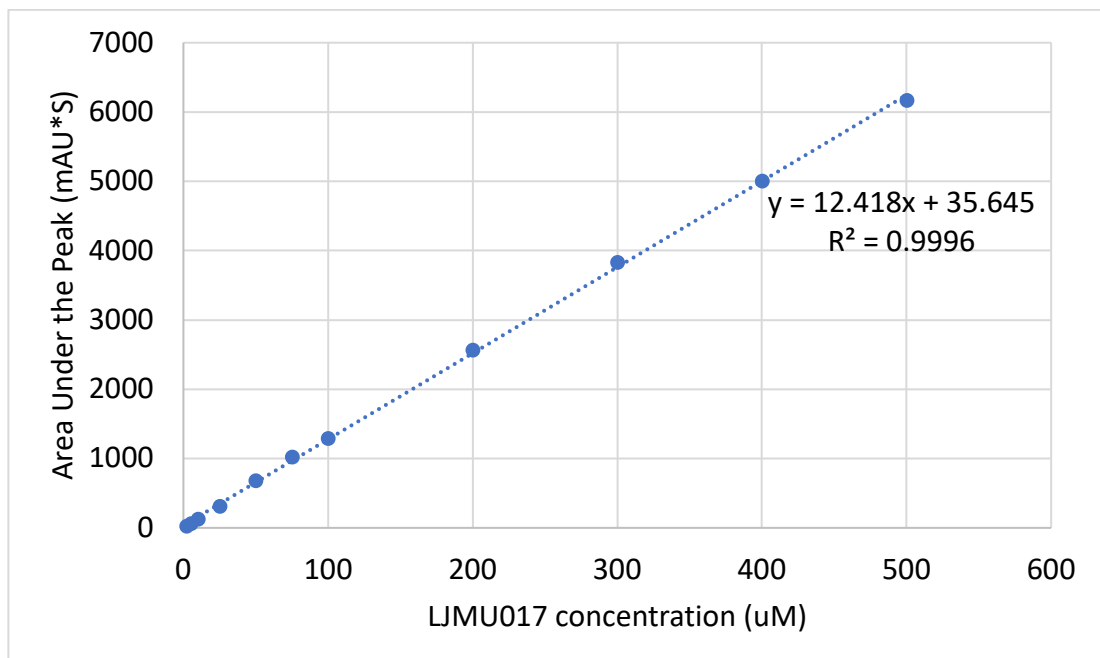


Figure S 125. LJM017 calibration curve in PBS aq. solution (5 % DMSO).

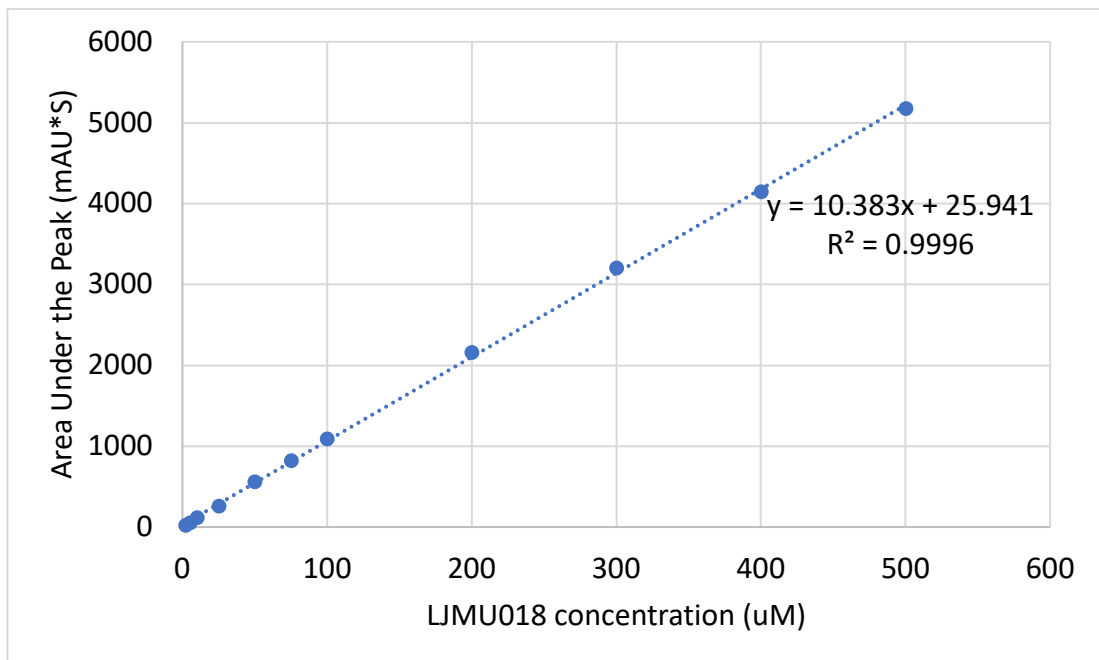


Figure S 126. LJM018 calibration curve in PBS aq. solution (5 % DMSO).

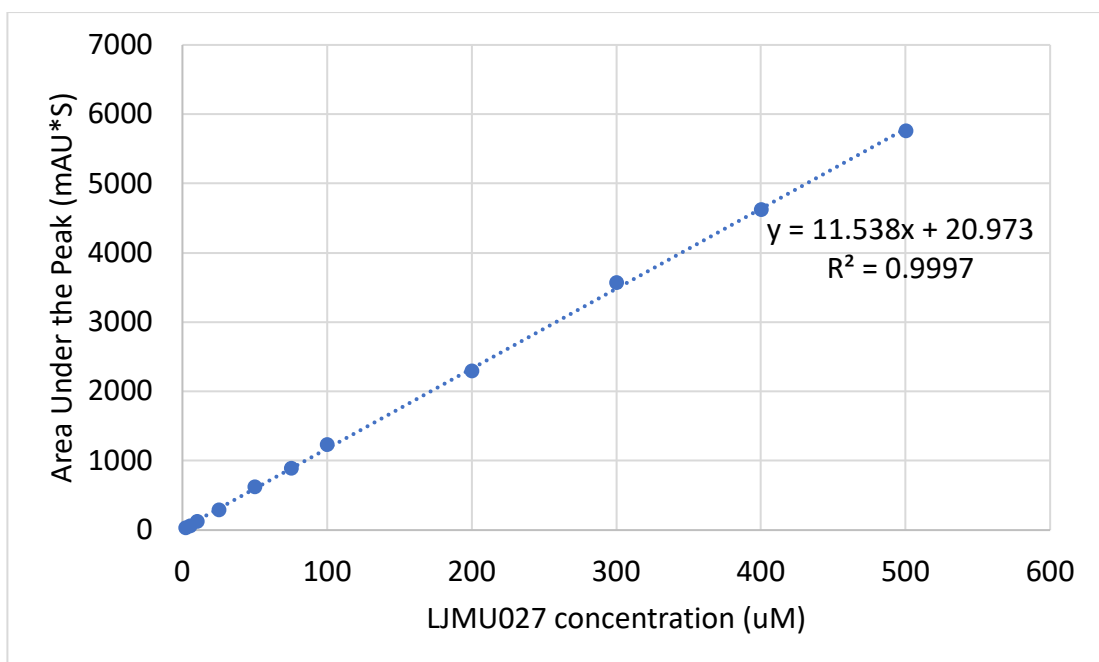


Figure S 127. LJM027 calibration curve in PBS aq. solution (5 % DMSO).

7.2.6 Plasma protein binding (PPB) experiments

7.2.6.1 PPB assessment via HSA precipitation method

Table S.3. HSA precipitation method full dataset ($n=3$).

HSA (μM)	P006 bound (%)	LJMU027 bound (%)	LJMU017 bound (%)	LJMU018 bound (%)
0	0.00	0.00	0.00	0.00
10	9.05 ± 1.26	9.29 ± 0.32	5.53 ± 0.06	16.93 ± 1.55
25	6.34 ± 4.08	18.24 ± 0.89	18.57 ± 0.49	25.71 ± 3.86
50	3.26 ± 2.86	24.55 ± 0.61	30.59 ± 0.04	40.24 ± 0.55
80	2.27 ± 3.39	40.08 ± 0.94	43.15 ± 0.32	51.05 ± 0.28
100	3.15 ± 3.03	45.17 ± 0.44	49.52 ± 0.25	58.13 ± 1.56
150	4.75 ± 1.61	55.11 ± 0.37	60.98 ± 0.11	63.64 ± 0.85
200	-1.04 ± 3.40	62.20 ± 0.52	65.98 ± 0.28	72.04 ± 0.93
250	-1.16 ± 1.74	65.28 ± 0.99	70.97 ± 0.35	75.30 ± 0.96
400	9.90 ± 1.07	74.49 ± 0.57	78.85 ± 0.40	81.94 ± 0.86

7.2.6.2 PPB assessment via equilibrium dialysis

Table S.4. RED method full dataset ($n=2$).

	[Peptide] in white chamber (μM)	[Peptide] in red chamber (μM)	unbound peptide (%)	bound peptide (%)
P006	104.73 ± 5.31	143.11 ± 6.96	73.18	26.82
LJMU027	113.29 ± 1.23	138.80 ± 4.39	81.62	18.38
LJMU017	98.02 ± 5.75	119.68 ± 6.66	81.90	18.10
LJMU018	141.55 ± 5.29	184.42 ± 5.90	76.76	23.24

7.2.6.3 PPB assessment via ultrafiltration

Table S.5. Ultrafiltration method full dataset ($n=2$).

	[peptide] in filtrate sol.	Peptide filtrated compared to PBS sample (%)
P006	55.68 ± 3.08	103.52 ± 5.64
LJMU027	9.17 ± 2.28	69.66 ± 14.47

Table S.6. Filtration test to assess the extent of nonspecific binding to UF device (n=2).

	Filtration	[HSA] (μM)	[peptide] in filtrate sol.	Peptide filtrated compared to PBS sample (%)
LMU027	No	0	51.33 ± 0.63	-
LMU027	Yes	0	24.14 ± 2.38	48.83 ± 3.91
LMU027	Yes	100	14.35 ± 0.07	30.41 ± 0.50
LMU027	Yes	200	16.34 ± 4.43	34.17 ± 7.93
LMU027	Yes	300	14.58 ± 6.09	30.85 ± 11.84
LMU027	Yes	400	11.93 ± 2.14	25.88 ± 3.71

7.3 Chapter 5 – supporting information

7.3.1 Calibration curves for formulation studies

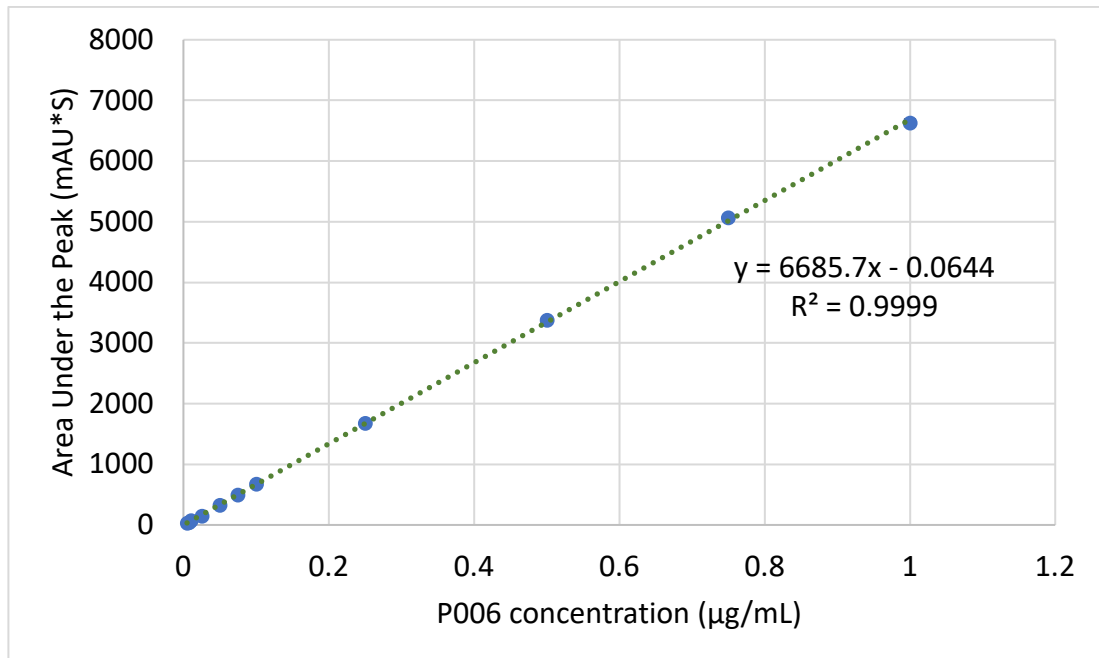


Figure S 128. P006 calibration curve in H_2O .

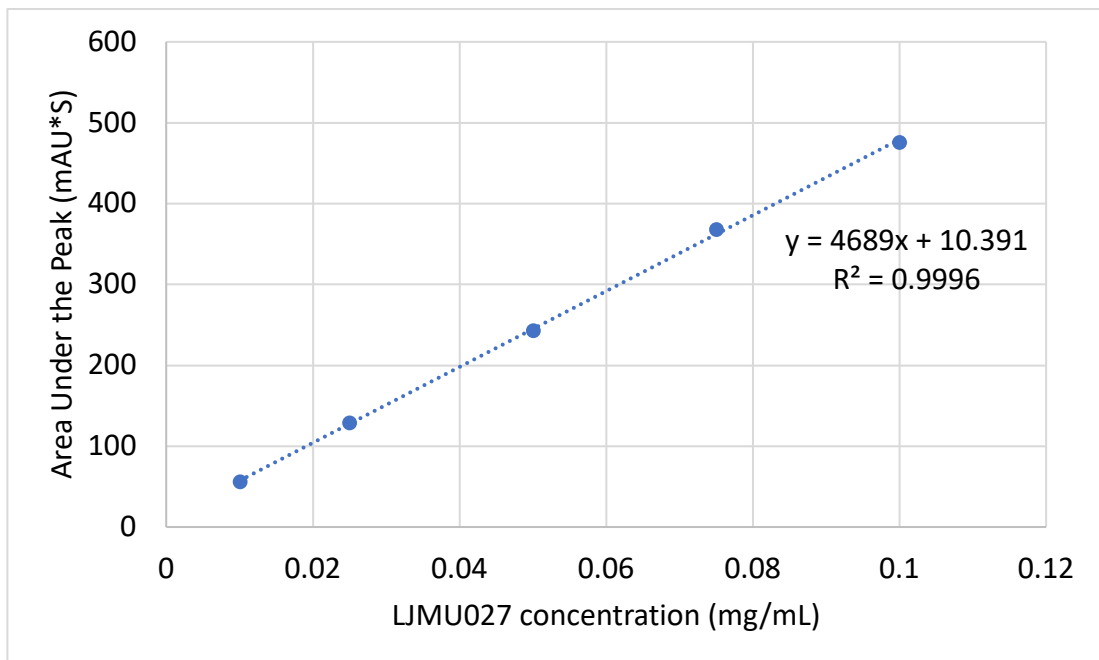


Figure S 129. LJM027 calibration curve in H_2O .

7.3.2 Table results NPs optimisation

Table S.7. Taguchi Design of Experiment for blank PLGA NPs optimisation.

Exp. No. (n=3)	Amount PLGA (mg)	% PVA	OP:AP ratio	Average size (nm)	PDI	Z-potential (mV)
1	10	1	01:04	121.27 ± 10.21	0.20 ± 0.02	0.65 ± 1.43
2	10	2.5	01:07	189.43 ± 61.68	0.34 ± 0.05	0.47 ± 0.43
3	10	5	01:10	251.67 ± 76.45	0.62 ± 0.09	0.02 ± 0.40
4	20	1	01:07	142.20 ± 5.35	0.14 ± 0.04	1.64 ± 0.47
5	20	2.5	01:10	204.07 ± 10.92	0.20 ± 0.01	-0.10 ± 0.52
6	20	5	01:04	482.90 ± 48.51	0.14 ± 0.00	0.35 ± 0.53
7	30	1	01:10	159.30 ± 6.31	0.10 ± 0.01	0.20 ± 1.84
8	30	2.5	01:04	261.03 ± 13.97	0.08 ± 0.02	1.29 ± 2.15
9	30	5	01:07	578.00 ± 30.62	0.07 ± 0.02	0.07 ± 1.03